ELASTIC-PLASTIC FINITE ELEMENT ANALYSIS OF SEMI-HOT FORGING DIES

A THESIS SUBMITTED TO
THE GRADUATE SCHOOL OF NATURAL AND APPLIED SCIENCES
OF
MIDDLE EAST TECHNICAL UNIVERSITY

BY

MURAT HALİSÇELİK

IN PARTIAL FULFILLMENT OF THE REQUIREMENTS
FOR
THE DEGREE OF MASTER OF SCIENCE
IN
MECHANICAL ENGINEERING

MAY 2009

Approval of the thesis:

ELASTIC-PLASTIC FINITE ELEMENT ANALYSIS OF SEMI-HOT FORGING DIES

submitted by **MURAT HALİSÇELİK** in partial fulfillment of the requirements for the degree of **Master of Science in Mechanical Engineering Department, Middle East Technical University** by,

Prof. Dr. Canan Özgen
Dean, Graduate School of **Natural and Applied Sciences** _____

Prof. Dr. Süha Oral
Head of Department, **Mechanical Engineering** _____

Prof. Dr. Haluk Darendeliler
Supervisor, **Mechanical Engineering, METU** _____

Prof. Dr. Mustafa İlhan Gökler
Co-supervisor, **Mechanical Engineering, METU** _____

Examining Committee Members:

Prof. Dr. Metin Akkök
Mechanical Engineering, METU _____

Prof. Dr. Haluk Darendeliler
Mechanical Engineering, METU _____

Prof. Dr. Mustafa İlhan Gökler
Mechanical Engineering, METU _____

Prof. Dr. Sıtkı Kemal İder
Mechanical Engineering, METU _____

Prof. Dr. Can Çoğun
Mechanical Engineering, Gazi University _____

Date: _____

I hereby declare that all information in this document has been obtained and presented in accordance with academic rules and ethical conduct. I also declare that, as required by these rules and conduct, I have fully cited and referenced all material and results that are not original to this work.

Name, Last Name: Murat Halisçelik

Signature :

ABSTRACT

ELASTIC-PLASTIC FINITE ELEMENT ANALYSIS OF SEMI-HOT FORGING DIES

Halisçelik, Murat
M.Sc., Department of Mechanical Engineering
Supervisor: Prof. Dr. Haluk Darendeliler
Co-Supervisor: Prof. Dr. Mustafa İlhan Gökler

May 2009, 113 pages

Semi-hot or warm forging is an economical alternative to the conventional forging processes by combining advantages of hot and cold forging processes.

In this study, a new forging process sequence and design of the preform die for a part which has been produced by hot forging are proposed to be produced by semi-hot forging. Thermo-mechanical finite element analyses are performed over the stages of forging process. The billet and the dies are modeled as elastic-plastic bodies. Effects of preform die geometry on the die stresses and the forging load are investigated using finite element method. Comparison of the results obtained by using two different commercial finite element analysis programs is done for semi-hot and hot forging temperature ranges. The forging temperatures are determined for the particular part and the experiments are conducted by using the 1000 ton forging press. The parts are produced without any defects and material wastage in

the form of flash is reduced. The numerical results are also compared with the experimental results and a good agreement is achieved.

Keywords: Semi-hot Forging, Warm Forging, Hot Forging, Finite Element Method, Die Stress Analysis, Metal Forming

ÖZ

YARI SICAK DÖVME KALIPLARIN ELASTİK-PLASTİK SONLU ELEMANLAR ANALİZİ

Halisçelik, Murat
Yüksek Lisans, Makina Mühendisliği Bölümü
Tez Yöneticisi: Prof. Dr. Haluk Darendeliler
Ortak Tez Yöneticisi: Prof. Dr. Mustafa İlhan Gökler

Mayıs 2009, 113 sayfa

Yarı sıcak veya ılık dövme, sıcak ve soğuk dövme işlemlerinin avatajlarını birleştirerek, geleneksel dövme işlemlerine ekonomik bir alternatif oluşturmaktadır.

Bu çalışmada, sıcak dövülerek üretilen bir parçanın yarı sıcak dövülerek üretilmesi için yeni bir dövme düzeni ve ön şekillendirme kalıp tasarımı sunulmuştur. Dövme işleminin aşamaları üzerinde termal mekanik analizler gerçekleştirilmiştir. Başlangıç malzemesi ve kalıplar elastik plastik cisimler olarak modellenmiştir. Önşekillendirme kalıplarının geometrisinin kalıp gerilimlerine ve dövme kuvvetine etkileri sonlu elemanlar metoduyla incelenmiştir. İki adet farklı ticari sonlu elemanlar analiz programından alınan sıcak ve yarı sıcak dövme sıcaklık aralıklarındaki sonuçları karşılaştırılmıştır. Belirli parça için dövme sıcaklığı belirlenmiş ve 1000 tonluk dövme presi ile deneyler yapılmıştır. Parçalar hatasız

olarak üretilmiş ve çapak şeklindeki malzeme kaybı azaltılmıştır. Sayısal sonuçlar, deneyin sonuçlarıyla kıyaslanmış ve tutarlılık sağlanmıştır.

Anahtar Kelimeler: Yarı Sıcak Dövme, Ilık Dövme, Sıcak Dövme, Sonlu Elemanlar Metodu, Kalıp Gerilim analizi, Metal Şekillendirme

To My Family and Fiancée

ACKNOWLEDGEMENTS

I would like to express my appreciation and thankfulness to my supervisor Prof. Dr. Haluk Darendeliler and my co-supervisor Prof. Dr. Mustafa İlhan Gökler for their encouragement, guidance, advice and support that created this study.

I also would like to thank to management of METU-BILTIR Research & Application Center for the facilities provided for my work. Thanks go to Halit Şahin, Ali Demir, Hüseyin Ali Atmaca, Sinem Demirkaya and Gökhan Biçer for their supports and efforts.

I also would like to thank to Mr. Cevat Kömürcü, Mrs. Tülay Kömürcü from AKSAN Steel Forging Company.

I owe Seda Gül and Zeynep Sude Bostancı for their precious help, support and friendship.

I would like to thank Ufuk Penekli for his invaluable collaboration and friendship.

Thanks to all my colleagues in FİGES, leading Kaan Özsoy, Berkan Büyükdağlıoğlu, Derya Akkuş and my manager Hakan Oka. Further, thanks go to Onur Doğan, Mert Çakar, Koray Atılgan and Hüseyin Sabri Aliefendioğlu from ASELSAN.

Further, thanks go to Levent Yılmaztürk, Suat Memiş, Onur Yıldız, Tarık Sekmen, Sonat Deniz, Süleyman Arslan, Erdem Budak, Yiğit Doğancı and Gülçin Kayhan for their supports and encouragement.

The special thanks go to my parents Emine Halisçelik and Ediz Halisçelik for their infinite support, and to my brothers Kaan Halisçelik, Hakan Halisçelik.

TABLE OF CONTENTS

LIST OF FIGURES

LIST OF TABLES

CHAPTER 1

INTRODUCTION

1.1 Forging Process

Forging process is perhaps the oldest manufacturing process used to fabricate metal products. In early time's metals such as bronze, copper, gold and wrought iron were forged to produce hand tools and weapons. Later at the end of 18^{th} century, during the industrial revolution, processes were devised to satisfy large demands for metal products. The past 100 years have seen the development of new types of equipment and new materials with special properties and applications in forging industry [1].

In forging process, an initially simple part is plastically deformed between tools in order to obtain a desired complex configuration. The input material is in billet, rod or slab form. The tools having the negative image of the desired geometry, impart pressure on the deforming material through the material die interface. Forging process usually produces little or no scrap and generates the final geometry in a very short time, usually in one or a few strokes of a press or hammer.

Among all manufacturing processes, forging has a special place because it greatly reduces material waste; ensure good surface finish and tolerances in the manufacture of engineering components. Forged components are more reliable than parts machined from bar stock or plate; because properly developed grain flow in forgings closely follows the outline of components [2]. Today, forging is used in different industries for

the manufacturing of variety parts such as; small bolts, pins as well as gears, cam and crankshafts, connecting rods, valves, landing gear components, etc.

Forging industry try to make improvements in all areas of forging in order to keep pace with other metal forming processes. The design and control of forging processes depend on an understanding of the characteristics of the workpiece material, the conditions at the tool workpiece interface, the equipment used and the finished product requirements. The traditional trial-and-error method has some problems of high scrap rate, low efficiency and operator experiences dependency. The formulation of sophisticated mathematical analyses of forming processes has led to higher quality products and increased efficiency in the metalworking industry.

1.2 Classification of Forging Processes

There are various classifications for forging process. In general, forging processes can be classified as conventional production and special forging processes. Conventional production forging processes include all hot, cold and warm working operations with open or closed dies by use of forging hammers, presses. The second category involves forging done by less common types of forging equipment such as roll forging, wheel and rotary forging, etc.

1.2.1 Conventional Production Forging Processes

Conventional production forging processes can be classified according to:

- Working temperature as hot forging, cold forging and warm forging
- Die type as closed die and open die
- Machine type as hammer, mechanical press, hydraulic press, screw press

1.2.1.1 Classification According to Working Temperature

Forging process can be classified according to their working temperature as hot forging, cold forging and warm forging.

In hot forging, the forging operation is applied to metals having temperature above recrystallization temperature. This is acquired by preheating the billet to high temperatures. The main advantage of hot forging is that the strain hardening effects are negated by the recrystallization process simultaneously with deformation of the metal. Also a great degree of deformation can be achieved due to reduced flow stresses and yield strength. Another advantage is the increase in ductility of the workpiece. However, high energy requirements for heating systems, formation of scale layer due to reactions between the metal and the surrounding atmosphere, less precise tolerances and dimensional accuracy due to thermal contraction and uneven cooling are the main disadvantages of hot forging process [3].

In cold forging, the material is forged below its recrystallization temperature usually around room temperature. Better surface finish and dimensional control can be achieved compared to that of hot forging, but small range of materials can be utilized. Intermediate anneals may be required to compensate for loss of ductility that accompanies strain hardening. Also high forming forces are needed and the tool stresses are quite high [3].

Warm forging process is performed near the recrystallization temperature of the material. Temperature range is usually between 600 °C and 900 °C [4]. The range is generally below the temperature at which scale forms. Compared with hot and cold forging, warm forging has a number of advantages that makes it used increasingly as a manufacturing method.

1.2.1.2 Classification According to Type of Die Set

Forging process can be classified according to type of die set as open die forging and closed die forging.

Open die forging is also referred as hand, smith, hammer and flat die forging. Most of open die forgings are produced in pair of flat dies or dies of very simple shape. Schematic representation of open die forging is shown in Figure 1.1. The dies do not confine the workpiece and it can flow except where contacted by the dies. An open die forging may weight as little as a few kilograms or as much as 6000 Newtons. Highly skilled press operators are needed to produce complex shapes. Also geometry of the forging can not be fully controlled. Operator needs to orient and position the workpiece in every stage to get the desired shape. Parts produced by open die forging have less accuracy and dimensional tolerance.

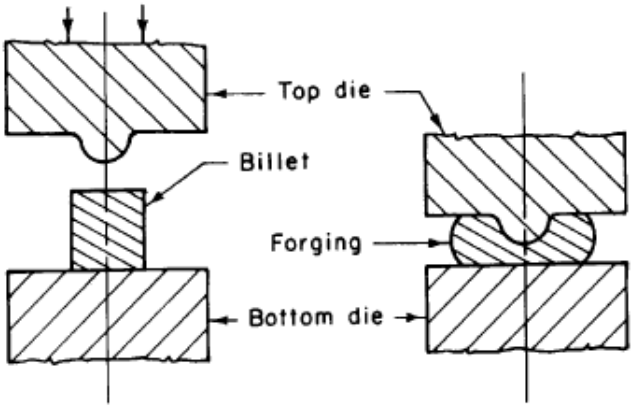

Figure 1.1 Open Die Forging [6].

In closed die forging, workpiece is plastically deformed between the dies having negative form of the desired part. Upper and lower dies mate at the parting plane. During forging process, the workpiece flow in the die cavity and with proper die design it acquires the shape of the cavity. Very complex shapes with closer dimensional tolerances than open die forging can be produced with usually some preforming steps. The final shape is forged in a finisher impression cavity. Schematic representation of closed die forging is shown in Figure 1.2. Closed die forgings are usually designed to require minimal subsequent machining. Generally forging stock is cut to a length to provide the volume needed to fill the die cavity. Excess metal is squeezed out of the die forming flash. Flash cools rapidly during the process and become stronger than the material inside die cavity and acts as a brake to slow the outward flow of metal. This result in increasing the pressure inside and narrow sections of die cavities can be filled. However high pressures formed by flash reduce die life and require additional power. After forging process the flash is trimmed off as scrap. Flash can account for 20 to 45% of the starting material [3].

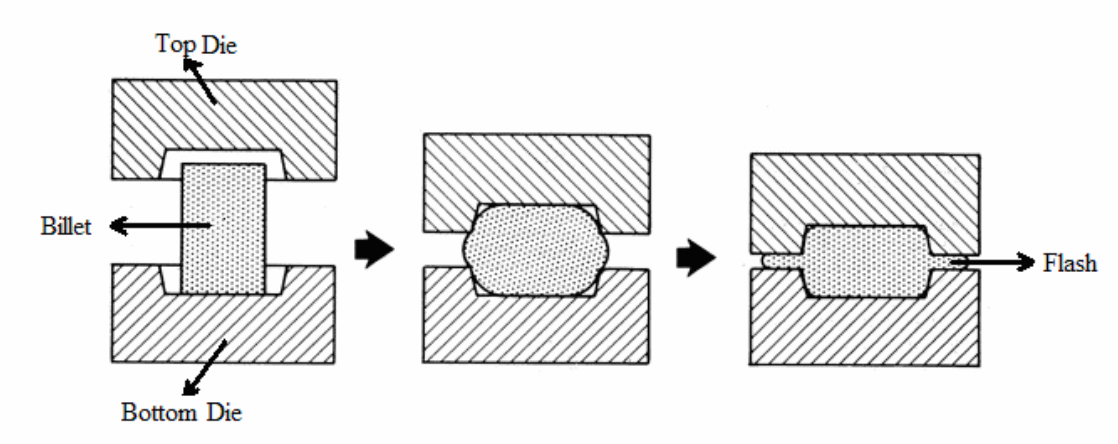

Figure 1.2 Closed Die Forging [5].

In the recent years flashless forging has been introduced that result in minimal material wastage. Volume of the metal must be controlled within very narrow limits to achieve complete filling of the die cavity. A thin film or ring flash may form in the clearance between the upper punch and die, but it is easily removed by blasting or tumbling operations, and does not require a trim die. Additional cost due to more complex design and need for better lubrication are the disadvantages of this process [7].

1.2.1.3 Classification According to Machine Type

Forging process can be classified according to machine type used as hammer, hydraulic press, mechanical press, screw press. Schematic illustrations of forging equipments are shown in Figure 1.3.

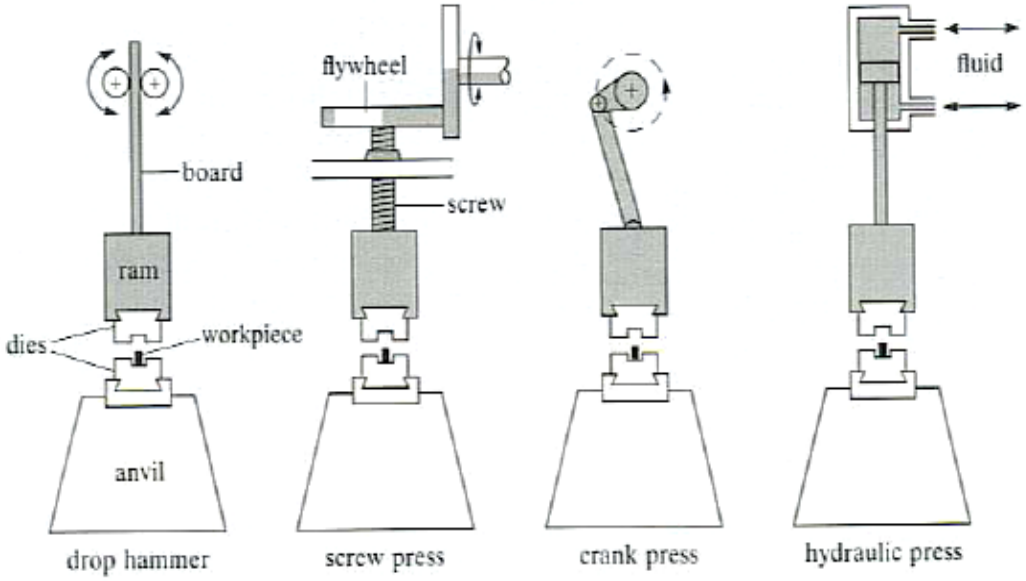

Figure 1.3 Schematic Illustrations of Forging Equipments; (a) Drop hammer, (b) Screw press, (c) Crank press, (d) Hydraulic press [4].

Forging hammers, such as board drop hammers, power drop hammers or air-lift gravity drop hammers, generally have a weighted ram moving vertically to cause an impact force against a stationary component in order to deform it plastically with each blow. The exception is the counterblow hammer in which the striking force develops from opposite movement of rams meeting at the midpoint. Since the deformation results from dissipating the total kinetic energy of the ram, hammers are energy-restricted machines. During forging the ram strikes the workpiece with repeated blows and thus shapes the metal in a stepwise fashion. Subsequent surface finish operation may be needed, since close dimensional tolerances can not be obtained by hammer forging [8].

Hydraulic presses are operated by large pistons driven by high pressure hydraulic or hydro-pneumatic systems. These presses have low speed and limited load that can be applied. Pressing speed can be continuously varied and controlled during the process permitting the control of metal flow velocities. Pressing load is constant during the entire stroke. Although close tolerances can be obtained, forging time may require several seconds which can cause chilling of the workpiece and overheating of the dies [9].

Mechanical presses differ from hammer and hydraulic presses in that they force two working surfaces together by offset cams, cranks and other rigidly connected mechanical systems that translate rotary motion into reciprocating linear motion. Mechanical presses are displacement-restricted machines. The stroke of mechanical presses is shorter and ram velocity is slower. The highest forging load develops at the end of the stroke before the direction of the ram movement is reversed. Compared to hammer forging, mechanical presses result in accurate close tolerance parts and higher production rates.

Screw presses use energy stored in a flywheel to provide the force for deforming the workpiece. Flywheels rotational energy is converted to linear motion by a threaded screw attached to the flywheel on one end and to the ram on the other end. Die stresses and effects of temperature of the workpiece are minimized in screw presses which results in good die life. Also impact speed is much greater than with mechanical presses. Screw presses are widely used in Europe for job-shop hardware forging, forging of brass and aluminum parts, precision forging of turbine and compressor blades and hand tools [1].

1.2.2 Special Forging Processes

Special forging processes can be classified as roll forging, rotary, shear forming and forging high energy rate forging.

In roll forging process, cross sectional area of bars or billets are reduced by passing them between two driven rolls that rotate in opposite directions. Rolls have one or more matching grooves. Generally shaping of long, thin and tapered parts are produced by roll forging. Typical examples are airplane propeller blade half sections, tapered axle shafts, tapered leaf springs, hand shovels and spades.

Rotary forging, also known as orbital forging, is a two die forging process that deforms only a small portion of the workpiece at a time in a continuous manner. In rotary forging, the axis of the upper die is tilted slightly causing the forging load applied to a small area of the workpiece. Rotary forgings are limited mainly to production of symmetrical parts and generally considered to be a substitute for hammer or press forging. The primary advantage is the requirement of low axial force resulting in lower machine and die deflections and therefore making highly accurate parts.

Shear forming, otherwise known as hydrospinning, spin forging, flow turning, is a process that combines spinning with rolling process. It changes the shape of a plate or a ring by applying force through pressure rolls operating against the workpiece, which is held by a turning mandrel.

In high energy rate forging, sometimes called high velocity forging, stored energy is used to accelerate the ram to high velocities generating forging force. It generates parts with good accuracy in dimensional tolerances; however workpiece must me capable of undergoing extremely rapid deformation rates. High speed machines are smaller than conventional forging machines and require a lower capital investment. Dies must be designed carefully to withstand high impact. Main disadvantage of the process is the limitation of shape and size. Only symmetrical parts with size limit about 11 to 12 kg for carbon steel forgings can be manufactured [1].

1.3 Forging Defects

Forging defects can be defined as the flaws resulting from improper forging operations. They can be categorized in terms of their general source as; fracture related problems (die contact surface cracking, internal bursts or chevron cracks), metal flow related defects (shear bands, folds, laps) and material selection or utilization problems (underfill, high scrap loss, poor dimensional control).

1.3.1 Fracture Related Problems

Internal fracture occurs by mechanisms such as triple point cracking at hot working temperatures or inhomogeneous deformation that cause internal defects such as internal burst or chevron cracking.

Internal fractures are the most dangerous type of defect since it can not be detected visually. Internal defects acts as initiation sites for further crack propagation during service loads. Microetching and ultrasonic inspection methods are widely used for identifying such regions.

1.3.2 Flow Related Problems

These types of defects are commonly related to improper die, perform design and lubrication system which lead to problems in the distribution of metal. Most types of flow related defects occur in hot forging [12].

1.3.2.1 Laps and Folds

Laps are formed when the material folds over its surface during forging. They frequently occur where vertical and horizontal sections intersect. Also in vertical cavities laps may form from nonuniform metal flowing when the metal fills the cavity. As a result a discontinuity with a sharp notch is created.

The die corner radius is a critical tool dimension. Most frequently improper selection of fillet radii is the cause of forming laps. In progressing through a forging sequence, the die corners should become tighter so that the workpiece fillets are initially large and progressively become smaller as the forging steps are completed [12].

1.3.2.2 Shear Bands

Shear defects are also known as flow through defects because they are formed from excessive metal flow past a filled detail of the part. Flow through defects are formed when metal is forced to flow past a recess after the recess has filled or when material

in the recess has ceased to deform because of chilling. They can also occur when trapped lubricant forces metal to flow past an impression.

1.3.3 Defects Due to Control, Material Selection or Utilization Problems

The efficiency and productivity of a forging operation depends on material selection and control, equipment cost, dimensional control and amount of scrap loss. Material control and selection have significant effects on mechanical properties of the product.

Problems such as underfill, part distortion, poor dimensional control, tool overload, excessive tool wear and high scrap loss may arise if no attention is paid to material control, selection and utilization.

Underfill may be due to insufficient starting mass or may be flow related. Improper fill sequence, insufficient forging pressure, insufficient preheat temperature and lubricant build up in die corners may lead to underfill. A change in the workpiece shape or change in the deformation sequence is needed to eliminate the problem.

1.4 Previous Studies

In this section the related studies are summarized.

Saraç [13] studied forging process of a part in hot and warm forging temperature ranges which needed improvements in accuracy of part dimensions and energy concepts. Process at hot forging temperature range is analyzed by a finite volume analysis. A new perform design was proposed and the forging process was simulated using thermo-mechanically coupled finite element method. In the analysis, dies were modeled as elastic objects enabling them to deform up to the yield point of the material. As a result of simulations plastic deformations were found in the finish dies

below initial billet temperature of 1000 °C. Also experimental study was conducted and results of the simulations were compared to the experimental study.

Aktakka [14] investigated hot and warm forging process of a part being used in automotive industry. Finite volume analysis had been performed in the range of hot and warm forging temperatures and experiments had been conducted. Since the results of the experiments did not correspond to the results of the simulations, a second set of finite volume analysis had been made with the data from experiments. Results of second series of simulations were observed to be in good agreement with the experiment results.

Civelekoğlu [15] analyzed the effect of different workpiece materials on hot forging operation. Eye bolts and runner blocks are examined in the study. As workpiece material 100Cr6, C45, C60, X20Cr13 and 42CrMo4 were selected and experiments were conducted. From the experiments, it was observed that flow stress of the material used as billet strongly effects die fill and workpiece dimensions. Also results had been discussed by considering effective stress distributions and temperature effects.

Mheta, Al-Zkeri and Gunasekera [16], evaluated MSC SuperForge by comparing its simulation results with the results of Deform 3D. A 3D extrusion process using a streamlined die design, that produces a relatively complex shape, was selected for the evaluation. As a secondary objective shear extrusion dies are investigated. Shear extrusion dies are easier to design and less expansive than the streamlined extrusion dies although they produce higher extrusion loads. As a result the finite volume program MSC SuperForge was effectively used to simulate various feeder plate designs for a shear die extrusion process and the results were in good agreement with the simulation results of Deform 3D.

Abachi [17] investigated analysis of die wear on dies provided by a forging company. Finite volume analyses with die wear were conducted. Results from computer simulation were compared with the measurement on the worn die taken from industry. Some modifications were made to analyses parameters after the results of the simulations had some disagreements with the experiment results. It was concluded that assuming constant dimensional wear coefficient was a good approximation for the case study.

Öztürk [18] investigated aluminum forging process of a part which is being produced with steel material at hot forging temperature range. The proposed forging process was simulated for Al 7075 and Al 6061 at several temperatures by a finite volume program. The experimental study was conducted and results were compared with the results of simulations. Single stage operation for the process produced folds in the finished part and as a result of simulations two staged forging process was considered successful. And also it was found that maximum effective stresses for Al 6061 are lower compared to the Al 7075.

Kim, Kim, Kang [19] explained the effects of lubricant and surface treatment on the life of forging dies. The thermal load and thermal softening, that occur when there is contact between the hotter billet and the cooler dies, may cause wear, thermal cracking and fatigue. Because the cooling effect and low friction are essential to long die life, the proper selection of lubricant and surface treatment is very important in hot forging process. Experiments were conducted to obtain the friction factor and the surface heat transfer coefficients in different lubricants and surface treatments. For lubrication, oil base and water base graphite lubricants were used. As surface treatment conditions ion nitride and carbon nitride were used. The methods for estimating die service life are presented in this study.

In the study of Iwama and Morimoto [20] development of countermeasures to improve the duration of punch's life in warm forging was investigated. It was found that to improve die life, a dry adhesion layer which binds strongly to the die is essential.

In the study of Fai, Chow and Chui [21], various combinations of punch and die were analyzed to evaluate the feasibility of axisymmetric warm forging process. A method for predicting the critical shapes of billets was proposed by comparing simulation results such as die filling and load-stroke curves with experiments.

1.5 Aim and Scope

Semi-hot or warm forging process has better forming precision than hot forging and has better formability than cold forging process. However, die damage is a serious problem in warm forging process due to high die stresses compared to hot forging process. Traditional trial-and-error methods for developing a complete manufacturing process is heavily experience based, and in many cases it causes material wastage, high energy consumption, unacceptable products, loosing time and money. Computer simulations may eliminate these.

The main scope of this study is to investigate feasibility to reduce the forging temperature for a particular industrial part and to analyze the die stresses developed during the forging process.

In this study, a detailed analysis of a part which has been produced by hot forging in Aksan Steel Forging Company [22], Ankara is performed using finite element method. The billet and dies have been analyzed by elastic-plastic finite element analysis including thermal and friction effects in order to produce the part with less scrap material and to reduce the forging process temperature.

The basic principals of warm forging process will be given in Chapter 2. General information about the finite element method and steps to define the forging process in a finite element analysis program will be given in Chapter 3. In Chapter 4, firstly the simulations and results for the current practice in the factory will be given. Then comparison of results of two commercial finite element analysis programs, MSC Superform [33] and Deform 3D [30], will be given for the proposed method by Saraç [13]. A new forging process sequence and finite element analyses of effects of the preform die geometries and forging temperatures will also be presented in Chapter 4. The experimental study is carried out in METU-BILTIR Center Forging Research and Application Laboratory for the proposed process sequence will be presented and will be compared to the results of the computer simulations in Chapter 5. Conclusion and recommendations about future work will be given in Chapter 6.

CHAPTER 2

WARM FORGING PROCESS

2.1 History and Characteristics of Warm Forging

Large production numbers are required due to the highly increasing demand for precision parts in especially automotive industry. Since the growth of automotive industry in 1950s cold forging process is used in serial mass production of a wide range of components. Limitations to the economical production of parts of complex geometry in large size and in certain alloys revealed the potential of warm forging process.

After conventional hot and cold forging processes, warm forging became very important with regards to cost savings by near net shapes production. Warm forging process is mostly combined with cold forging process. The process was first introduced in Japan and the Far East in the 1970s and has been in continual development. Today, the warm forging process is also known as semi-hot forging and majority of warm forgings are made in steel for the automotive industry [23].

Warm forging process is applied within a temperature range between 600 °C and 900 °C. In comparison to hot and cold forging processes, warm forging process offers the following advantages [23]:

- Reduced forming loads compared with those for cold forging.

- Greater ductility compared with those for cold forging.
- Improved accuracy compared with those for hot forging.
- Better surface finish and less scale amount compared with those for hot forging.
- Enhanced product properties through grain refinement and controlled phase transformations in heat treatable steels.
- A potential for the reduction of products costs.

A detailed comparison of the characteristics of hot, warm, cold forging processes is given in Table 2.1.

Table 2.1 Comparison of Typical Process Characteristics [23, 24].

Characteristic	Hot forging	Warm forging	Cold forging
Shape spectrum	Arbitrary	Rotationally symmetrical if possible	Mainly rotationally symmetrical
Weight of the part	5 g - 1500 kg	100 g - 50 kg	1 g - 50 kg
Steel grade	Any	C desirable, other alloying elements <10%	Low alloyed steels (C<0.45%, other elements <3%)
Normally achievable accuracy	IT 12 – IT 16	IT 9 – IT 12	IT 7 – IT 11
Economical lot size	Min. 500 pieces	Min. 10,000 pieces	Min. 3,000 pieces
Surface quality	Low	Medium	High
Intermediate treatments	none	generally none	annealing/phosphating
Die life	5,000 - 10,000 parts	10,000 - 20,000 parts	20,000 - 50,000 parts
Energy requirement (per kg gross of forging)	460 - 490 J	400 - 420 J	400 - 420 J

2.2 Workpiece Material for Warm Forging

Materials used in forging operations are mainly unalloyed, low-alloy and high-alloy carbon steels, non-ferrous light and heavy alloys such as aluminum, magnesium, titanium and copper and their alloys.

Aluminum and magnesium forgings offer low weight components however they are used in applications where the temperatures do not exceed 150 °C. Copper forgings are corrosion resistant and have high thermal and electrical conductivity. Titanium forgings exhibit high strength, low weight and high corrosion resistance.

In warm forging process, most engineering steels may be used but there are limitations to deformation depending on chemical composition and forging temperature. Different classes of steels have characteristics which influence the choice of working temperature [23].

- Carbon Steels: These steels are generally forged at temperatures over 600 °C since they may be brittle between temperatures 200 °C and 550 °C depending on the rate of deformation.
- Alloy Steels: Any temperature in the warm forging range may be used, depending on circumstances.
- Austenitic Stainless Steels: Temperatures between 200°C and 300°C are commonly used. Temperatures over this range are not recommended due to the lack of a suitable lubricant for such application.

Table 2.2 provides a summary of most important steel material groups and information on whether the steel is suitable for hot forging (H), warm forging (W) or cold forging (C) processes.

Table 2.2 Selection of Steels for Forging Operations [25].

Material Group	No.	DIN 1654	Suitable for Cold (C), Warm (W), Hot (H) Forging
General Structural Steel	1.0303	QSt 32-3	C
	1.0160	UPSt37-2	H
	1.0224	UQSt-38	C
	1.0538	PSt50-2	H
Case-hardening Steels	1.0301	C10	W, H
	1.1121	Ck10	C, W, H
	1.1122	Cq10	C, H
	1.0401	C15	W, H
	1.1141	Ck15	C, W, H
	1.7131	16MnCr5	C, W, H
Heat-treatable Steels	1.6523	21NiCrMo2	C
	1.1151	Ck22	C
	1.1152	Cq22	C
	1.0501	C35	W, H
	1.1181	Ck35	C, W
	1.1172	Cq35	C, W, H
	1.0503	C45	W, H
	1.1191	Ck45	C, W, H
	1.1192	Cq45	C
	1.1193	Cf45	W
	1.1213	Cf53	W
	-	Cf60	W
Alloyed Heat-treatable Steels	1.5508	22B2	C
	1.7076	32CrB4	C
	1.7033	34Cr4	C, W, H
	1.7035	41Cr4	C, W, H
	1.7218	25CrMo4	C, W, H
	1.7220	34CrMo4	C, W, H
	1.7225	42CrMo4	C, W, H
	1.6582	34CrNiMo6	C, H
Stainless Steels	1.4016	X6Cr17	C, ferritic
	1.4006	X10Cr13	C, martensitic
	1.4024	X15Cr13	C, H, austenitic
	1.4303	X5CrNi18-12	C, austenitic
	1.4567	X3CrNiCu18-9	C, austenitic
Roller Bearing Steel	1.3505	100Cr6	C, W

2.3 Tool Materials and Heat Treatment of Tool Steel

Severe mechanical loading and thermal stresses are exposed by the tooling in warm forging process. Tool components suffer considerable loading, and in addition thermal and tribological stresses are superimposing on the surface, leading to continuous wear. Materials used for warm forging are required to have high strength, high toughness and high hardness. For an economical die life, extremely good wear and tempering resistance are necessary.

During warm forging process, the specific stresses in the tools ranges at approximately 50-60 % compared to cold forging tools and approximately twice as high as in hot forging tools [24].

Schmoekel, Sheljaskow and Speck [27] summarized the requirements necessary in tool steel for warm forging as:

- Resistance to deformation
- Resistance to fracture
- Wear resistance
- Temper resistance
- Thermal shock resistance
- Economy

Currently a mixture of hot work steels, cold work steels, high speed steels are being used for warm forging. Hot work tool steels are often used, but these may wear or deform relatively quickly so that the tools soon become out of tolerance. High speed steel tooling may be employed to meet the extra strength and hardness requirements but is limited to use in particular parts because of its inherent lack of toughness and therefore thermal shock resistance. Cold work tool steels have inadequate toughness

levels, and are not temper resistant, loosing their high hardness rapidly in warm forging temperatures. There is also a variety of patented steels from various tool steel manufacturers.

Best tool life is achieved with high speed steels as their load carrying capacity exceeds warm forging steels. However long cooling time is needed since only indirect cooling and air ventilation is appropriate during production. This is due to low temperature shock resistance of high speed steels. Because of this characteristic cooling time needs to be extended and this limits the maximum number of production strokes.

Hot work steels are used as tool materials when production numbers are high. Addition of chromium, molybdenum and vanadium increase toughness and resistance to thermal shock. Although they have lower load carrying capacities production output is compensated by modification of the forging process or increase of temperature.

Nickel alloys can be used to achieve excellent tool lives. These alloys, such as Iconel 78, have high fatigue strength at high and low load alterations, high thermal shock resistance and high toughness. However these alloys have high costs and usually used for tool parts with comparatively low weight [23].

Even though carbide steels are well suited for forging process, they are not used in warm forging as they fail after any interruption of the process and related temperature drop [26].

Investigations for developments in die materials for warm forging process are concentrated on tool steels which are derived from hot forging tool steels having relatively low carbon content. These steels demonstrate superior wear and heat resistance properties as well as very good thermal shock resistance [25].

Tool loads for warm forming are cyclic and nearly as high as for cold forging, at the same time tools are in contact with warm workpieces causing thermal shocks. The surface expansion of the workpiece can be very great resulting in severe tribological conditions. To secure a stable process and consistent product accuracy, wear and fracture resistance must be high.

Usually tool steels are in form of soft annealed condition when supplied from the manufacturer. The machining is done in this stage and heat treatment must be applied to the tool in order to achieve required hardness for operation. After heat treatment tool is then ground and polished to its finished state. Heat treatment process consists of one or two preheating stages, hardening stage, quenching stage, tempering stage and stress relieving stage. These stages are performed in a salt bath or a vacuum furnace and the surface of the tooling is protected from oxidation.

The success of hardening and tempering depends on correct temperature and time of treatment as well as correct cooling after the heat treatment. Accurate heat treatment is very important in using the tool steel in its full potential. An inaccurate heat treatment can easily destroy the essential properties of the material and cause the tool to fail.

2.4 Tool Design

For an adequate tool design, tool material selection must be correct and process planning must be optimized. To achieve this following data are needed [23]:

- Physical properties of work-piece material
- Number of components to be forged
- Forging loads and tools stresses
- Forging temperature
- Production rate

- Kinematics of forging machine
- Geometric limits to shape of tools

Warm forging process usually consists of many stages. In the early stages shape of the workpiece is developed and in the later stages finished shape is refined or dimensional accuracy is improved.

2.5 Tool Failure

A very important factor affecting the performance and economics of warm forging process is the service life of tooling. Initiation and propagation of die damage can be caused by a number of mechanisms. Failures of tooling occur due to either wrong material selection or due to heat treatment or machining procedures have not been optimized. Design errors such as sharp corners, undersized fillet radii, thin sections and sudden variations in section thickness are often the causes of die failure.

To decrease the likelihood of die failure the following steps can be taken [28]:

- Design that is compatible with the die material selected and with the planned processing procedure.
- Selection of a heat treating procedure that is compatible with design and processing procedure.
- Selection of material that is compatible with design and processing procedure.
- Control of the specified heat treating procedure.
- Control of the grinding and other finishing operations.
- Control of die setup (particularly alignment) in the equipment.
- Control of die operation, specifically avoidance of overloading.

2.6 Lubrication

Lubricants play an important role in forging process such as reducing forging loads, cooling the tools and acting as parting compounds. The requirements of die lubricants for warm forging process are:

- Good film formation on hot dies
- Good lubricating properties to reduce friction, therefore reduce forging loads
- Good release properties

Insulating qualities are important since it is usually desirable in forging metals at high temperatures to minimize chilling of the workpiece by the dies.

Various types of lubricants are used, and they can be applied by swabbing or spraying. The simplest way is high flash point oil swabbed onto the dies. Colloidal graphite suspensions in either oil or water are also frequently used. Synthetic lubricants can be employed for light forging operations. The water base and synthetic lubricants are extensively used because of their cleanliness.

Some lubrication systems blow air/water mist mixture sequentially for cooling and then spray a lubricant. Large amounts of heat can be extracted more economically with this method then by applying more lubricant to the system.

In warm forging process the use of an additional billet coating is recommended, as it assures additional lubrication next to the die lubricant in order to reduce the forces and increase the life of the tools. The billet coatings used include graphite in a fluid carrier or water base coatings used in conjunction with phosphate conversion coating of the workpiece. Advantages and limitations of some lubricant types are given in Table 2.3 [29].

Table 2.3 Advantages and Limitations of Some Lubricant Types [29].

Type of lubricant	Advantages	Limitations
Water Base Graphite	• Eliminates smoke and fire • Provides die cooling • Easily extended with water	• Must be applied by spraying for best results
Water Base Synthetic	• Eliminates smoke and fire • Cleaner than oils or water base graphite • Easily diluted • Does not need agitation after initial mixing • Reduces clogging of spray equipment • Does not transfer dark pigment to part	• Must be sprayed • Lacks lubricity of graphite for severe forging operations
Oil Base Graphite	• Fluid film lends itself to either spray or swab application • Has good performance over a wide temperature range (up to 540 °C)	• Generates smoke, fire, and noxious odors • Explosive nature may shorten die life • Has potentially serious health and safety implications for workers

CHAPTER 3

FINITE ELEMENT METHOD

3.1 Introduction

It is difficult to analyze forging process for complex parts with analytical methods and numerical methods are preferred for a complete analysis. The finite element method is a numerical technique where the bodies to be analyzed are divided into small finite number of domains. Using finite element simulations reduce lead times and costs by eliminating unnecessary trials. The information from simulations can be used to evaluate forging process and tool design in the designing stage as well as in the troubleshooting stage. Results can be used to obtain parts without any defects and making improvements in tool life.

Finite element analysis of forging process is usually a nonlinear problem coupled with heat transfer. Nonlinear behavior results from geometric nonlinearities such as large strains, large deflection, stress stiffening, material nonlinearities such as plasticity, hyperelasticity, creep and boundary nonlinearities such as contact [34]. Nonlinear analysis is more complex and computationally expensive than the linear analysis. Solutions of nonlinear problems require incremental solution schemes and in implicit methods system is analyzed using iterative series of linear approximations with corrections. Many iterations are needed to converge to an equilibrium. Commonly Newton-Raphson method is used as iterative procedure.

For describing finite element problems two different approaches are used which are Eulerian method and Lagrangian method. In the Eulerian method, finite element mesh is fixed in space and the material flows through the mesh. In the Lagrangian method finite element mesh is attached to the material and moves through space along with the material. The mesh is updated to new positions after each increment. Although Eulerian method is suitable for steady state processes [30], Lagrangian method is more conveniently used in metal forming simulations [31].

3.2 Finite Element Analysis of Forging Process

In this study finite element models are prepared in commercial software Deform 3D [30]. To define a complete thermo-mechanical analysis in Deform 3D following steps are completed:

1. Part Description: Includes all data associated with a part including geometry mesh temperature and boundary conditions.
2. Material Data: Includes data describing the behavior of material under the forging process conditions
3. Interaction Conditions: Describes how the objects interact with each other, including contact, friction and heat transfer between objects.
4. Simulation Controls: Includes the conditions of processing environment, amount of discrete time steps to model the process, types of physical processes involved and controls about the simulation process and remeshing criteria to be used.
5. Running the Simulation: Includes performing the numerical calculations to solve the problem.
6. Post-processing: Postprocessor features a graphical user interface to view geometry, strain, stress and other simulation data.

3.2.1 Defining Part Description

The first step in the analysis is to define the die and billet geometries. After modeling the billet mesh is generated.

In Deform there are five part modeling types available which are rigid, elastic, plastic and elastic-plastic. Rigid objects are modeled as non-deformable materials and it is recommended when the tools have much higher yield stress than the workpiece [30]. Elastic material behavior is useful in situations when tooling deflection can have significant influence on the shape of the part and if the yield strength is not exceeded. Plastic deformations are modeled as rigid plastic or rigid viscoplastic material depending on characteristics of materials. The formulation assumes that the material stress increases linearly with strain rate until a threshold strain or strain rate and deforms plastically beyond that. In elastic-plastic definition, objects are treated as elastic until yield point is reached. Then any portions of the object that reach the yield point are treated as plastic, while the remainder is treated as elastic. It provides a realistic simulation of elastic recovery, strains due to the thermal expansion and residual stress calculation. Elastic-plastic definition requires more computational time and may have difficulties with convergence.

The most common initial condition is the material temperature and the most common boundary conditions are heat exchange with environment, prescribed velocity and force, symmetry and shrink fit [30].

3.2.2 Defining Material Data

In order to have an accurate simulation it is important to define accurate material properties covering the working temperatures of the process modeled. In this study, elastic-plastic material definition defined as tabulated data format is used for the

workpiece and the dies. For a thermo-mechanically coupled analysis thermal expansion, heat capacity, conductivity and emissivity data are also used.

3.2.3 Defining Friction, Heat Transfer and Press Conditions

The critical variables to be defined between contacting objects are friction factor, interface heat transfer coefficient, contact relation, separation criterion and object positioning.

The friction coefficient may be specified as a constant, a function of time or a function of interface pressure. The friction types available are shear and coulomb friction. Constant shear friction also known as Tresca's friction model is used mostly in bulk-forming simulations. The frictional stress in the constant shear model is defined by:

$$F_s = m\,k \tag{3.1}$$

Where F_s is the frictional stress, k is the shear yield stress and m is the friction factor. This states that the friction is a function of the yield stress of the deforming body. For forging operations involving high contact pressures, constant shear model is more appropriate [33].

Coulomb friction is used when contact occurs between two elastically deforming objects. The frictional stress in the Coulomb law model is defined by:

$$F_s = m\,p \tag{3.2}$$

Where p is the interface pressure between two bodies and m is the friction factor.

The interface heat transfer coefficient specifies the coefficient of the heat transfer between two objects in contact. It is determined by the interface pressure, amount of

sliding, and interface temperature [30]. This can be specified as constant or a function of time.

Definition of press type that is used and objects positioning is also defined in this step. Different machines such as screw press, mechanical press, hydraulic press and hammer can be defined as well as translational and rotational movement controls.

3.2.4 Remeshing

In bulk forming processes workpiece is exposed to high deformations and therefore finite element mesh experience high distortion during the analysis. High distortion of element may cause the analysis to fail. In order to avoid such problems it is necessary to assign new mesh by remeshing. In remeshing procedure first a new mesh is assigned and then solution information from old mesh is interpolated on to the new mesh and simulation goes on. Deform uses an automatic remeshing subroutine to deal with the mesh degradation. The remeshing criteria window contains a group of parameters that control when and how often the mesh will be regenerated. The most used control parameter is the interference depth parameter [30]. Remeshing is triggered when an element edge of meshed body has been penetrated by the master object by a specified amount.

CHAPTER 4

FINITE ELEMENT ANALYSIS OF FORGING

In this chapter a part currently forged at 1150 °C at AKSAN Steel Forging Company and related dies are analyzed by finite element method (FEM). A photograph of the sample part is given in Figure 4.1.

Figure 4.1 Sample Forged Part [22].

For the sample part two studies were completed in METU-BILTIR Center, where in one the process has been investigated and a process design has been proposed by using

finite volume and finite element method [13] and in the other forging of the part with aluminum material has been analyzed [18].

4.1 The Current Practice in Factory

Four forging stages are utilized in the company consisting of two upsetting stages, a performing stage and a finishing stage. Initial billet has a diameter of 30 mm and a height of 30 mm. The billet material used is St 52-3.

First two stages of the forging process are upsetting the initial billet in the rolling direction between flat dies. Since the operation is performed in the hot forging temperature range, scale layer is formed on the outer surface of the billet. During upsetting stages, the scale layer is removed and a sufficient shape is prepared for the subsequent stages. However, because of open die forging, dimensions can not be controlled and varieties of geometries are obtained. In the third stage upsetted billet is forged in perform die sets. Finally finish dies are used to obtain the finish geometry.

After the finishing stage forged part is trimmed and a hole is punched out in the hexagonal cavity. Due to the problems in the forging stage, finally cold ironing is applied to match the geometric dimensions needed. Another problem in the forging stage is excessive wear and flash amount.

Die sets in the upsetting operations are flat dies having the material of AISI L6. The perform and finish dies are also made from same material. Upsetting, perform and finish forging operations are performed with 1000 ton eccentric mechanical press. Trimming and punching operations are performed with a trim press of 250 ton capacity.

4.1.1 Modeling of Forging Part, Billet and Dies

The model of the finished part is given in Figure 4.2. Technical drawing of the part is given in Appendix A.

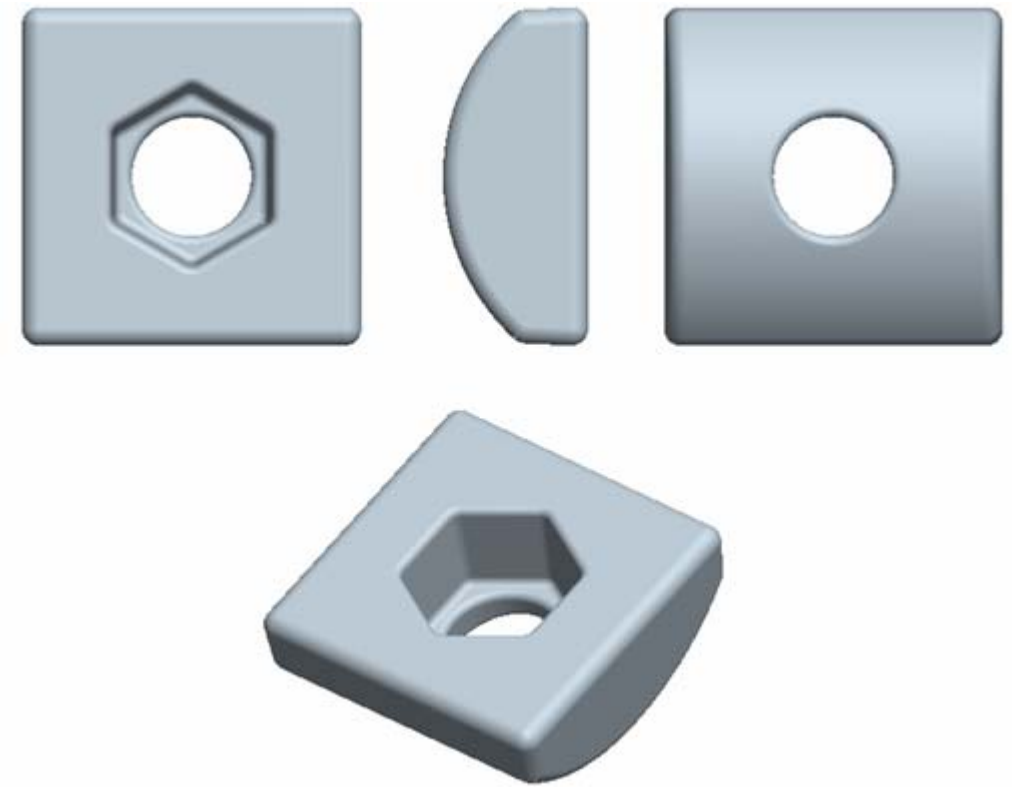

Figure 4.2 Views of 3D Model of the Part.

The finished part has a width and length of 40 mm. The height of the part is 17 mm. Hexagonal cavity on the part is critical and has a dimension of 19 mm.

The models of current perform die used in the factory are given in Figure 4.3 and the models of finish die are given in Figure 4.4.

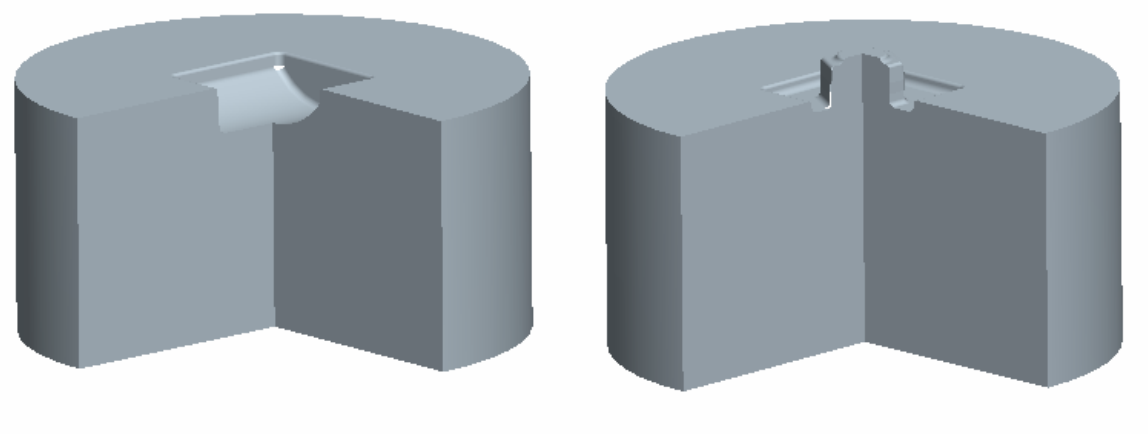

Figure 4.3 Preform Dies Used in the Factory.

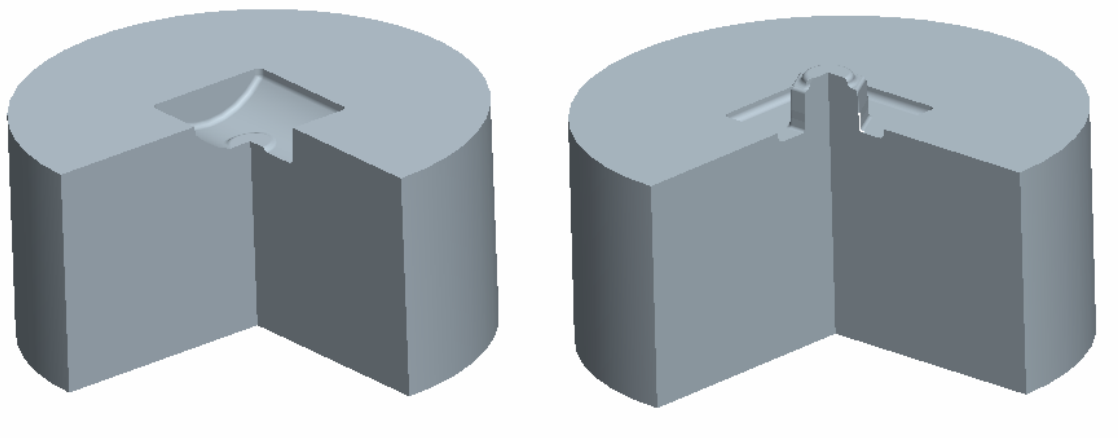

Figure 4.4 Finish Dies Used in the Factory.

4.1.2 Analysis of Forging Process Using Finite Element Method

Finite element models are prepared in commercial software Deform 3D [30]. Results such as die filling success, flash formation, material flow, stress, strain and temperature distributions are examined.

4.1.2.1 Modeling of Billet and Die

In the upsetting stages 34773 elements are used in order to model the billet with an average edge length of 0.25 mm. View of billet after mesh generation is shown in Figure 4.5.

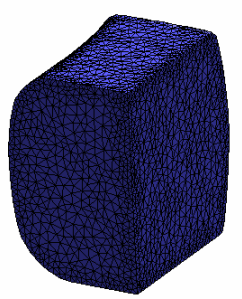

Figure 4.5 View of Billet After Mesh Generation.

In the upsetting stages the dies are assumed as rigid bodies. For perform and finish dies elastic-plastic material model is used in the analysis and a fine mesh is utilized around the die cavities. There are 26089 elements in the upper preform die, 31006 in the lower preform die. Similarly, for the elastic-plastic analysis of the dies for finishing operation 31825 elements are used in the upper finish die and 33117 elements in the lower finish

die. The preform and finish die after mesh generation are shown in Figure 4.6 and Figure 4.7, respectively.

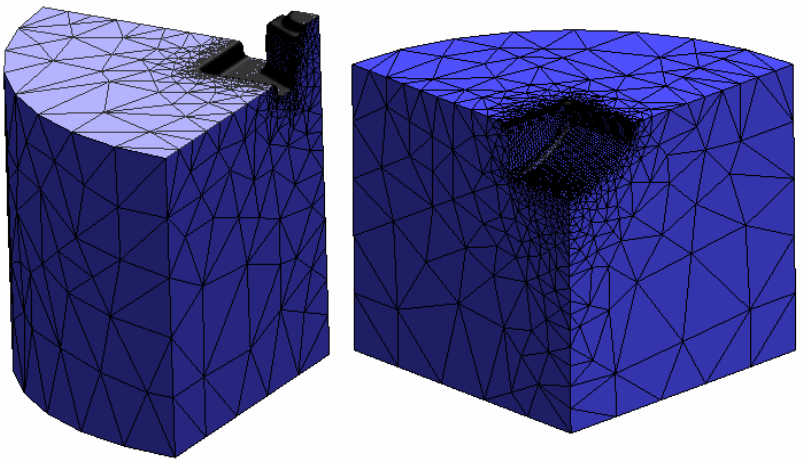

Figure 4.6 Preform Dies After Mesh Generation.

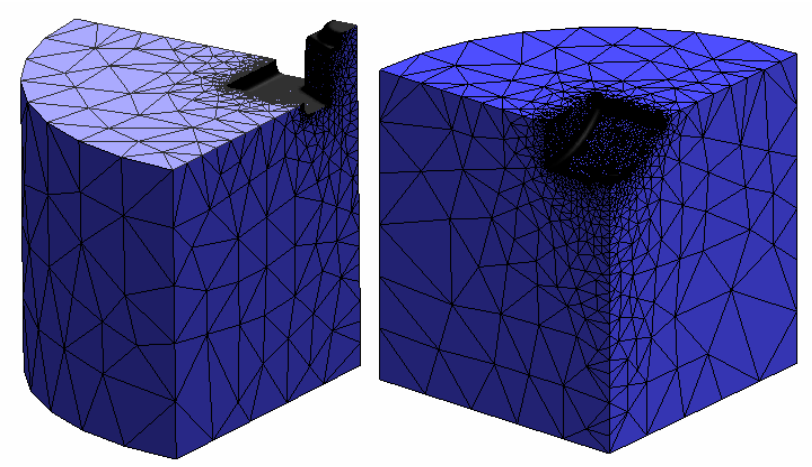

Figure 4.7 Finish Dies After Mesh Generation.

Initial temperature for the billet is taken as 1150 ºC and for the dies as 250 ºC. Environment temperature is defined constant as 20 ºC. Symmetry and heat exchange with environment are enforced at nodes as the boundary conditions.

4.1.2.2 Material Data

The workpiece material is carbon steel AISI 1020. The chemical composition of AISI 1020 is given in Table 4.1, the mechanical and thermal properties are given in Table 4.2 [35].

Table 4.1 Chemical Composition of AISI 1020 [35].

AISI 1020 (DIN 1.0402)	C %	Si %	Mn %	P %	S %
	0.18-0.23	≤ 0.4	0.3-0.6	0.04	0.04

Table 4.2 Mechanical and Thermal Properties of AISI 1020 [35].

Tensile Strength	475-640 MPa
Yield Strength	295 MPa
Elongation at Rupture	36.50%
Modulus of Elasticity	190-210 GPa
Poison's Ratio	0.27-0.3
Density	7870 kg/m³
Hardness	111 HRB
Thermal Conductivity	51.9 W/m-K
Heat Capacity	0.486 J/g-°C
Thermal Expansion	11.7 µm/m-°C
Emissivity	0.75

Die materials are assigned as AISI L6 from programs material database. The chemical composition of AISI L6 is tabulated in Table 4.3, the mechanical and thermal properties of AISI L6 are given in Table 4.4 [36].

Table 4.3 Chemical Composition of AISI L6 [36].

	C %	Si %	Mn %	P %	S %	Cr %	Mo %	Ni %	V %
AISI L6	0.65-0.75	0.5	0.25-0.8	0.03	0.03	0.6-1.2	0.45-0.55	1.5-2	0.07-0.12

Table 4.4 Mechanical and Thermal Properties of AISI L6 [36].

Tensile Strength	655 MPa
Yield Strength	380 MPa
Elongation at Rupture	25%
Reduction of Area	55%
Modulus of Elasticity	200 GPa
Poison's Ratio	0.28
Density	7860 kg/m³
Hardness	93 HRB
Thermal Conductivity	50.71 W/m-K
Heat Capacity	0.414 J/g-°C
Thermal Expansion	11.3 µm/m-°C
Emissivity	0.7

4.1.2.3 Friction and Press Parameters

In the analyses, constant shear model is used. The friction factor is assumed as 0.3 which is was also used in other similar studies [14, 15, 38].

In this analysis, an eccentric mechanical press of 1000 ton capacity being used in the forging company is defined. The parameters required to specify the movement of a mechanical press are:

1. Displacement of the punch for the mechanical press representing the total stroke of the press per cycle: 125 mm.
2. Strokes per time representing the frequency of the press blows: 90 rpm corresponding 1.5 stroke per second.
3. Current die stroke which is the value of the stroke length for which die is in contact with the workpiece: The value is taken as 106.2 mm meaning the die will move 18.8 mm to finish the stroke as the flash thickness is about 2 mm.
4. Direction in which the stroke is applied: -Y direction.
5. Connecting rod length which has an influence on the speed of the ram: 665 mm.

4.1.2.4 Remeshing and Other Parameters

For remeshing criterion, penetration distance of 0.8 with a relative setting is defined; when the distance from the middle of the edge to the die surface is divided by the original length of the edge exceeds the magnitude of the specified value, remeshing will be triggered. In the analysis proper time step selection is important. Movement about 1/3 the length of an element length is defined in one step. Also maximum primary die displacement of 125 mm is defined for the stopping criterion.

4.1.2.5 Visualization of Finite Element Results

The results obtained by the finite element modeling are given for upsetting, preform and finish stages.

4.1.2.5.1 Upsetting Stage

The equivalent stress values obtained at the maximum punch stroke of first and second upsetting stages are given in Figure 4.8.

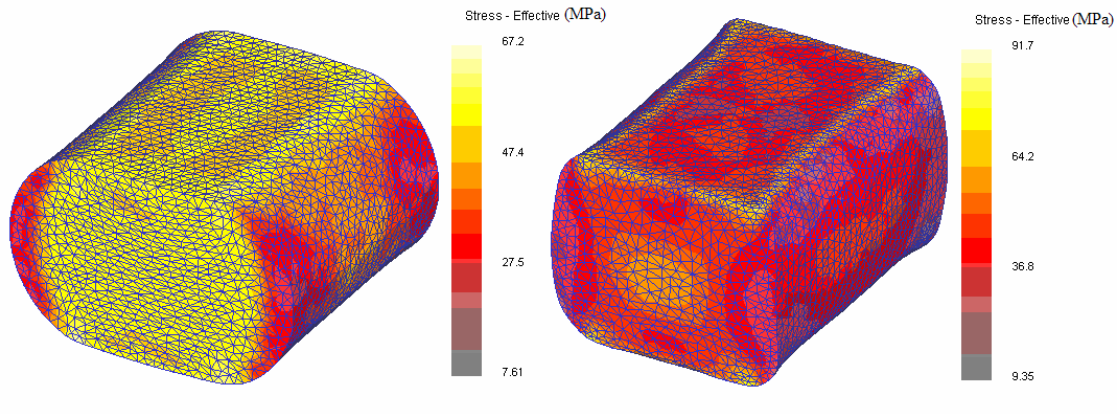

Figure 4.8 Maximum Equivalent Stress Values Obtained After the First and Second Upsetting Stages.

It is observed that the maximum equivalent stress is 67 MPa after the first upsetting operation and 92 MPa after the second upsetting operation.

The geometry of the billet and the dimensions obtained after the first and second upsetting stages are given in Figure 4.9. It is seen that almost a rectangular cross-section of 28.8 mm x 22 mm x 38.4 mm is obtained after the upsetting stage.

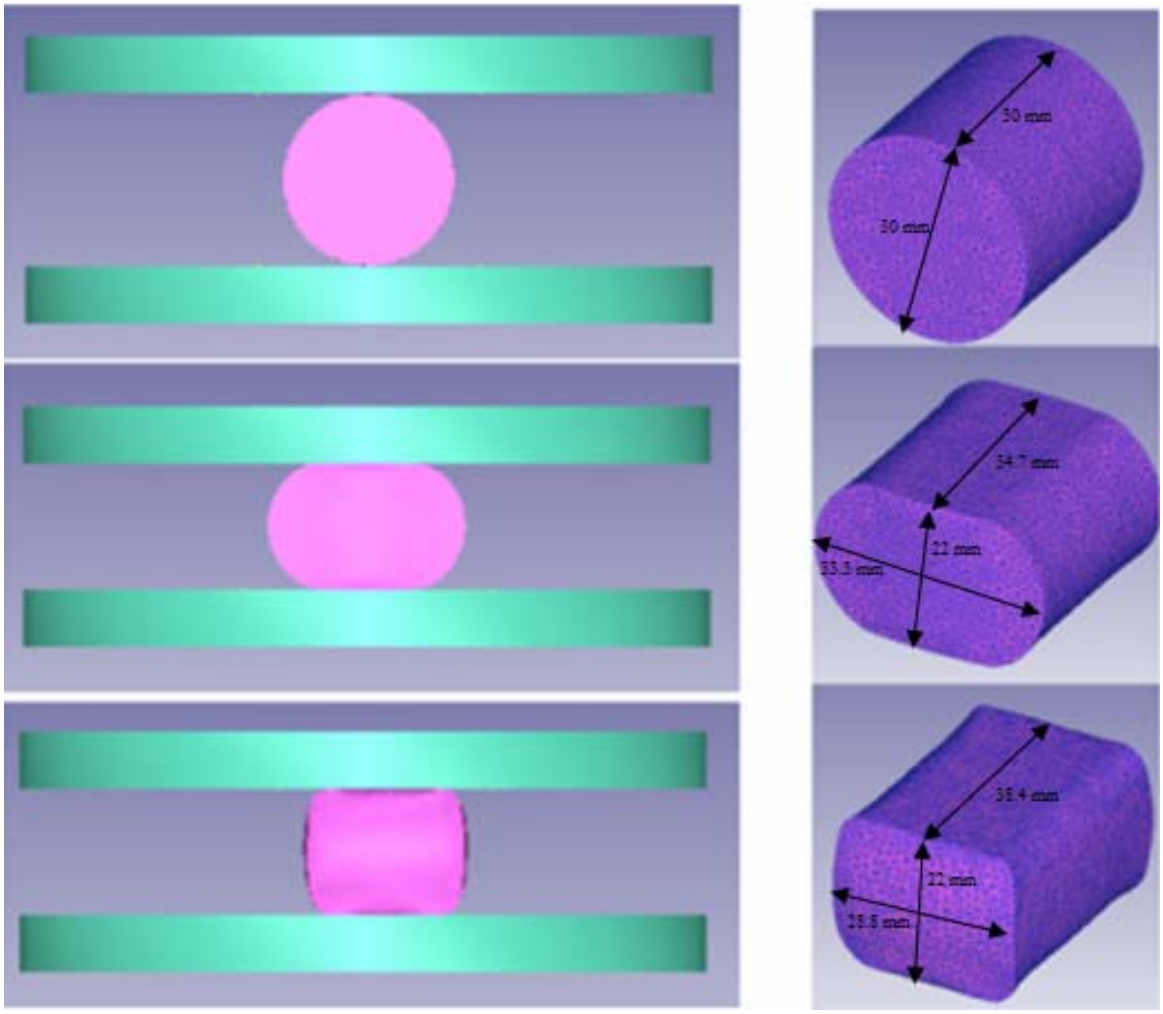

Figure 4.9 Geometry and Dimensions of the Billet After the Upsetting Stages.

4.1.2.5.2 Preform Stage

The residual stress and the temperature distribution obtained at the end of the preform stage are shown in Figure 4.10 and Figure 4.11. The equivalent stress distribution obtained at the maximum stoke are given in Figure 4.12 for the upper die and Figure

4.13 for the lower die. The temperature distributions for upper and lower die are given in Figure 4.14.

It is observed that maximum value of the residual stress is 78 MPa and maximum temperature of 1168 °C is obtained after the preform stage.

The maximum equivalent stress on the upper preform die is around the edges of the hexagonal protrusion and has a value of 551 MPa which is lower than the yield strength of the die material. In the lower die the maximum equivalent stress is 745 MPa which is also lower than the yield strength. No plastic deformation is observed in the preform stages.

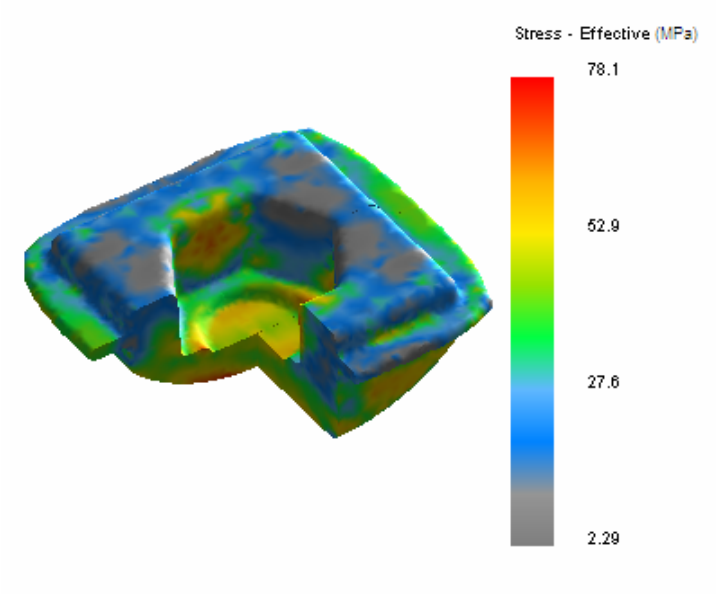

Figure 4.10 Residual Stress Values on the Preformed Part.

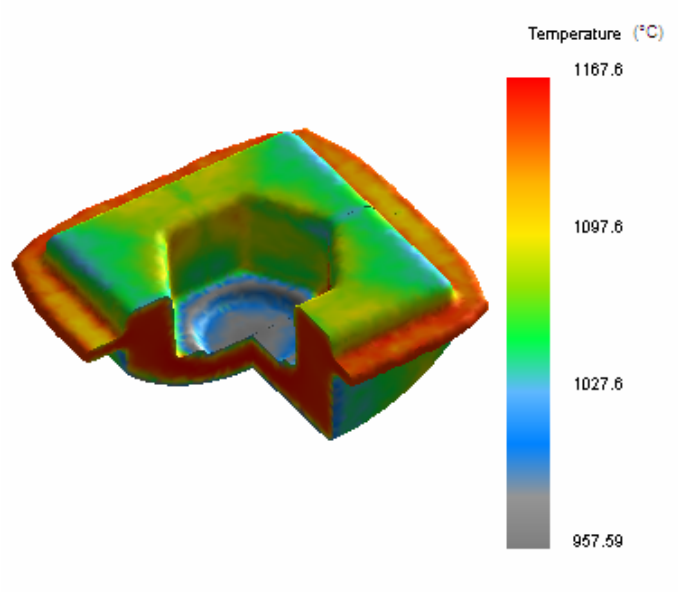

Figure 4.11 Temperature Distributions on the Preformed Part.

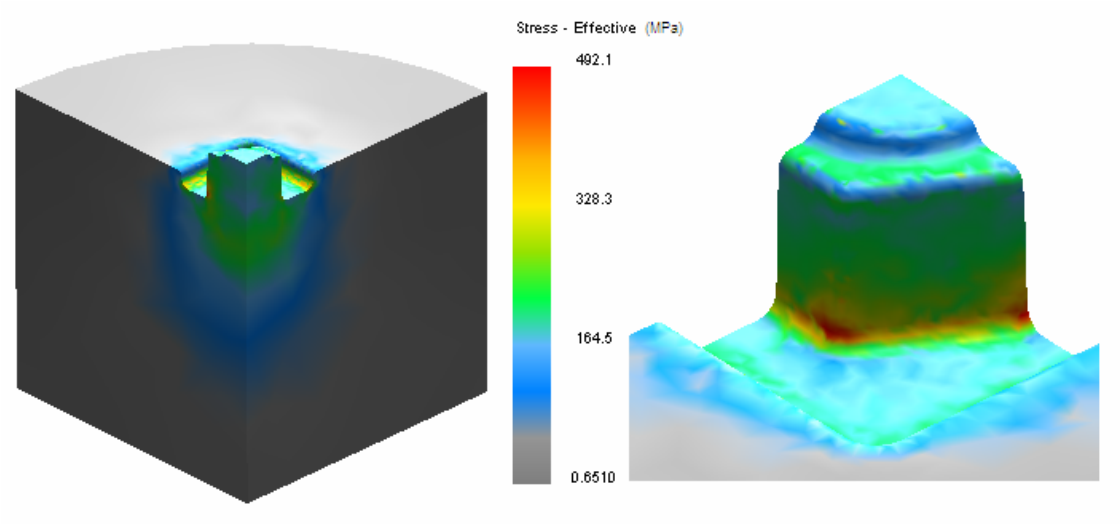

Figure 4.12 Maximum Equivalent Stress Distributions on the Upper Preform Die.

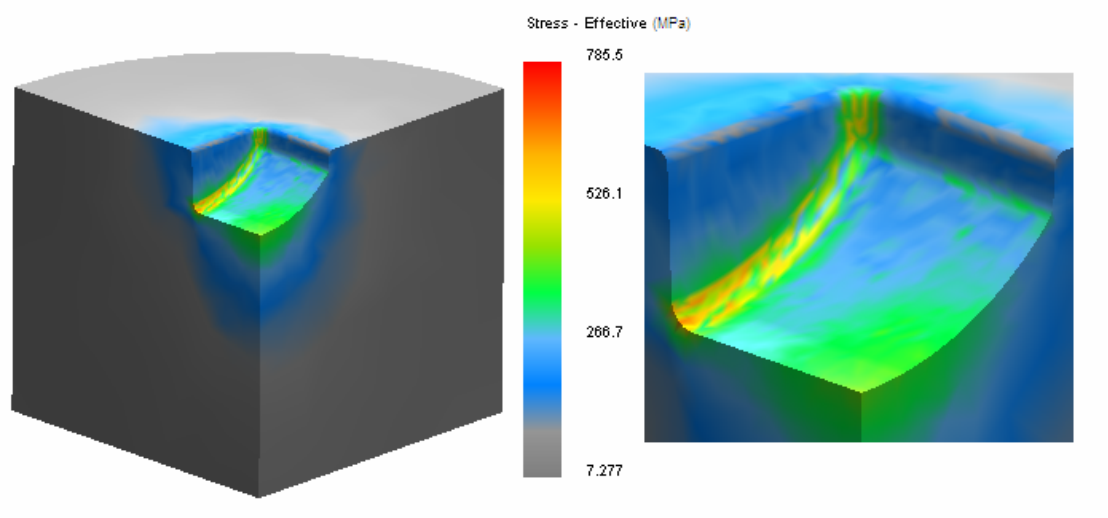

Figure 4.13 Maximum Equivalent Stress Distributions on the Lower Preform Die.

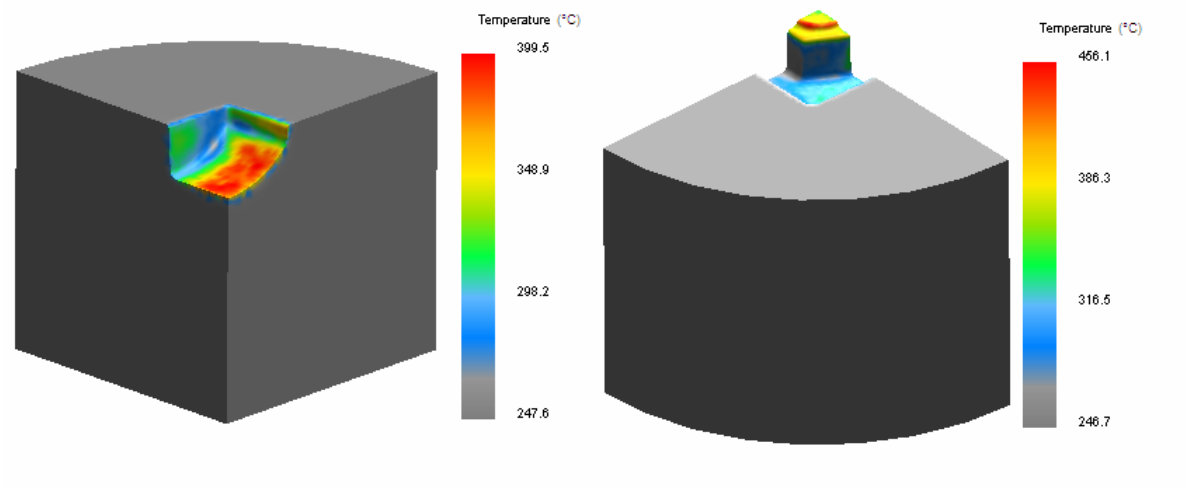

Figure 4.14 Temperature Distributions on the Upper and Lower Preform Die.

4.1.2.5.3 Finish Stage

The residual stress and the temperature distributions obtained at the end of the finish stage are shown in Figure 4.15 and Figure 4.16. The equivalent stress distribution obtained at the maximum stoke are given in Figure 4.17 for the upper die and Figure 4.18 for the lower die. Plastic strain values for the lower finish die are given in Figure 4.19. The temperature distributions for upper and lower die are given in Figure 4.20.

It is observed that the maximum value of the residual stress is 207.3 MPa and the maximum temperature of 1165 °C is obtained after the finish stage.

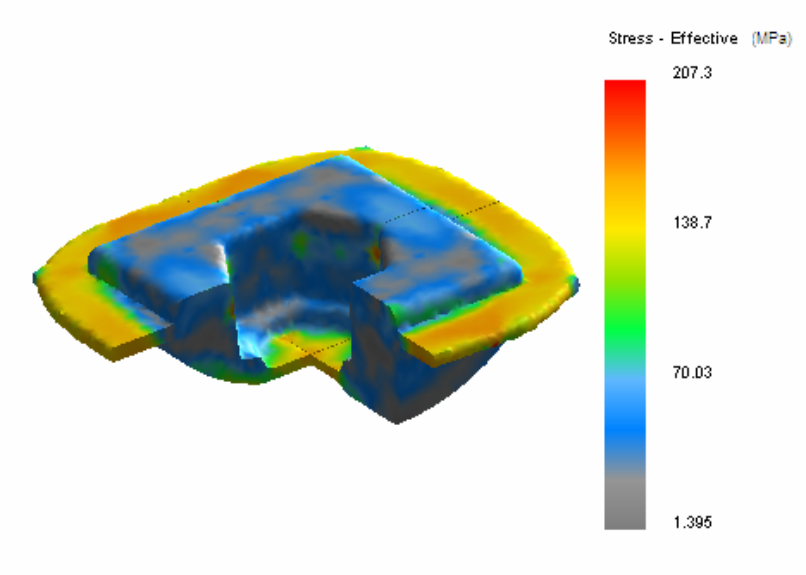

Figure 4.15 Residual Stresses on the Finished Part.

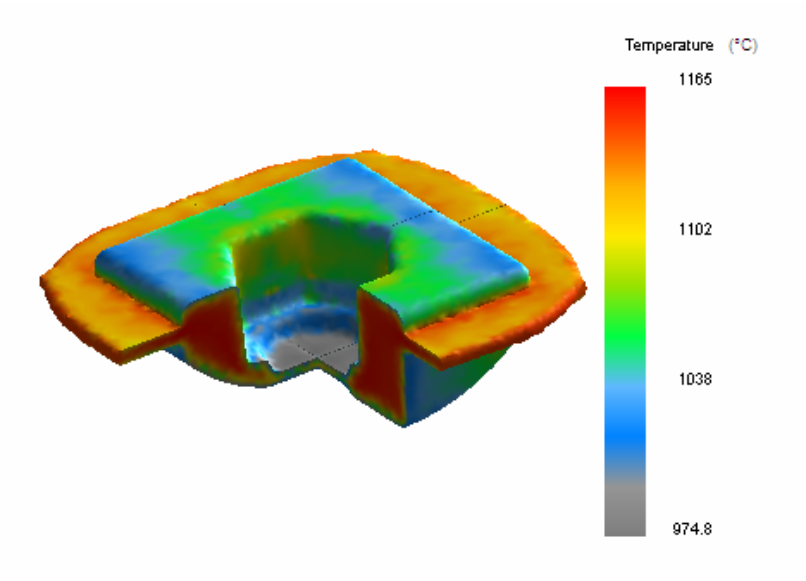

Figure 4.16 Temperature Distributions on Finished Part.

The maximum equivalent stress on the upper finish die is 767.6 MPa and on the lower finish die is 904.5 MPa. The maximum equivalent stress in lower finish die is observed to be above the yield strength of the material. Hence plastic deformation is expected to occur in the die. In the upper finish die no plastic deformation is observed. From the simulation results, it is clear that the amount of flash is quite high. Also it is observed that the flash distributions in the preform and finish parts are similar to the formed parts. In the simulations billet is located at the desired place between dies, during the production, the billet can not be placed precisely and symmetrical flash distribution can not be obtained in the forged parts.

Results show that some modifications must be made to the dies and process sequence in order to reduce stresses on the dies.

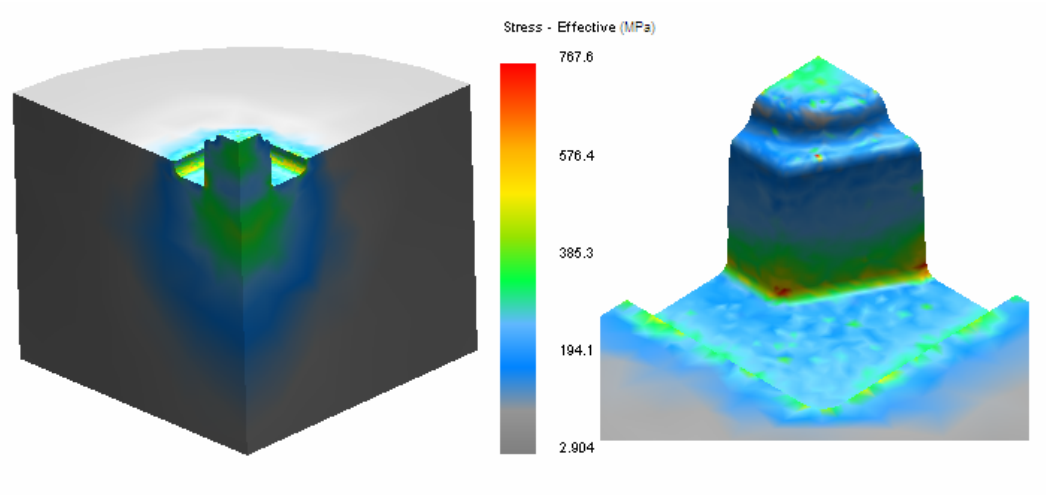

Figure 4.17 Maximum Equivalent Stress Distributions on the Upper Finish Die.

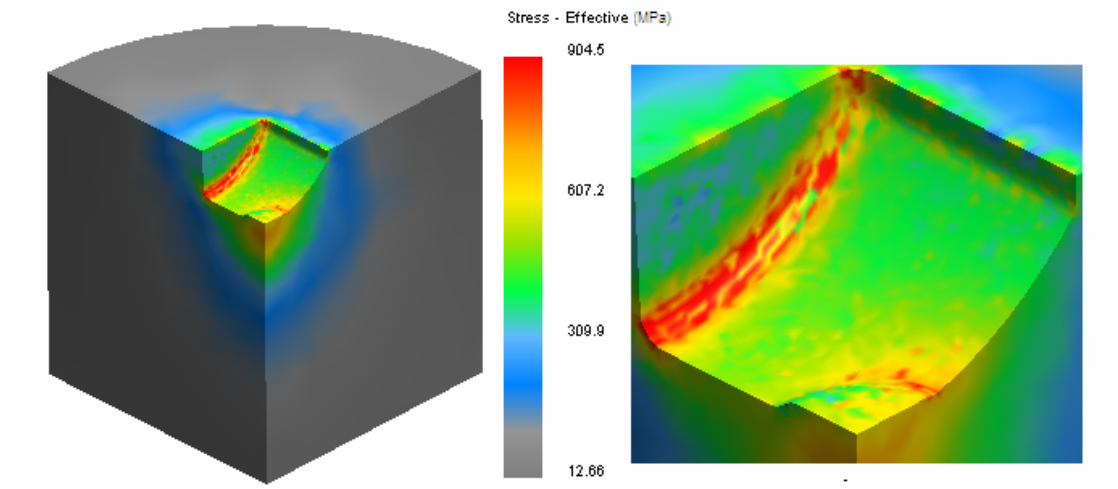

Figure 4.18 Maximum Equivalent Stress Distributions on the Lower Finish Die.

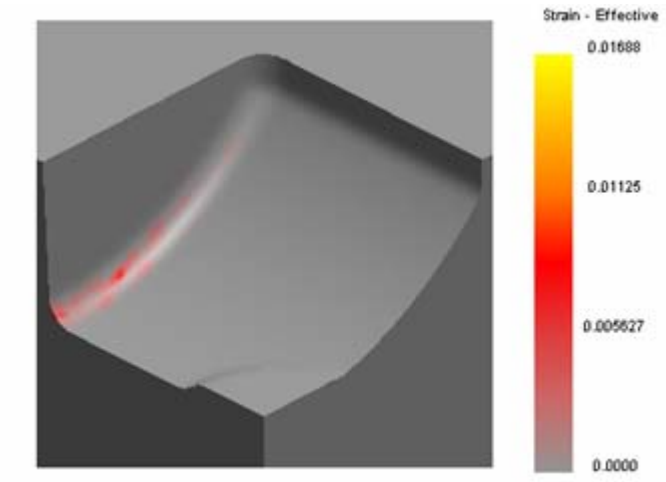

Figure 4.19 Plastic Strain on the Lower Finish Die.

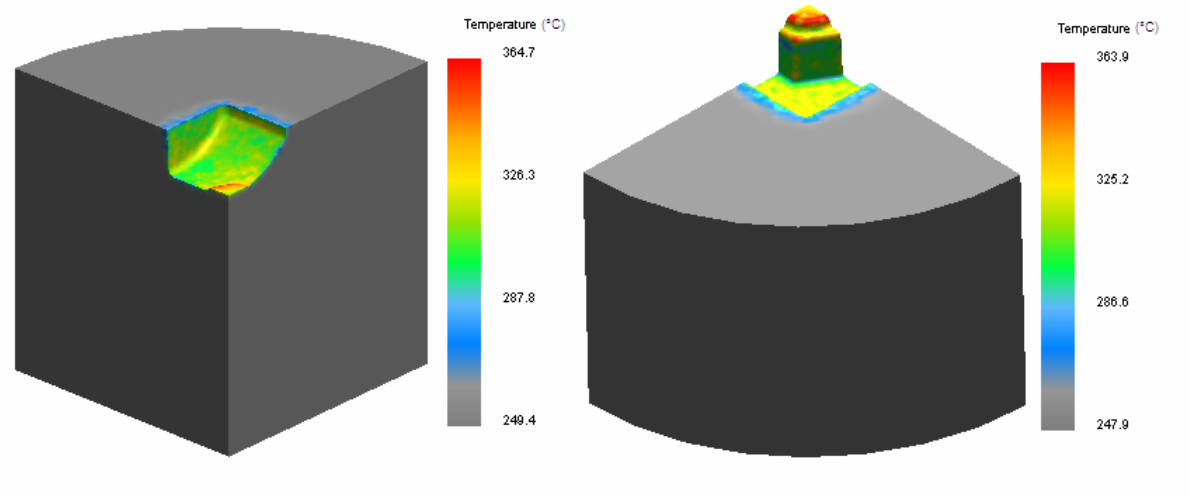

Figure 4.20 Temperature Distributions on the Lower and Upper Finish Die.

4.2 Proposed Method by Saraç [13]

In this section, finite element analysis results obtained by Deform 3D will be compared to the results of MSC Superform, previously done by Saraç [13]. In Saraç's study simulations were conducted at hot and semi-hot temperature ranges for proposed die sets and the practice in the factory with MSC Superform. Same die sets, initial billet, material and process conditions will be used for the analyses in Deform 3D. Results such as stress, strain and temperature distributions will be compared.

4.2.1 Modeling of Billet and Dies

The billet was designed to be 35 mm x 35 mm x 17 mm square billet. For the mesh of the quarter billet 29595 elements are used with an average edge length of 0.35 mm. The billet mesh is given in Figure 4.21.

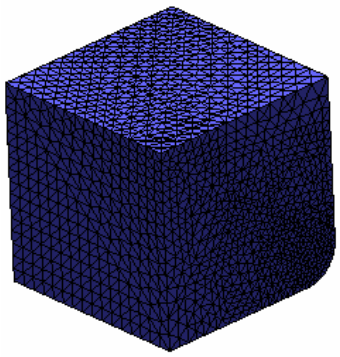

Figure 4.21 View of the Billet After Mesh Generation.

There are 21000 elements in the upper preform die, 28000 elements in the lower preform die, 31000 elements on upper finish die and 32500 elements on the lower

finish die. Views of the preform dies and finish dies are shown in Figure 4.22 and Figure 4.23, respectively.

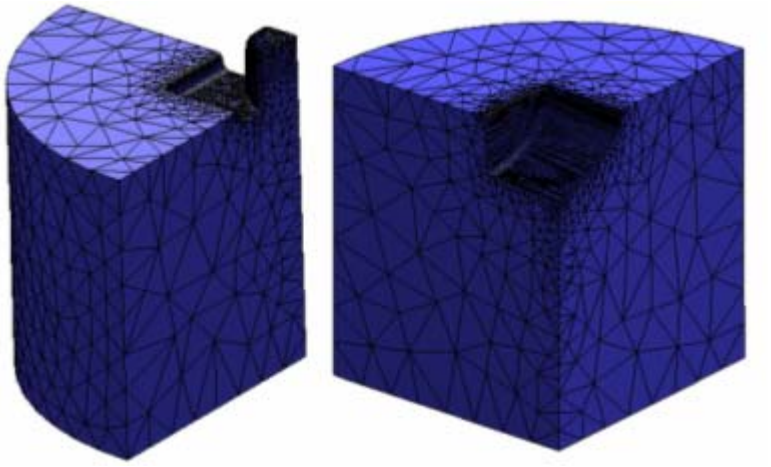

Figure 4.22 Views of the Preform Dies After Mesh Generation.

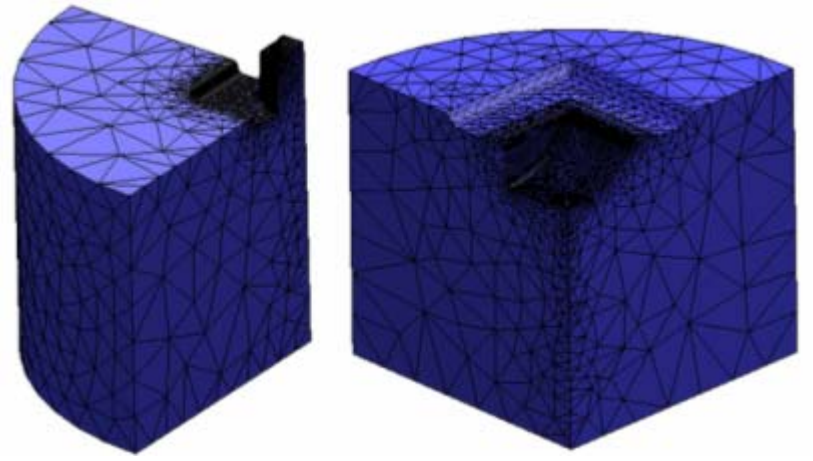

Figure 4.23 Views of the Finish Dies After Mesh Generation.

The preform and finish die dimensions are given in Appendix B.

Initial temperature for the billet is taken in the range 850 ºC – 1000 ºC at increments of 50 ºC and also 1150 ºC is used as the initial temperature in one of the runs. Initial temperatures for the dies are taken as 200 ºC.

4.2.2 Material Data

The workpiece material carbon steel AISI 1020. For the dies, material is Dievar which is a high performance chromium-molybdenum-vanadium alloyed hot work tool steel which offers a very good resistance to heat checking, gross cracking, hot wear and plastic deformation [38]. The mechanical and thermal properties of Dievar are tabulated in Table 4.5 and chemical composition is given in Table 4.6 [38]. Tensile properties at elevated temperatures are given in Figure 4.24. Since the elastic-plastic die stress analyses are conducted, flow curve of the material which has been obtained at different temperatures by Öztürk [18] is utilized.

Table 4.5 Mechanical and Thermal Properties of Dievar [38].

Temperature (°C)	20	400	600
Density (kg/cm³)	7800	7700	7600
Modulus of Elasticity (MPa)	210000	180000	145000
Tensile Strength, R_m (MPa)	1480	1290	905
Yield Strength, $R_{p0.2}$ (MPa)	1210	1025	655
Coefficient of Thermal Expansion (1/°C)	-	12.7 x 10-6	13.3 x 10-6
Thermal Conductivity (W/m°C)	-	31	32

Table 4.6 Chemical Composition of Dievar [38].

	C %	Si %	Mn %	Cr %	Mo %	V %
Dievar	0.35	0.20	0.50	5.00	2.30	0.60

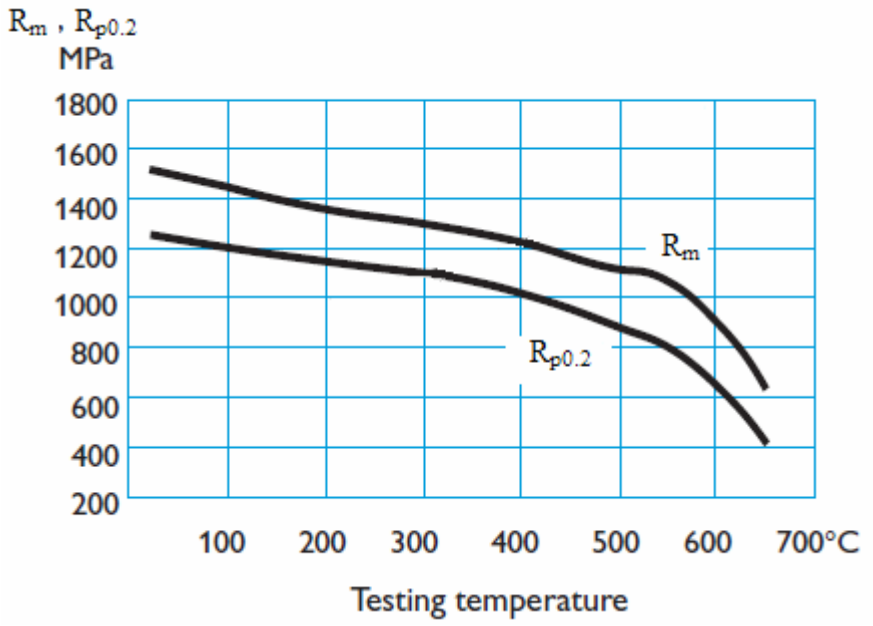

Figure 4.24 Tensile Properties of Dievar at Elevated Temperatures [38].

4.2.3 Friction and Press Parameters

The friction factor is assumed as 0.3 for hot forging temperature range and as 0.25 for semi-hot forging temperature range [6, 32].

In the analyses, 1000 ton mechanical press is used. The parameters to specify the movement of the press are taken as:

1. Displacement for the mechanical press is 110 mm.
2. Strokes per time is 100 rpm.
3. Current die stroke is taken as 106.2 mm for preform stage since the flash thickness is 2.2 mm and 105.5 for finishing stage since the flash thickness for this stage is 2 mm.
4. Connecting rod length is specified as 750 mm.

Maximum primary die displacement of 110 mm is defined for the stopping criterion.

4.2.4 Visualization of Finite Element Results

The maximum equivalent stress, temperature and the maximum equivalent plastic strain distributions for the preform and finish dies, the residual stresses on the preformed and finished part are presented. As an example the results are shown for initial billet temperature of 850 °C in Figures 4.25-4.36.

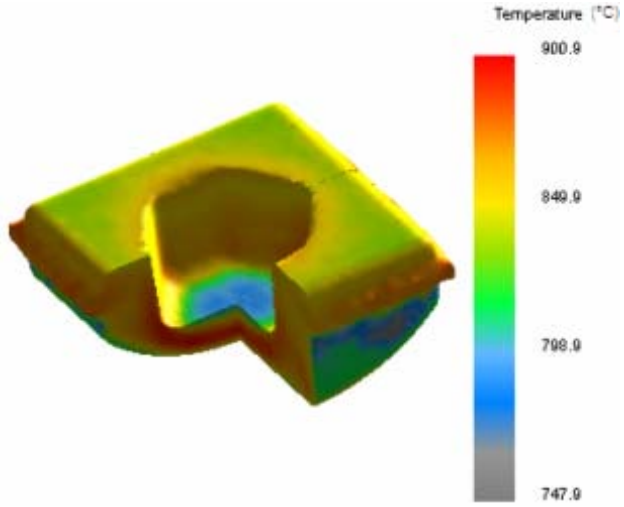

Figure 4.25 Temperature Distributions for Billet Temp. of 850 °C.

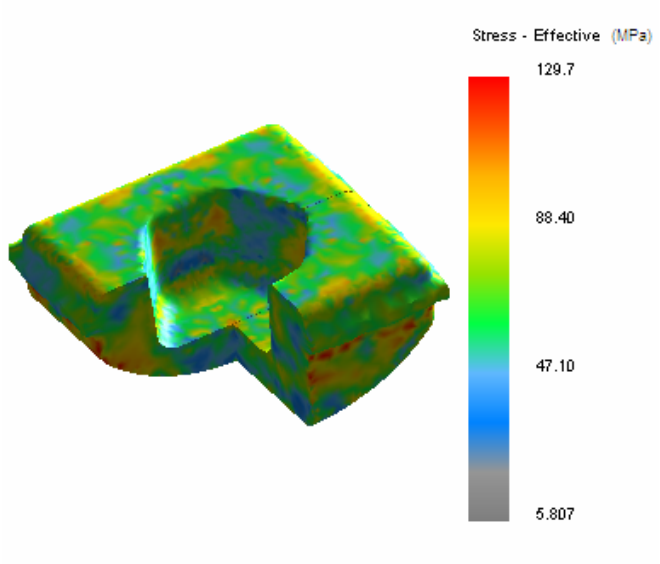

Figure 4.26 Residual Stresses on the Preformed Part for Billet Temp. of 850 °C.

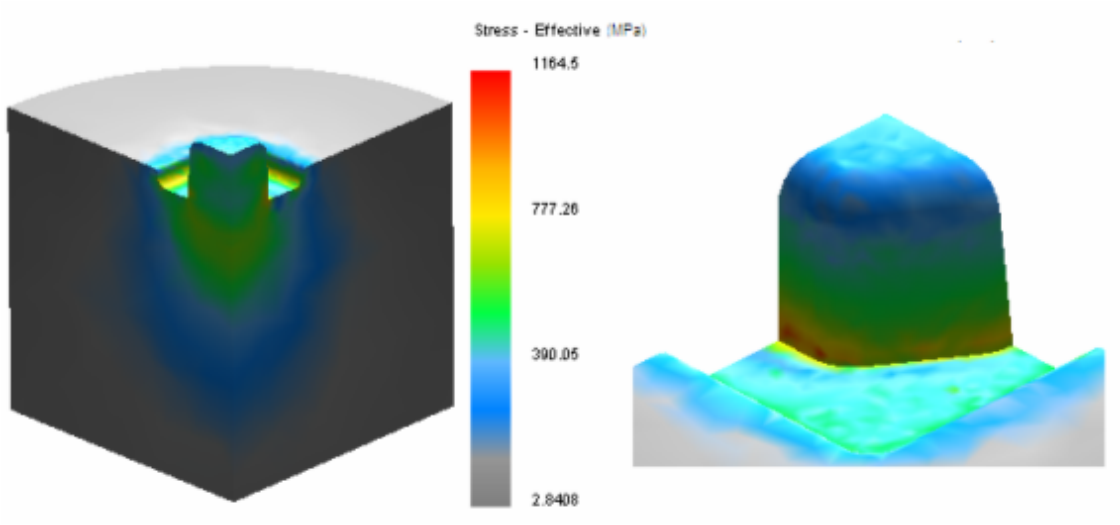

Figure 4.27 Max. Equiv. Stress Distributions on the Upper Preform Die for Billet Temp. of 850 °C.

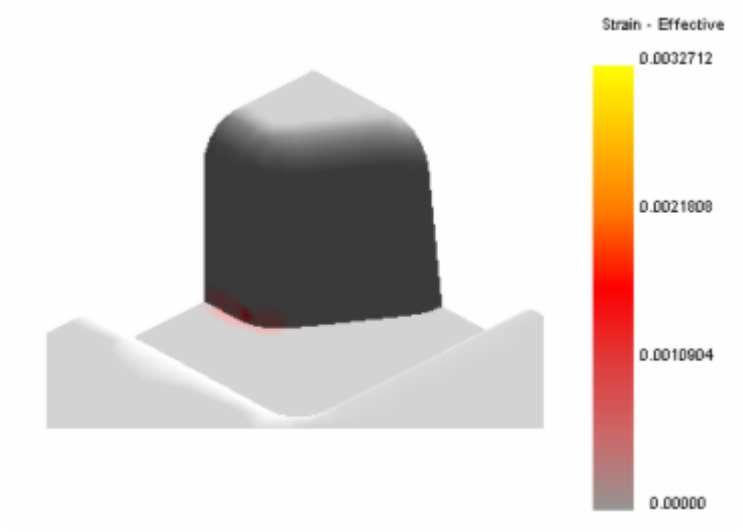

Figure 4.28 Plastic Strain on the Upper Preform Die for Billet Temp. of 850 °C.

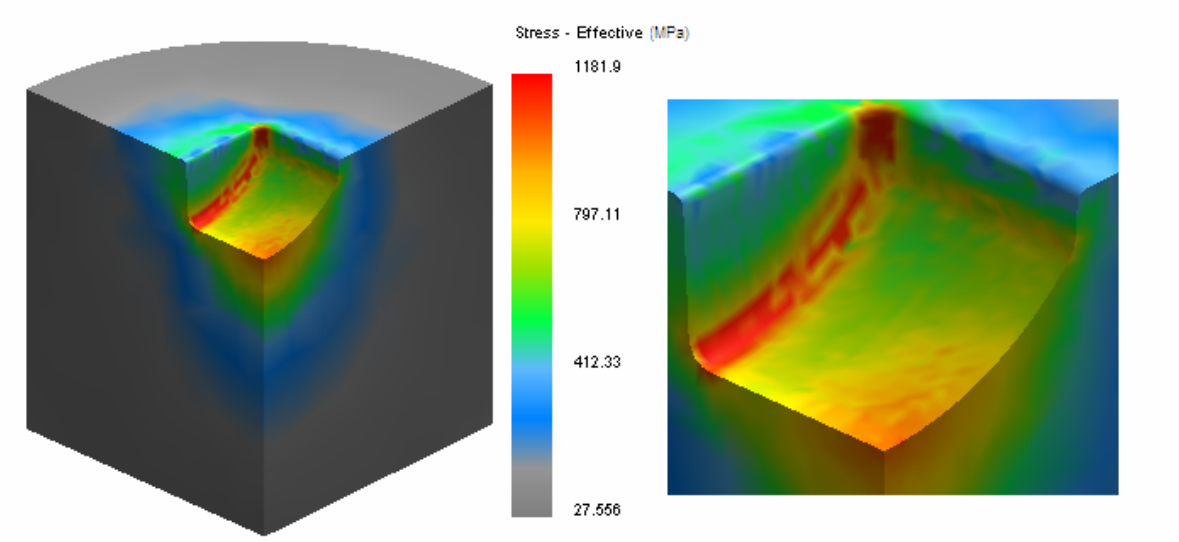

Figure 4.29 Max. Equiv. Stress Distributions on the Lower Preform Die for Billet Temp. of 850 °C.

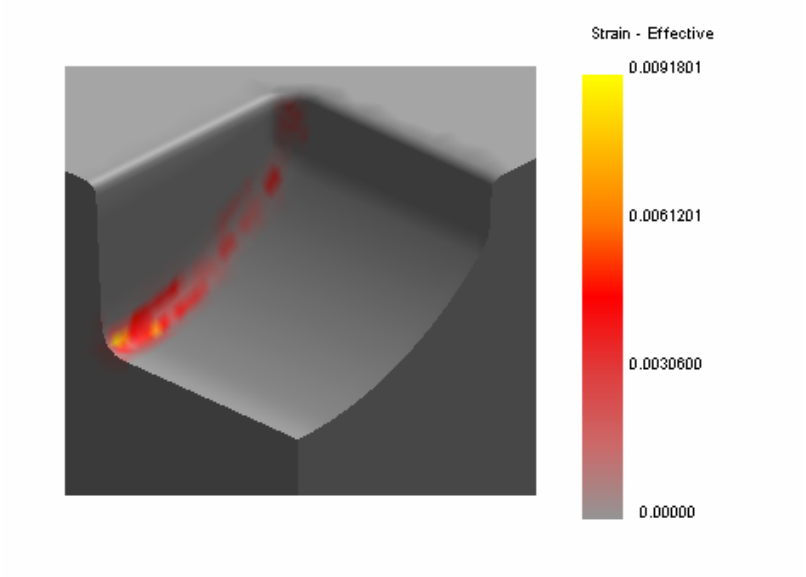

Figure 4.30 Plastic Strain on the Lower Preform Die for Billet Temp. of 850 °C.

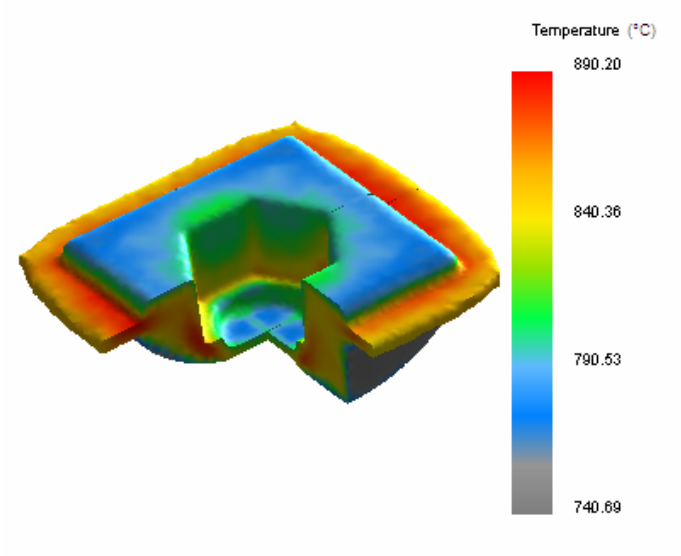

Figure 4.31 Temp. Distributions on the Finished Part for Billet Temp. of 850 °C.

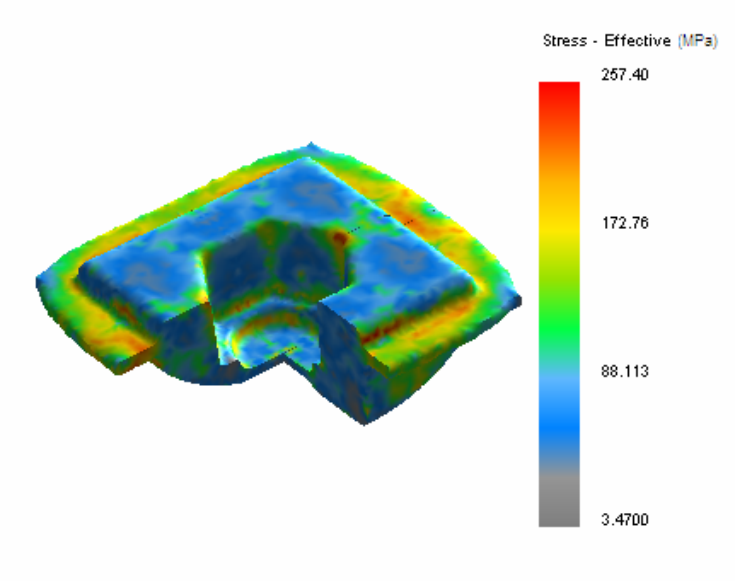

Figure 4.32 Residual Stresses on the Finished Part for Billet Temp. of 850 °C.

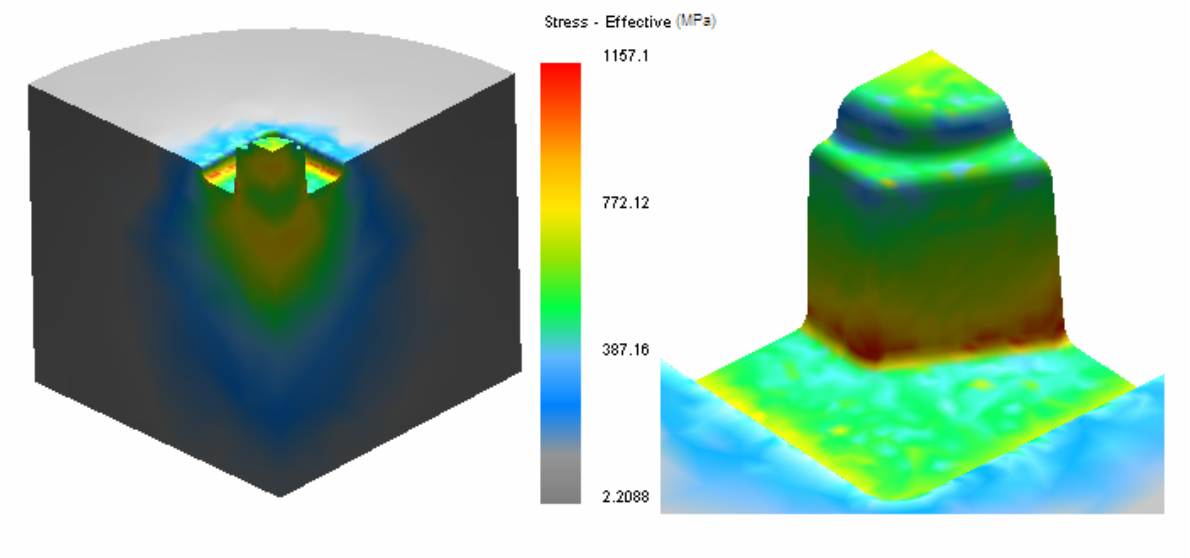

Figure 4.33 Max. Equiv. Stress Distributions on the Upper Finish Die for Billet Temp. of 850 °C.

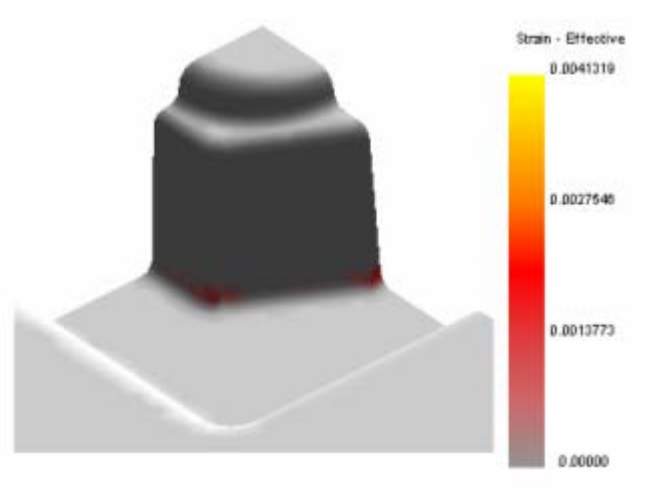

Figure 4.34 Plastic Strain on the Upper Finish Die for Billet Temp. of 850 °C.

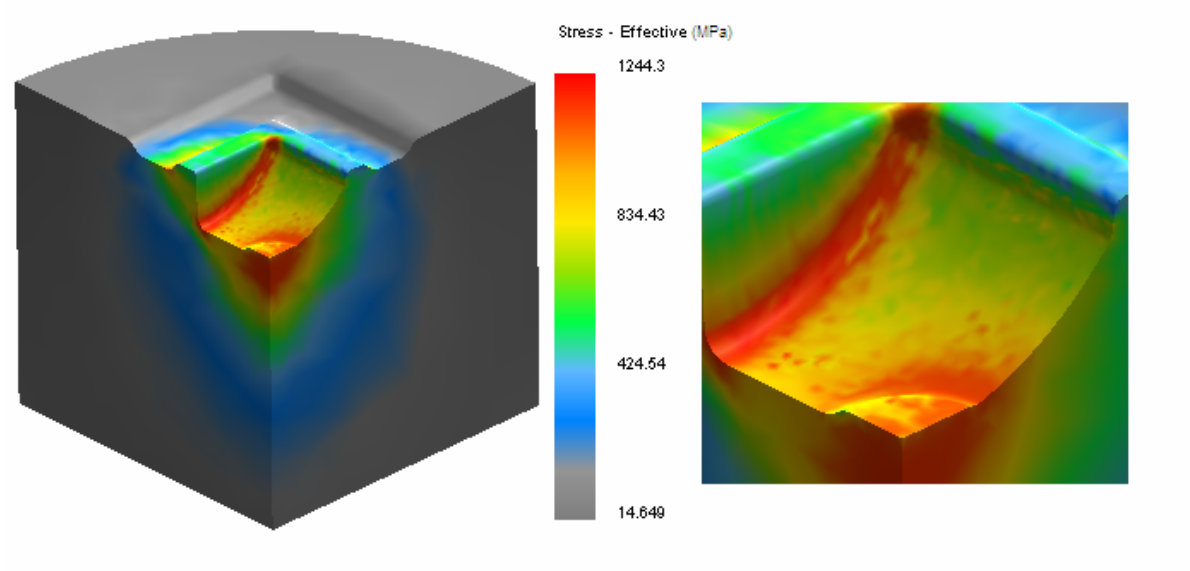

Figure 4.35 Max. Equiv. Stress Distribution on the Lower Finish Die for Billet Temp. of 850 °C.

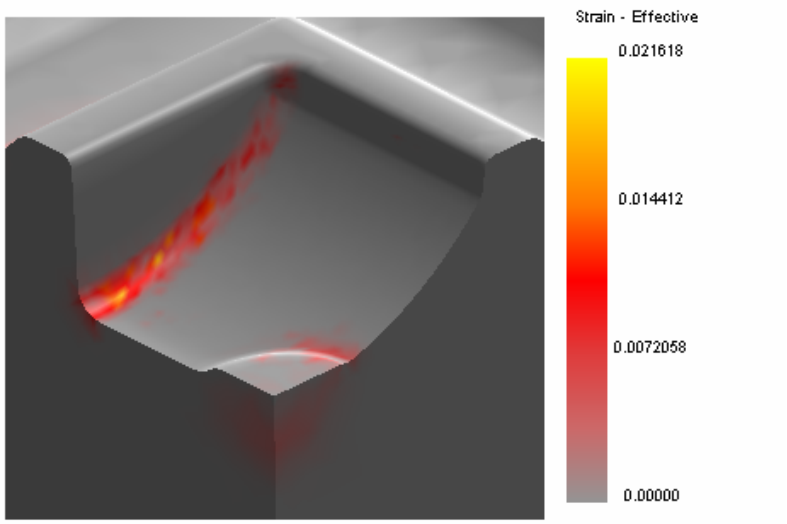

Figure 4.36 Plastic Strain on the Lower Finish Die for Billet Temp. of 850 °C.

4.2.5 Discussion of the Finite Element Results

From the simulation results, it is observed that the stress and temperature distributions occur at the similar locations on the preform and finish dies for different billet temperatures. As the temperature of the billet decreases, equivalent stress values increases in the dies.

For the billet temperature of 1150 °C, the maximum equivalent stresses on the preform dies are 484 MPa for upper die and 732 MPa for the lower die. For the finish dies the values are 603 MPa for the upper and 913 MPa for the lower die. The values are lower than the yield strength of proposed die material whereas higher than the die material used in the current practice in the factory.

For the billet temperature of 1000 °C, the maximum equivalent stress on the lower finish die exceeds the yield strength of the die material. Plastic strains are observed on the lower finish die by Deform 3D, whereas MSC Superform showed no plastic deformation.

In the simulations for the billet temperatures of 950 °C and below, maximum equivalent stress values exceeding the yield strength of the material are observed on the finish dies similar to the results of MSC Superform. Also it is observed that maximum stresses and temperature occur at similar locations with the results of MSC Superform for the simulated billet temperatures. These locations are the round and middle sections of the cavity for the lower dies and bottom of the hexagonal protrusion for the upper dies.

For the billet temperature of 900 °C, plastic deformation is observed on the upper finish die by Deform 3D, whereas MSC Superform showed no plastic deformation. For the lower finish dies both programs predicts plastic deformation.

For the billet temperature of 850 °C, local plastic deformation is observed on the finish dies by both programs. Also plastic deformation is predicted on the upper and lower preform dies by Deform 3D.

From comparison of Deform 3D and MSC Superform analyses, it is observed that the equivalent stress, equivalent plastic strain and the temperature distributions are in good agreement with each other in elastic deformation range for both billet and the dies.

The comparisons of the results are given in Table 4.7 for the proposed dies by Saraç and in Table 4.8 for the dies of current practice in the factory. In Saraç's [13] study, since the dies are elastic bodies, the values that are exceeding the yield strength of the die material were not given.

Table 4.7 Comparisons of the Results for the Dies and the Parts.

	Deform 3D	**MSC Superform [13]**	**Deform 3D**	**MSC Superform [13]**	**Deform 3D**	**MSC Superform [13]**
Billet Temperature (°C)	1150		1000		950	
Max. Equiv. Stress on Upper Preform Die (MPa)	483.7	468.06	730.8	715.51	817.8	795.11
Max. Equiv. Stress on Lower Preform Die (MPa)	732.1	690.25	936.9	919.67	963.7	940.69
Max. Equiv. Stress on Upper Finish Die (MPa)	602.8	578.29	862.8	807.44	983.2	950.17
Peak Temperature on Upper Finish Die (°C)	448.2	452.51	417.1	414.90	392.5	400.21
Max. Equiv. Stress on Lower Finish Die (MPa)	913.4	885.64	1163.0	1109.46	1184.8	***
Peak Temperature on Lower Finish Die (°C)	498.8	505.32	460.2	458.42	424.9	437.32
Plastic Equiv. Strain on Upper Preform Die	-	-	-	-	-	-
Plastic Equiv. Strain on Lower Preform Die	-	-	-	-	-	-
Plastic Equiv. Strain on Upper Finish Die	-	-	-	-	-	-
Plastic Equiv. Strain on Lower Finish Die	-	-	0.0073	-	0.0115	***
Residual Stress on Preformed Part (MPa)	71.7	69.90	82.4	78.00	93.9	83.00
Peak Temp. on Preformed Part (°C)	1160.0	1168.71	1029.4	1024.00	983.7	978.00
Residual Stress on Finished Part (MPa)	152.1	180.54	210.3	224.00	217.6	235.00
Peak Temp. on Finished Part (°C)	1132.3	1124.21	1003.1	995.00	990.5	982.00

** Yield Strength is exceeded.

Table 4.7 Comparisons of the Results for the Dies and the Parts [cont'd].

	Deform 3D	**MSC Superform [13]**	**Deform 3D**	**MSC Superform [13]**
Billet Temperature (°C)	900		850	
Max. Equiv. Stress on Upper Preform Die (MPa)	947.9	933.58	1164.5	1025.73
Max. Equiv. Stress on Lower Preform Die (MPa)	987.2	963.60	1181.9	1168.56
Max. Equiv. Stress on Upper Finish Die (MPa)	1144.8	1133.91	1157.1	***
Peak Temperature on Upper Finish Die (°C)	372.0	392.00	375.1	382.00
Max. Equiv. Stress on Lower Finish Die (MPa)	1209.4	***	1244.3	***
Peak Temperature on Lower Finish Die (°C)	407.2	424.00	399.8	410.00
Plastic Equiv. Strain on Upper Preform Die	-	-	0.0033	-
Plastic Equiv. Strain on Lower Preform Die	-	-	0.0092	-
Plastic Equiv. Strain on Upper Finish Die	0.0030	-	0.0041	***
Plastic Equiv. Strain on Lower Finish Die	0.0164	***	0.0216	***
Residual Stress on Preformed Part (MPa)	133.3	90.00	129.7	115.00
Peak Temp. on Preformed Part (°C)	939.2	932.00	900.9	886.00
Residual Stress on Finished Part (MPa)	221.3	236.00	257.4	262.00
Peak Temp. on Finished Part (°C)	945.5	935.00	890.2	846.00

*** Yield Strength is exceeded.

For all billet temperatures, maximum temperature locations on the dies are similar. Both programs results are in good agreement with each other. Higher temperature values are in locations which are in contact with the workpiece longest.

Table 4.8 Comparison of Results for the Current Practice.

	Results from MSC Superform [13]	Results from Deform 3D
Max. Equiv. Stress Upper Preform Die (MPa)	485	492.1
Max. Equiv. Stress Lower Preform Die (MPa)	800	785.5
Max. Equiv. Stress Upper Finish Die (MPa)	745	767.6
Max. Equiv. Stress Lower Finish Die (MPa)	***	904.5
Residual Stress on Preformed Part (MPa)	79	78.1
Residual Stress on Finished Part (MPa)	275	207.3

*** Yield Strength is exceeded

4.3 Proposed Forging Process

From the analyses results, it is observed that below the billet temperature of 1000 °C, plastic deformation occurs in the lower finish die for the proposed forging sequence of Saraç [13]. Also it is observed that further flash reduction is possible. In this section solutions to these problems will be proposed.

In current practice a rectangular shaped part is obtained from a round billet after the upsetting stages. Since the final product has a square dimensional shape and using a rectangular billet in forging operation results in non-uniform flash distribution. Also by using a square billet two upsetting stages are eliminated.

A rectangular billet of 34 mm x 34 mm x 17 mm is decided to be used after the computer simulations. In the current practice 33 grams of material is thrown away as scrap material. In the proposed forging process 11.8 grams of material is removed as excess material. A total of 12.1 % reduction in scrap material is obtained by reducing the billet material.

4.3.1 Finite Element Simulations of Proposed Forging Process,

In this section finite element analyses of the proposed forging process is presented.

4.3.1.1 Modeling of Billet and Dies

For the mesh of the billet 29712 elements are used with an average edge length of 0.35 mm. The preform and finish dies are the same with the previous analyses and the related data is given in section 4.2.1. Initial temperature for the billet is taken in the range 850 ºC – 1000 ºC at increments of 50 ºC and also 1150 ºC is used as the initial billet temperature. Initial temperature for the die is 200 ºC. Symmetry and heat exchange with environment are enforced at nodes in finite element mesh as the boundary conditions.

4.3.1.2 Material Data

The workpiece material is assigned as carbon steel AISI 1020. Die material are assigned as Dievar as given in Section 4.2.2. Both the workpiece and the dies are modeled as elastic-plastic bodies.

4.3.1.3 Press Parameters

In the analyses, 1000 ton mechanical press is defined. The parameters, to specify the movement of the press, are explained in Section 4.2.3. The flash thickness for preform stage is taken as 2.2 mm and for the finishing stage as 2 mm. Maximum primary die displacement of 110 mm is defined for the stopping criterion.

4.3.2 Discussion of Finite Element Results

The maximum temperature, equivalent stress and the residual stress results for the preform and finished part, the maximum equivalent stress, temperature, equivalent plastic strain and forging load results for the preform and finish dies are presented. As an example results are shown for billet temperature of 850 °C in Figures 4.37-4.50. In the figures for temperature and stress results, top and bottom values of the legend shows the maximum and minimum values of the results.

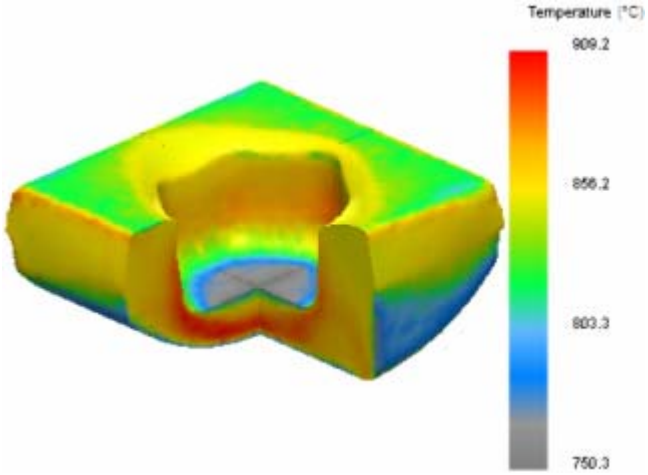

Figure 4.37 Temp. Distributions on the Preformed Part for Billet Temp. of 850 °C.

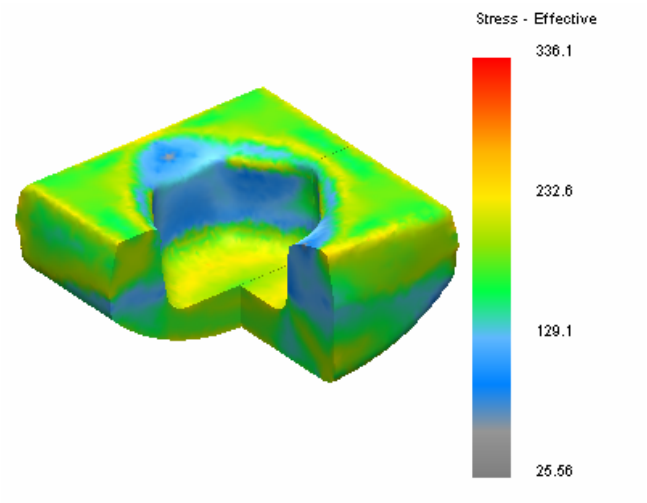

Figure 4.38 Max. Equiv. Stress Distributions on the Preformed Part for Billet Temp. of 850 °C.

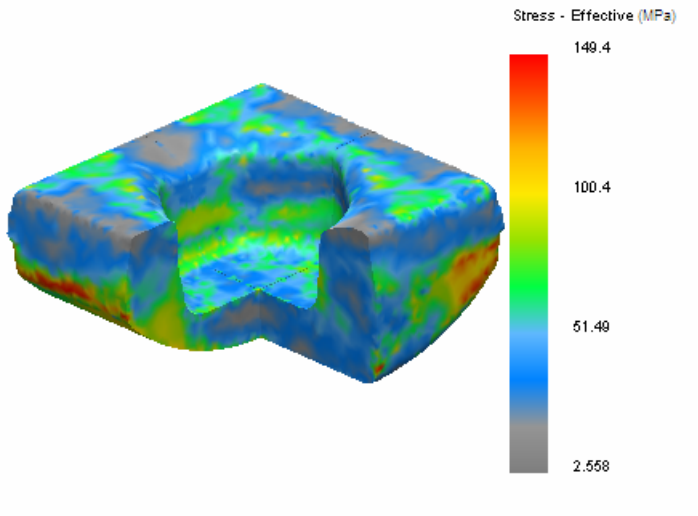

Figure 4.39 Residual Stresses on the Preformed Part for Billet Temp. of 850 °C.

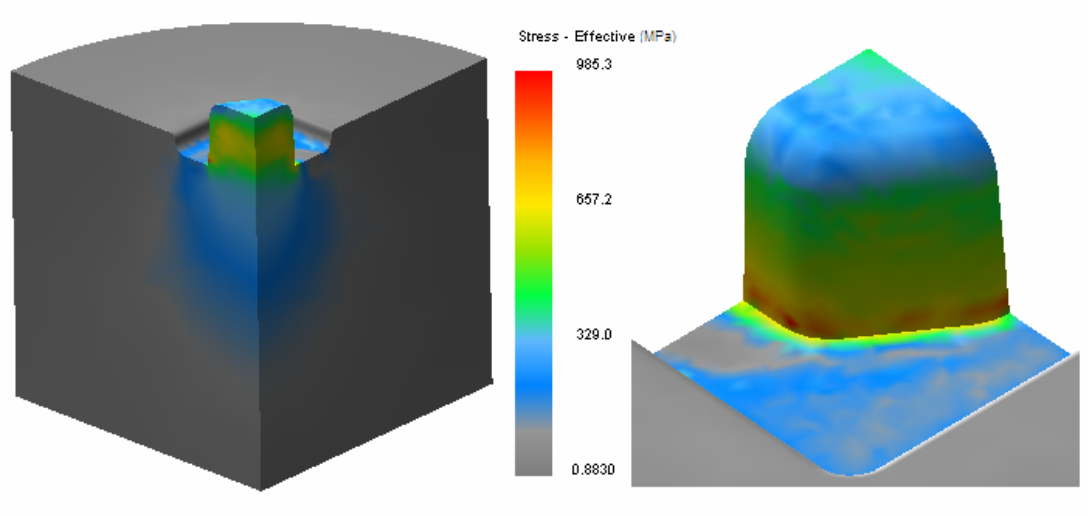

Figure 4.40 Max. Equiv. Stress Distributions on the Upper Preform Die for Billet Temp. of 850 °C.

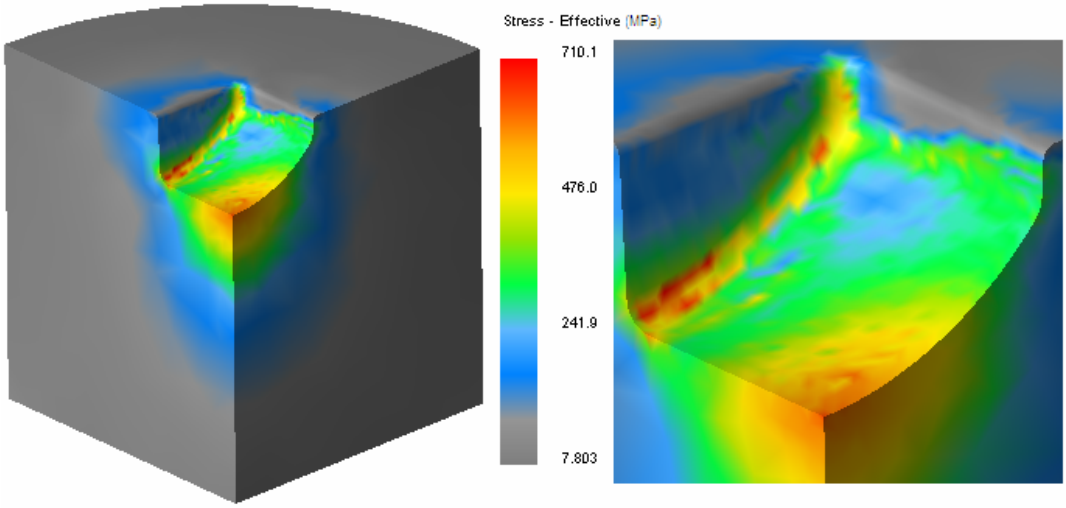

Figure 4.41 Max. Equiv. Stress Distributions on the Lower Preform Die for Billet Temp. of 850 °C.

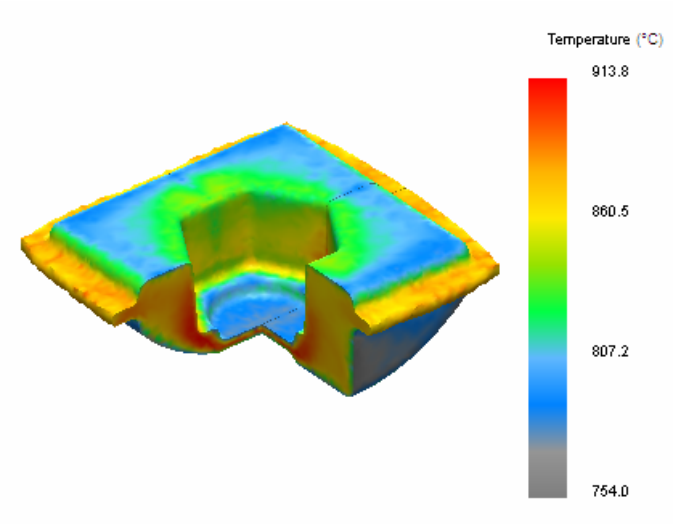

Figure 4.42 Temp. Distributions on the Finished Part for Billet Temp. of 850 °C.

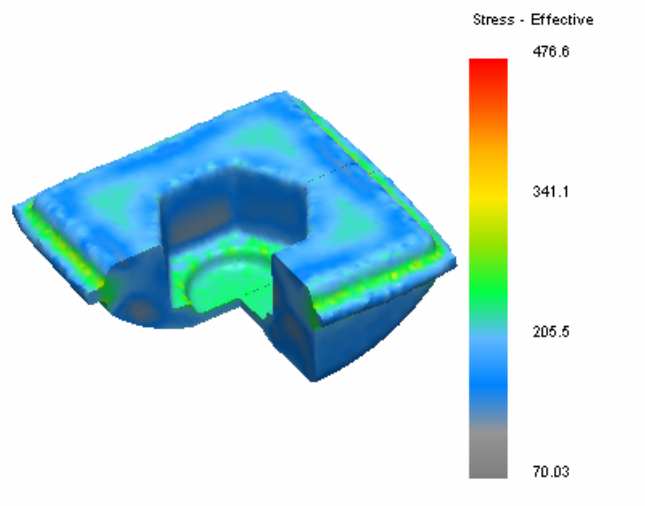

Figure 4.43 Max. Equiv. Stress Distributions on the Finished Part for Billet Temp. of 850 °C.

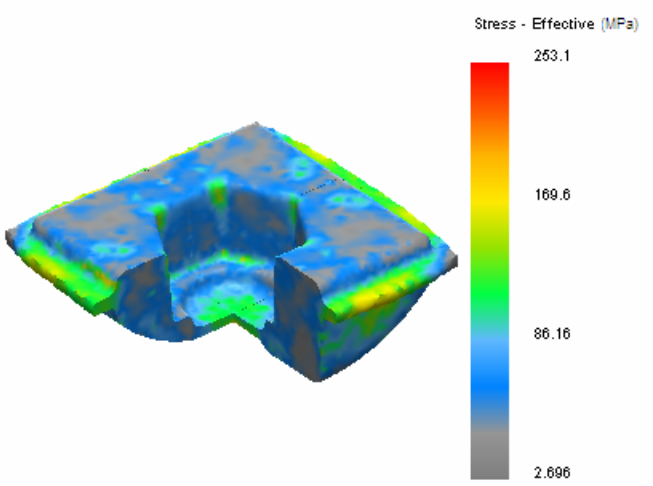

Figure 4.44 Residual Stresses on the Finished Part for Billet Temp. of 850 °C.

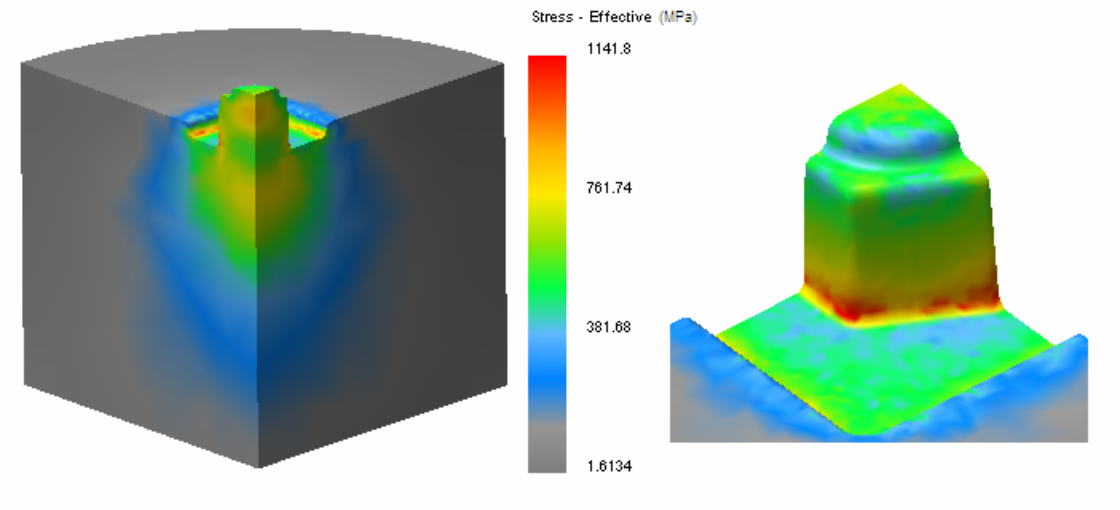

Figure 4.45 Max. Equiv. Stress Distributions on the Upper Finish Die for Billet Temp. of 850 °C.

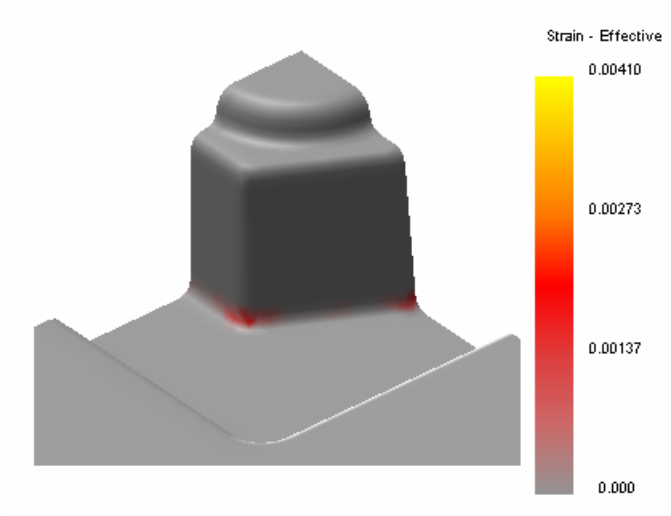

Figure 4.46 Plastic Strain on the Upper Finish Die for Billet Temp. of 850 °C.

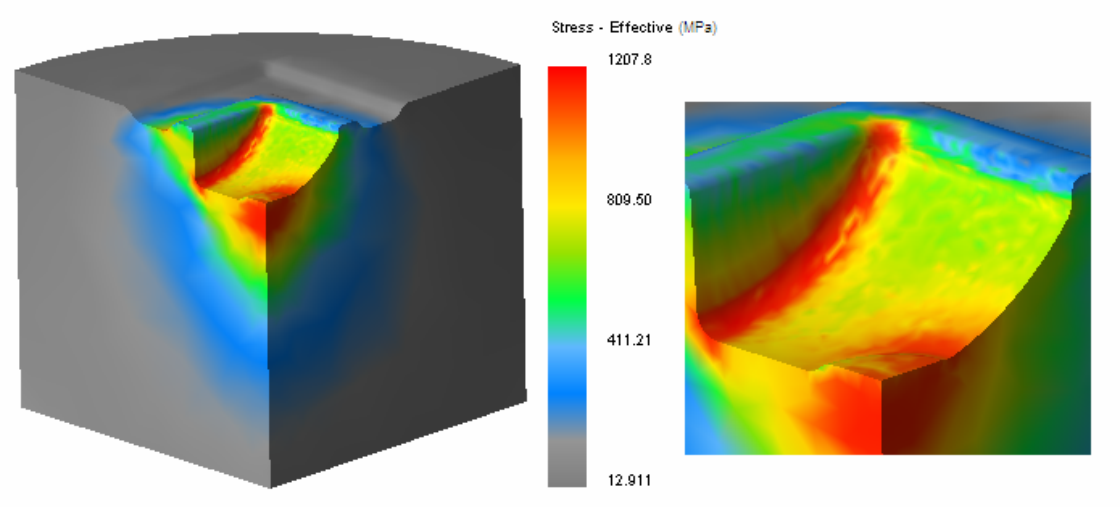

Figure 4.47 Max. Equiv. Stress Distributions on the Lower Finish Die for Billet Temp. of 850 °C.

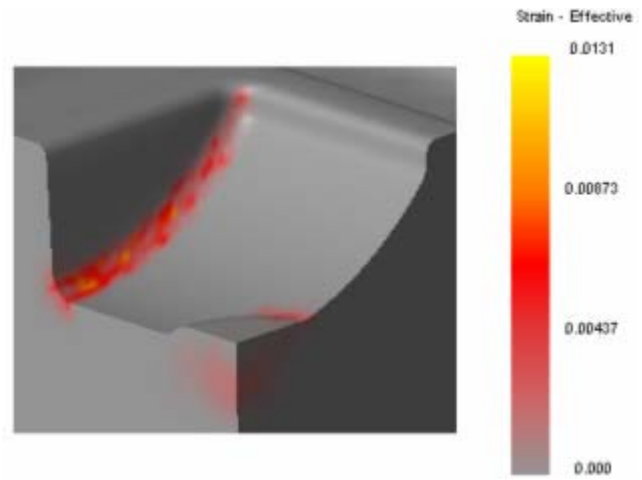

Figure 4.48 Plastic Strain on the Lower Finish Die for Billet Temp. of 850 °C.

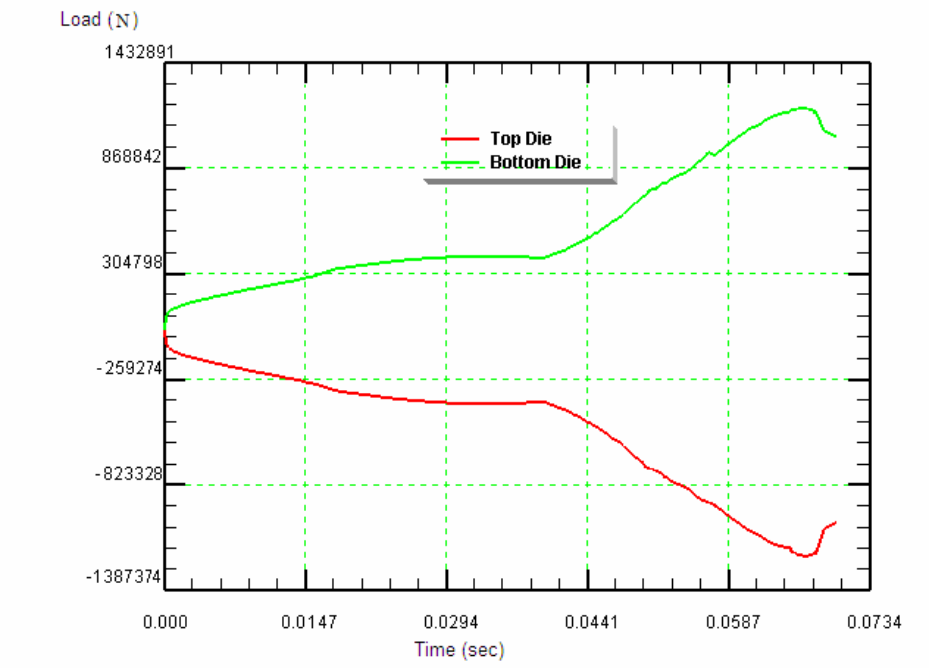

Figure 4.49 Load Curve for Preform Die for Billet Temp. of 850 °C.

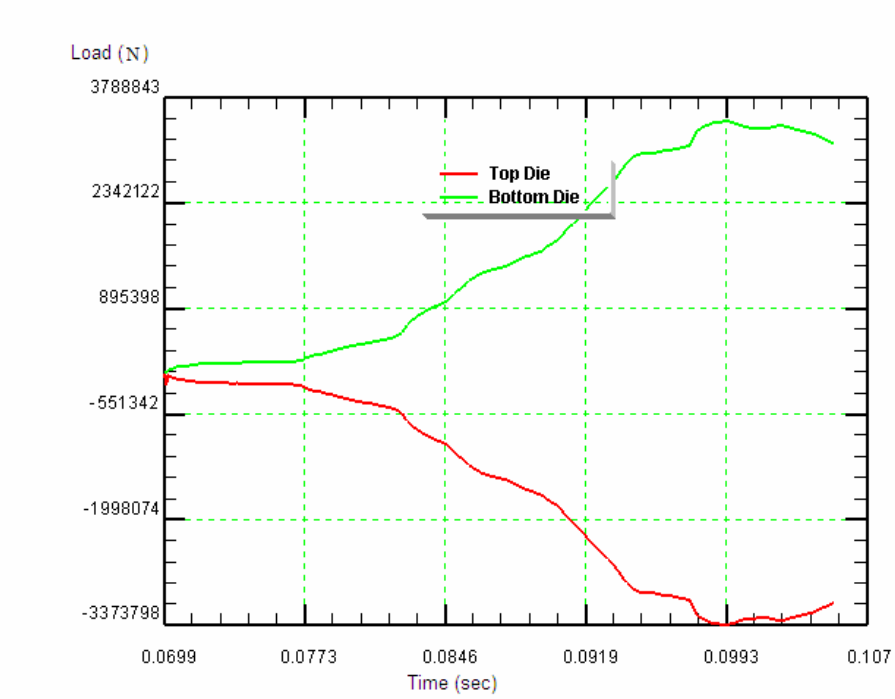

Figure 4.50 Load Curve for Finish Die for Billet Temp. of 850 °C.

The simulation results for all the temperatures show that the locations of maximum and minimum values of stress, strain and temperature are the similar but the numerical values are different. From the results it is observed that maximum stress and plastic strain locations are round section at the corner of the lower preform and finish dies and at the middle of the lower dies. For the upper preform and finish die maximum stress is located where the hexagonal extrusion starts. Higher temperature values are in locations where the dies contacts with workpiece longest.

The results for all billet temperatures analyzed are tabulated in Table 4.9.

Table 4.9 Simulation Results for the Proposed Forging Process.

Billet Temperature (°C)	1150	1000	950	900	850
Max. Equiv. Stress on Upper Preform Die (MPa)	430.0	668.2	792.3	923.8	985.3
Peak Temperature on Upper Preform Die (°C)	492.4	466.9	455.6	446.5	433.7
Max. Equiv. Stress on Lower Preform Die (MPa)	423.8	571.1	631.3	673.9	710.1
Peak Temperature on Lower Preform Die (°C)	438.4	412.3	401.5	392.8	384.3
Max. Equiv. Stress on Upper Finish Die (MPa)	588.3	840.3	976.4	1061.3	1141.8
Peak Temperature on Upper Finish Die (°C)	386.3	384.2	357.9	345.1	346.3
Max. Equiv. Stress on Lower Finish Die (MPa)	853.6	1132.4	1159.4	1183.4	1207.8
Peak Temperature on Lower Finish Die (°C)	401.2	376.9	371.3	357.5	360.1
Plastic Equiv. Strain on Upper Finish Die	-	-	-	0.0017	0.0041
Plastic Equiv. Strain on Lower Finish Die	-	0.0039	0.0091	0.0099	0.0131
Max. Load on Preform Die (ton)	62.2	72.5	85.0	99.0	116.0
Max. Load on Finish Die (ton)	137.0	240.0	271.0	302.0	344.0
Max. Equiv. Stress on Preformed Part (MPa)	176.10	246.69	281.06	297.54	336.1
Residual Stress on Preformed Part (MPa)	72.2	84.1	107.2	128.4	149.4
Peak Temp. on Preformed Part (°C)	1164.2	1031.9	983.8	942.2	909.2
Max. Equiv. Stress on Finished Part (MPa)	213.45	347.90	386.55	425.49	476.58
Residual Stress on Finished Part (MPa)	149.4	209.4	211.2	214.3	253.1
Peak Temp. on Finished Part (°C)	1128.8	998.2	986.6	943.0	913.8

Yield Strength is exceeded.

Simulation results show that, with the usage of proposed billet maximum equivalent stress values decreases at all temperatures. As expected, the maximum equivalent stress values and loads on the dies increase as the billet temperature is reduced. Similar to previous analyses, for the initial billet temperature of 1000 °C and below, plastic deformation occurs on the lower finish die. Plastic strain on the lower finish die reduces to 0.0039 from a value of 0.0073. Below initial billet temperature of 900 °C, plastic deformation on the upper finish die is also expected to occur according to the simulations. Different than previous analyses, for billet temperature of 850 °C, no plastic deformation is expected on the preform dies for the proposed billet.

From the simulation results it is observed that flash formation around the periphery of the finished part is reduced considerably compared to the current forging practice. Also there is no flash formation in the preform stage.

4.3.3 Finite Element Simulations of Preform Die Trials

In this section, preform die geometries are modified according to critical sections shown up by the results of the simulations performed. Critical dimensions are the radius of round at the tip of hexagonal extrusion (R_U), width (W) and height (H) of the hexagonal extrusion for the upper preform die and radius of the round (R_L) for the lower preform die (Figure 4.51). The dimensions used in the simulations, comparison of these values with Saraç's [13] study and forging process in the factory are given in Table 4.10. The materials and geometry of the finish dies are the same in the simulations.

Usage of 34 mm x 34 mm x 17 mm square billet in the previous simulations showed that the amount of flash is decreased and equivalent stress values on the dies are reduced. So in the preform trial simulations proposed billet is used.

Five different combinations of the parameters are used in the preform dies and initial billet temperature of 1000 °C is taken in all simulations for comparison.

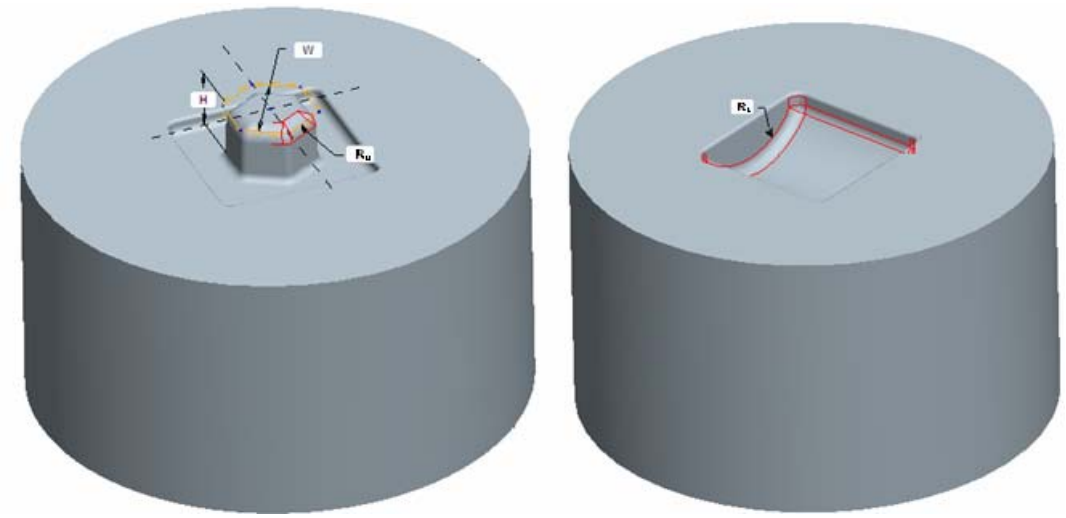

Figure 4.51 Parameters of Critical Dimensions for Upper and Lower Preform Die.

Table 4.10 Values of Preform Die Parameters used in simulations.

	Upper Preform Die			Lower Preform Die
	Radius of Round (R_U)	Width of hexagonal extrusion (W)	Height of hexagonal Extrusion (H)	Radius of Round (R_L)
Current Practice	1.5	21	13	2
Saraç's Study [13]	3	20.6	13	2
Trial 1	4	20.6	13	2
Trial 2	4	20.6	14	4
Trial 3	4	20.3	14.2	4
Trial 4	4	19.9	14.1	3
Trial 5	4	19.9	14.1	2

4.3.3.1 Modeling of Dies and Press Parameters

For each preform die, 3D models are prepared and then meshing is done similarly explained in Section 4.1.3. Approximately 22000 elements are used for each upper and lower preform dies. Initial temperature for the dies is taken as 200 ºC.

In the analyses, 1000 ton mechanical press is defined. The parameters, to specify the movement of the press, are taken as similarly explained in Section 4.2.3.

4.3.3.2 Finite Element Results and Discussion

The results such as maximum equivalent stress, strain, load and peak temperature values for the preform and finish dies, the maximum equivalent stress, temperatures and the residual for the preform and finished part are examined in the postprocessor. As an example results are shown for trial 4 in Figures 4.52-4.62.

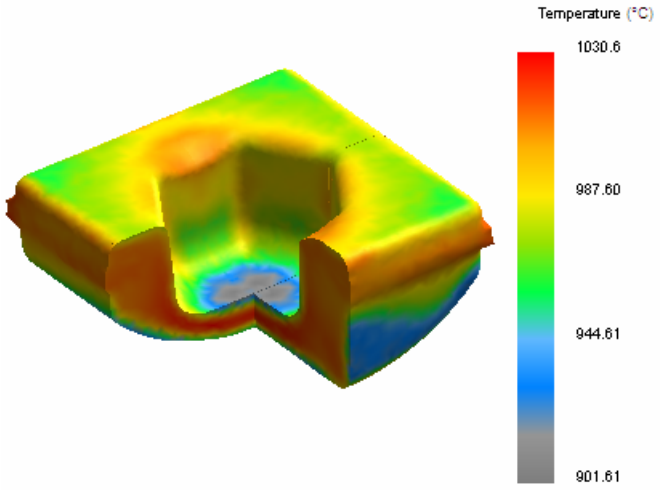

Figure 4.52 Max. Temperature Distributions on the Preformed Part for Trial 4.

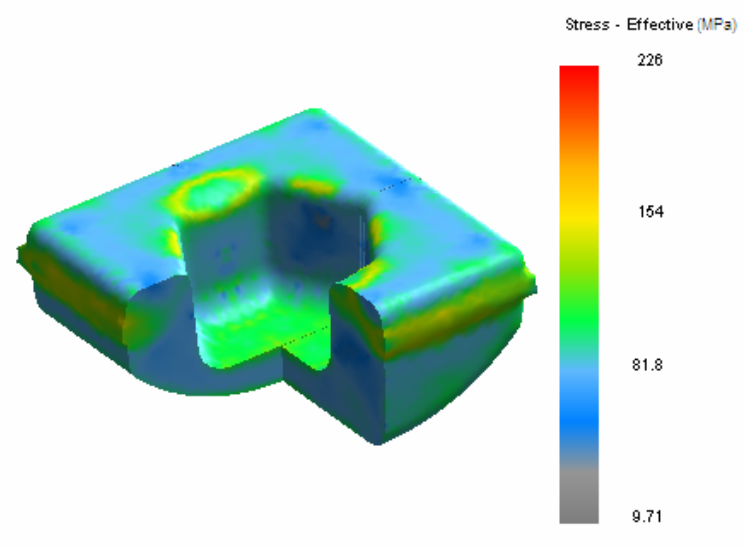

Figure 4.53 Max. Equiv. Stress Distributions on the Preformed Part for Trial 4.

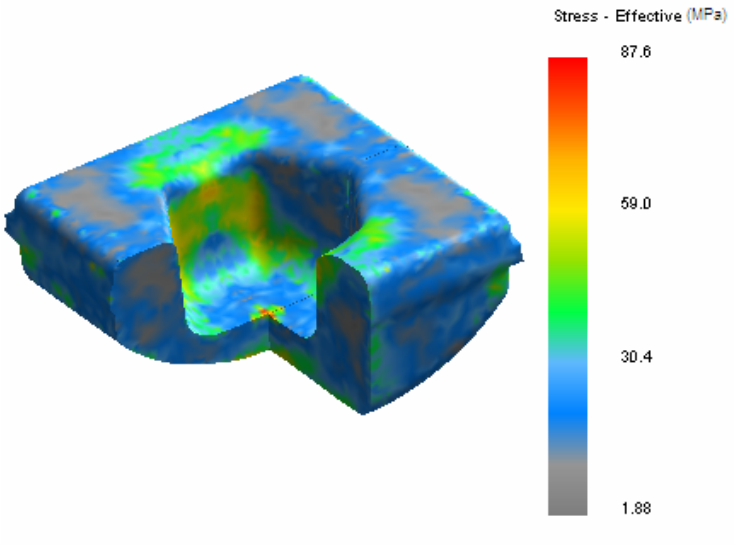

Figure 4.54 Residual Stresses on the Preformed Part for Trial 4.

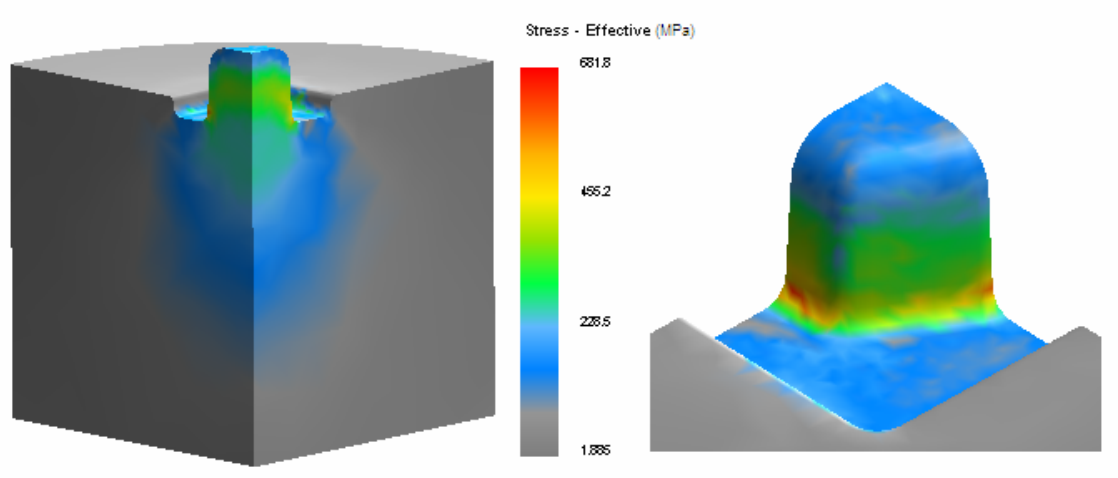

Figure 4.55 Max. Equiv. Stress Distributions on the Upper Preform Die for Trial 4.

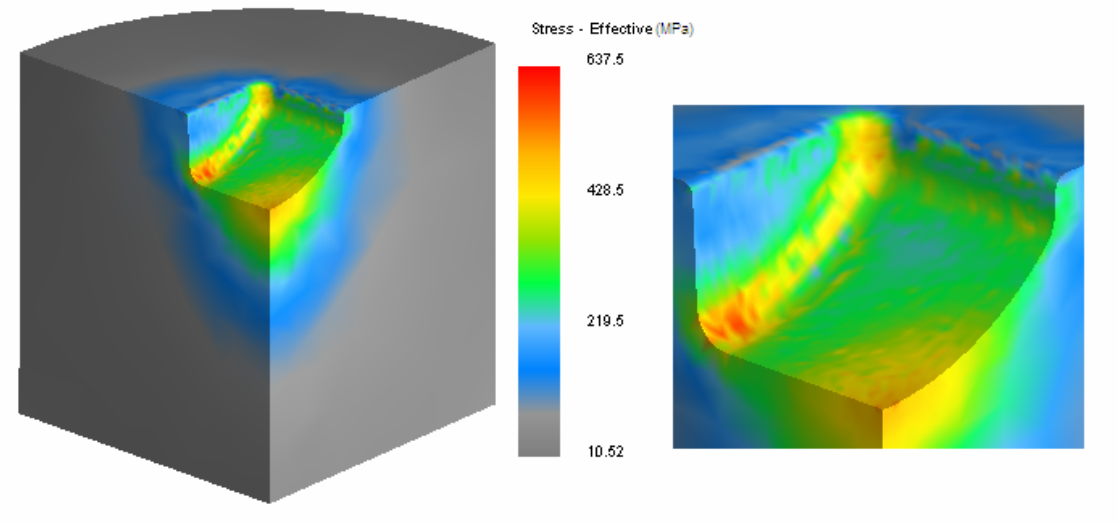

Figure 4.56 Max. Equiv. Stress Distributions on the Lower Preform Die for Trial 4.

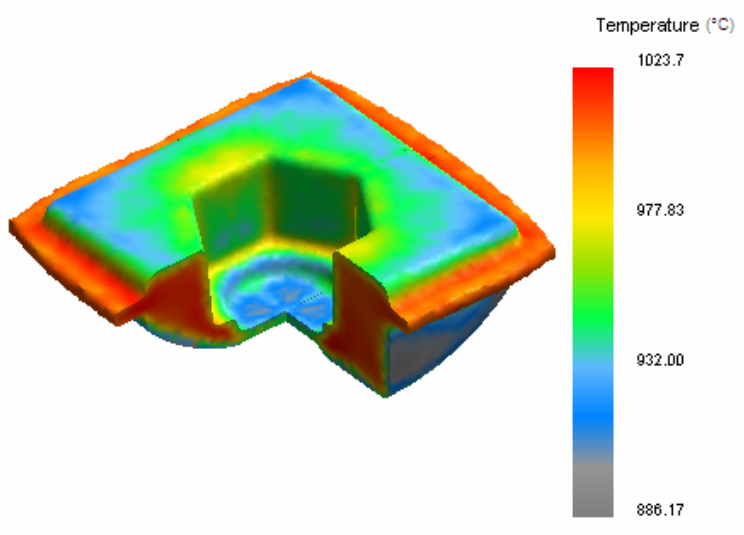

Figure 4.57 Max. Temperature Distributions on the Finished Part for Trial 4.

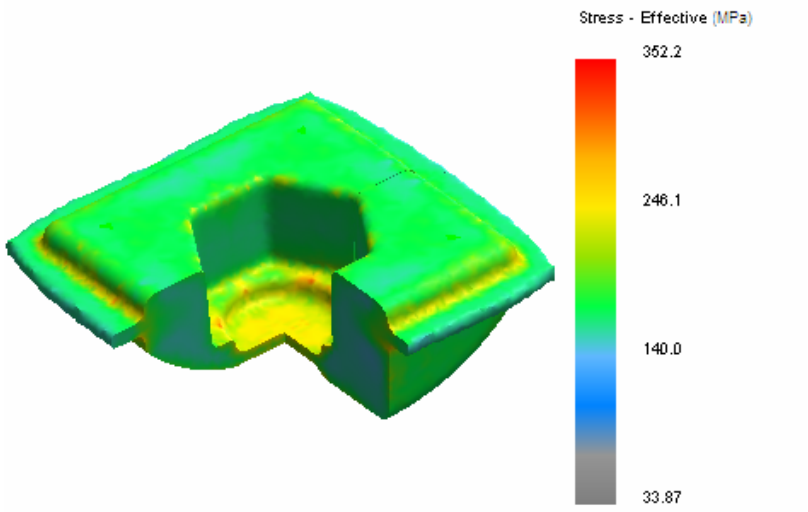

Figure 4.58 Max. Equiv. Stress Distributions on the Finished Part for Trial 4.

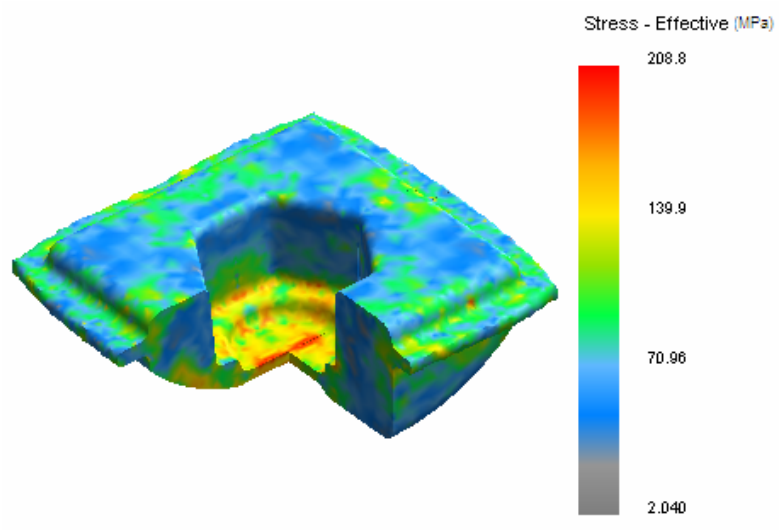

Figure 4.59 Residual Stresses on the Finished Part for Trial 4.

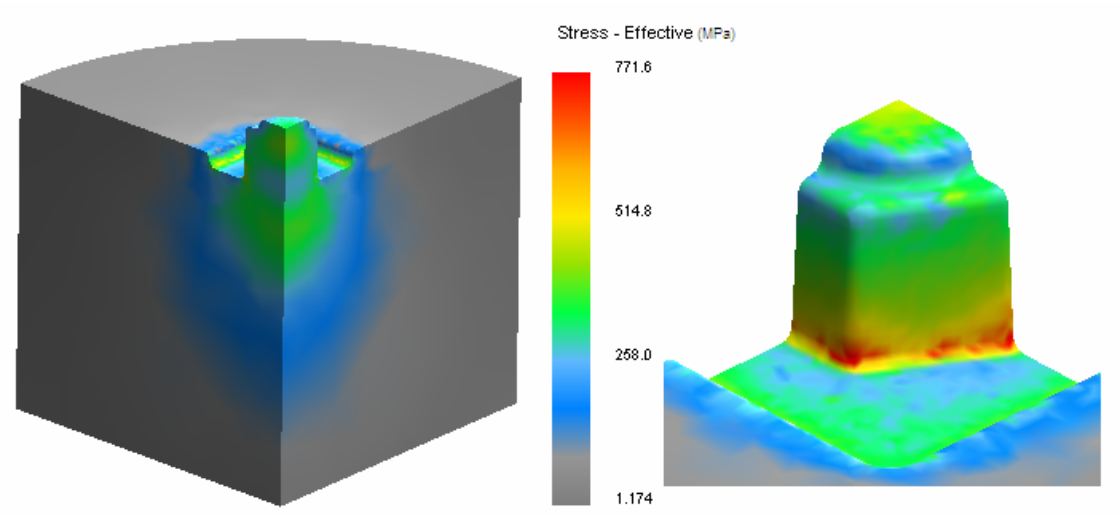

Figure 4.60 Max. Equiv. Stress Distributions on the Upper Finish Die for Trial 4.

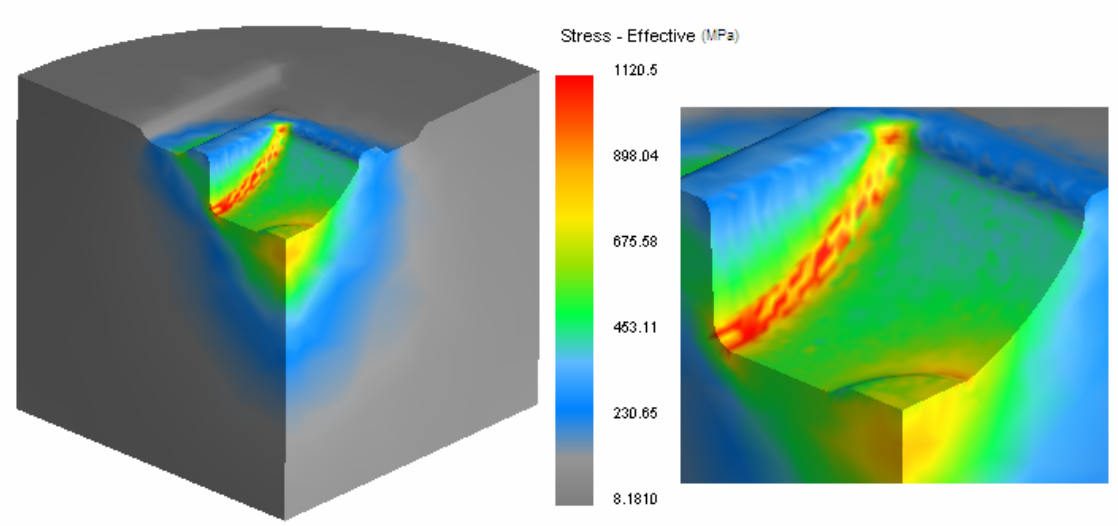

Figure 4.61 Max. Equiv. Stress Distributions on the Lower Finish Die for Trial 4.

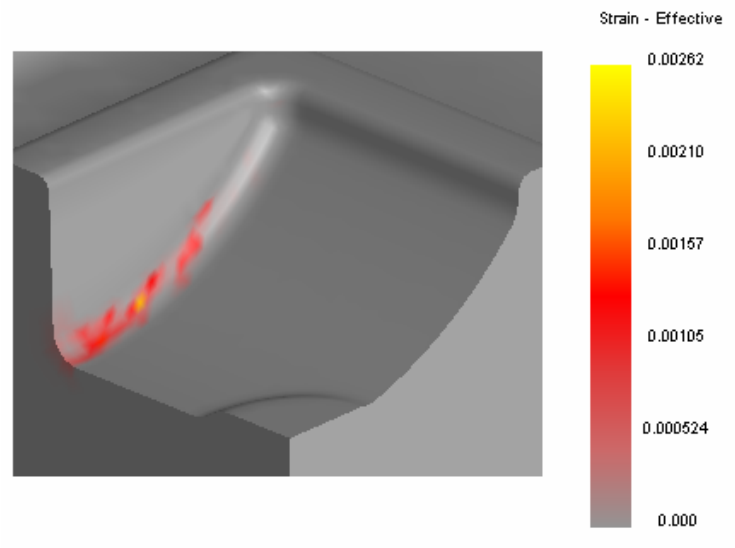

Figure 4.62 Plastic Strain on the Lower Finish Die for Trial 4.

The results for all billet temperatures analyzed are tabulated in Table 4.11.

Table 4.11 Simulation Results for the Trial Preform Die Geometries.

Trial Number	1	2	3	4	5
Max. Equiv. Stress on Upper Preform Die (MPa)	637.3	666.8	726.6	681.9	610.0
Peak Temperature on Upper Preform Die (°C)	455.0	478.0	464.6	510.9	490.4
Max. Equiv. Stress on Lower Preform Die (MPa)	526.3	701.7	683.8	637.5	732.5
Peak Temperature on Lower Preform Die (°C)	410.4	439.9	398.8	444.7	423.6
Max. Equiv. Stress on Upper Finish Die (MPa)	837.2	763.4	778.4	771.7	769.3
Peak Temperature on Upper Finish Die (°C)	365.3	368.4	366.3	351.9	338.6
Max. Equiv. Stress on Lower Finish Die (MPa)	1130.6	1128.1	1127.3	1120.5	1139.2
Peak Temperature on Lower Finish Die (°C)	378.3	382.3	380.1	367.0	352.6
Plastic Equiv. Strain on Lower Finish Die	0.0039	0.0037	0.0036	0.0026	0.0041
Max. Force on Preform Die (ton)	69.5	83.0	111.0	127.0	98.6
Max. Force on Finish Die (ton)	239.0	236.0	234.0	225.0	242.0
Residual Stress on Preformed Part (MPa)	233.8	228.2	210.1	226.0	217.3
Residual Stress on Preformed Part (MPa)	90.9	89.2	81.8	87.6	84.2
Peak Temp. on Preformed Part (°C)	1027.0	1030.5	1031.2	1030.6	1030.3
Max. Equiv. Stress on Finished Part (MPa)	366.5	334.7	301.0	352.2	330.9
Residual Stress on Finished Part (MPa)	209.5	207.6	200.7	208.8	207.0
Peak Temp. on Finished Part (°C)	1000.1	1025.4	1027.2	1023.7	1027.8

Yield Strength is exceeded.

From the simulation results of trial 1 it is observed that increasing the radius of the round section at the tip of the hexagonal protrusion has very small effect on the die stresses. The maximum load on the finish die is about the same with the simulation results in Section 4.3.2. However from the simulations it is observed that as the radius gets smaller the finished part is more susceptible to forging defects like folding. Because of this reason, for other trials it is decided to use the radius as large as possible.

The effect of height of hexagonal protrusion and radius of lower preform die is investigated in trial 2. Maximum equivalent stresses and forging load on the finish dies decrease. However the decrease is not sufficient and yield strength of the material is still passed over.

From the simulation results of trial 3, it is observed that decreasing width of the hexagonal protrusion decreases stress and forging load on the finish dies. However increasing height of the hexagonal protrusion is not possible because of the height of the protrusion in upper finish die.

In trial 4, width of the hexagonal protrusion is decreased further to the hexagonal protrusion of the finish die. Other changes are made to satisfy the volumetric calculations. From the simulation results it is observed that the forging load and the stress on the finish die decreases. Also plastic strains on the lower finish die decreases to a value of 0.0026.

Finally from the simulation results of trial 5, it is seen that decreasing radius of the round section in the lower preform die has a negative effect on the forging load and the stress values on the finish dies.

From the simulation results, best case is with preform die trial 4. However plastic deformation is expected to occur on the lower finish die. The value of maximum equivalent strain value is decreased to 0.0026 from a value of 0.0039. The maximum equivalent stress value is decreased to 1120.5 MPa from a value of 1132.4 MPa. Forging load of 225 ton is calculated from the results, which is 240 ton for the proposed forging sequence.

The simulation results suggest that although changing the preform die geometry decreases die stresses, plastic deformation still occurs in forging process for the lower finish die below initial billet temperature of 1000 °C. It can be concluded that one more preform stage or change in finish die geometry is necessary to overcome this problem. However increasing number of preform stages is not economical. Also it should be noted that the equivalent strain values on the dies are comparatively small. According to TS 4381-1 Standard, the value of a radius is allowable to 1.5 times its original value. So the plastic deformation of the dies can be tolerated to some limit.

CHAPTER 5

EXPERIMENTAL STUDY

In this chapter results of experiments which have been conducted for the proposed forging process will be explained. The experiments have been realized in METU-BİLTİR Center Forging Research and Application Laboratory.

5.1 Preparation of Experiments

Initially billets are prepared for the experiments. The material of the billet is AISI 1020 and supplied from a steel supplier in Ankara. Billets are cut to the defined lengths by Kesmak sawing machine and they are marked. The lengths of the billets are measured using a digital compass having an accuracy of ±0.1 mm, and weights are measured using a digital scale having an accuracy of ±0.01 g. Some of the billets and the digital scale is shown in Figure 5.1. Dimensions of the billets and their weights are tabulated in Table 5.1. Variations are observed in the dimensions and the weights of the billets are due to the cutting conditions of the sawing machine and dimensional variations of bought steel specimen.

The preform and the finish dies are fastened to the press after the billets are cut and numbered. The dies are located to the die holders and fastened by clamping elements as shown in Figure 5.2. Technical data of the press is given in Appendix C.

Figure 5.1 Photographs of the Billets Numbered and the Digital Scale.

Figure 5.2 Photographs of the Dies Fastened to the Press.

After mounting, the billets and dies are heated to the required temperatures. The billets are heated in 125 KVA- 3000 Hz induction heater which is available in the laboratory. The experiments are conducted at billet temperatures of 1150 °C and 1000 °C. During the experiments, temperatures of the billets are measured using by pyrometer having a temperature range of 600 °C – 1400 °C. The preform and finish dies are heated by two LPG heater flame guns to a temperature of approximately 200 °C. Temperature of the dies is measured in every 10 minutes using a portable optical pyrometer having a temperature range of -32 °C – 600 °C. Photograph of preheating of the dies is given in Figure 5.3.

Figure 5.3 Photograph of Preheating of the Dies.

5.2 Experimentation

In the experiments, one billet is heated to the forging temperature, one billet is forged to preform stage, one billet is forged to finish stage and kept. Then 10 billets are forged to preform stage and 10 billets are forged to finish stage.

After heating the billets to specified temperatures, temperature values are measured before the preform operation. Also lower and upper die temperatures are recorded. Then the billets are put on the preform die and forged. Billet temperature and die temperatures after forging are also measured. Preformed parts are then located on the finish dies whose temperatures are recorded before the operation. Following the forging of the parts, their temperature, upper and lower finish die temperatures are measured. The data recorded in the experiments for the workpiece and dies are given in Table 5.1 and Table 5.3, respectively. After the forged parts are cooled to room temperature, their dimensions and the flash thickness are measured by digital calipers. The results that are measured after the experiments are tabulated in Table 5.2.

Table 5.1 Experimental Data for the Workpiece.

Sample No	Stage No	Average Billet Length (mm)	Average Billet Mass (g)	Billet Temp. Before Forging (°C)	Preformed Part Temp. (°C)	Finished Part Temp. (°C)
1	0	17.02	152.68	1020.00	-	-
2	1	17.04	152.89	1035.00	1010.00	-
3	2	16.93	151.60	1030.00	986.00	900.00
4	1	17.00	152.41	1036.00	985.00	-
5	1	17.32	155.31	995.00	960.00	-
6	1	17.09	153.33	1040.00	1015.00	-
7	1	17.40	155.65	1045.00	1024.00	-
8	1	16.98	152.16	1034.00	1002.00	-

Table 5.1 Experimental Data for the Workpiece (cont'd).

Sample No	Stage No	Average Billet Length (mm)	Average Billet Mass (g)	Billet Temp. Before Forging (°C)	Preformed Part Temp. (°C)	Finished Part Temp. (°C)
9	1	17.06	152.99	997.00	963.00	-
10	1	17.20	154.21	1024.00	985.00	-
11	1	17.02	152.48	1035.00	991.00	-
12	1	17.10	153.39	1020.00	995.00	-
13	1	17.24	154.82	1000.00	935.00	-
14	2	17.17	153.99	1007.00	937.00	830.00
15	2	17.11	153.58	1020.00	980.00	854.00
16	2	17.15	153.94	1000.00	940.00	803.00
17	2	17.13	153.80	1068.00	1040.00	900.00
18	2	17.11	153.63	1055.00	1038.00	905.00
19	2	17.10	153.49	1037.00	1012.00	885.00
20	2	16.93	151.57	1000.00	930.00	830.00
21	2	17.30	155.18	1028.00	933.00	771.00
22	2	17.07	153.03	1005.00	927.00	845.00
23	2	17.14	153.92	1022.00	988.00	850.00
24	0	17.06	152.97	1157.00	-	-
25	1	16.92	151.34	1133.00	976.00	-
26	2	16.97	152.13	1160.00	1010.00	930.00
27	1	17.07	153.14	1175.00	1030.00	-
28	1	17.03	152.78	1160.00	1025.00	-
29	1	17.18	154.05	1172.00	1000.00	-
30	1	16.94	151.78	1145.00	1030.00	-
31	1	16.95	151.83	1165.00	1010.00	-
32	1	17.18	154.06	1160.00	1025.00	-
33	1	17.15	153.82	1170.00	1020.00	-
34	1	17.06	153.01	1155.00	1010.00	-
35	1	17.13	153.68	1180.00	1025.00	-
36	1	17.17	154.00	1175.00	1005.00	-
37	2	17.10	153.49	1120.00	1025.00	881.00
38	2	17.09	153.32	1160.00	1000.00	910.00
39	2	17.14	153.88	1158.00	981.00	890.00

Table 5.1 Experimental Data for the Workpiece (cont'd).

Sample No	Stage No	Average Billet Length (mm)	Average Billet Mass (g)	Billet Temp. Before Forging (°C)	Preformed Part Temp. (°C)	Finished Part Temp. (°C)
40	2	17.01	152.59	1130.00	965.00	880.00
41	2	17.15	153.94	1155.00	1010.00	935.00
42	2	17.19	154.08	1155.00	1000.00	890.00
43	2	17.22	154.44	1165.00	1005.00	905.00
44	2	17.00	152.45	1160.00	995.00	890.00
45	2	17.04	152.84	1170.00	1016.00	935.00
46	2	17.05	152.93	1180.00	1040.00	1010.00

Table 5.2 Results that are Measured After the Experiments.

Sample No	Width (mm)	Length (mm)	Height (mm)	Hexagonal Cavity Dimensions (mm)	Flash Thickness (mm)	mass (g)
1	34.00	33.99	17.01	-	-	151.51
2	38.65	38.70	19.45	19.70	-	152.17
3	40.01	40.08	17.12	19.03	2.07	151.01
4	38.87	38.98	19.30	19.68	-	151.48
5	38.75	38.77	18.87	19.50	2.93	154.31
6	38.48	38.86	18.80	19.66	2.90	152.53
7	38.80	38.99	19.28	19.54	-	154.96
8	38.78	38.93	19.17	19.54	-	150.08
9	38.66	38.85	19.30	19.63	3.20	151.05
10	38.20	38.78	19.35	19.70	-	153.14
11	38.87	38.82	18.90	19.80	-	152.17
12	38.76	38.86	18.72	19.55	-	152.99
13	38.81	38.92	19.20	19.62	-	154.29
14	40.07	40.01	17.16	19.05	2.08	153.69
15	40.02	40.01	17.02	19.03	2.04	152.94
16	40.01	39.99	16.99	19.03	2.00	153.4

Table 5.2 Results that are Measured After the Experiments (cont'd).

Sample No	Width (mm)	Length (mm)	Height (mm)	Hexagonal Cavity Dimensions (mm)	Flash Thickness (mm)	Mass After Forging (g)
17	40.04	40.03	17.08	19.02	2.08	153.57
18	40.04	40.02	17.00	19.03	2.04	153.34
19	40.05	40.00	17.18	19.02	2.11	152.98
20	40.00	39.98	16.98	19.02	1.99	150.83
21	40.00	40.01	17.19	19.04	2.10	154.07
22	40.02	39.99	17.01	19.03	2.02	152.17
23	40.10	40.03	17.02	19.03	2.02	153.32
24	34.04	34.10	17.05	-	-	152.45
25	38.72	38.70	18.55	19.52	2.60	151.06
26	40.06	40.00	17.05	19.04	2.04	151.96
27	38.67	38.66	18.59	19.63	2.53	152.28
28	39.00	38.87	18.50	19.56	2.48	152.44
29	38.75	38.72	18.60	19.53	2.58	153.66
30	38.76	38.72	18.57	19.52	2.60	151.36
31	38.78	38.75	18.60	19.56	2.66	151.51
32	38.85	38.79	18.65	19.54	2.66	153.49
33	38.90	38.74	18.63	19.66	2.55	153.48
34	38.78	38.70	18.70	19.58	2.65	152.9
35	38.81	38.77	18.63	19.60	2.64	153.33
36	38.79	38.76	18.65	19.59	2.61	153.61
37	40.03	40.01	16.99	18.99	2.00	153.31
38	40.05	40.00	16.99	19.05	2.03	153.02
39	40.06	40.01	17.01	19.03	2.04	153.64
40	40.03	40.01	17.04	19.06	2.06	152.24
41	40.03	40.02	17.14	19.04	2.08	152.88
42	40.02	40.01	17.10	19.03	2.07	153.92
43	40.03	39.99	17.05	19.02	2.04	154.25
44	40.06	40.00	17.06	19.05	2.05	152.01
45	40.03	39.98	17.02	19.07	2.05	152.15
46	40.05	40.03	17.09	19.05	2.09	152.73

Table 5.3 Experimental Data for the Dies.

	Preform Die				Finish Die			
Sample No	Lower Die Temp. Before Forging (°C)	Upper Die Temp. Before Forging (°C)	Lower Die Temp. After Forging (°C)	Upper Die Temp. After Forging (°C)	Lower Die Temp. Before Forging (°C)	Upper Die Temp. Before Forging (°C)	Lower Die Temp. After Forging (°C)	Upper Die Temp. After Forging (°C)
1	-	-	-	-	-	-	-	-
2	176	178	170	165	-	-	-	-
3	166	160	160	158	172	160	176	164
4	205	190	206	202	-	-	-	-
5	200	187	196	190	-	-	-	-
6	192	186	191	182	-	-	-	-
7	185	179	182	180	-	-	-	-
8	170	175	172	181	-	-	-	-
9	167	178	160	176	-	-	-	-
10	156	170	165	164	-	-	-	-
11	162	160	158	155	-	-	-	-
12	235	250	238	248	-	-	-	-
13	230	240	230	246	-	-	-	-
14	226	243	214	243	253	247	240	245
15	209	237	210	235	224	240	227	232
16	200	227	204	228	220	227	212	250
17	197	221	212	216	204	230	206	226

Table 5.3 Experimental Data of the Dies (cont'd).

	Preform Die				Finish Die			
Sample No	Lower Die Temp. Before Forging (°C)	Upper Die Temp. Before Forging (°C)	Lower Die Temp. After Forging (°C)	Upper Die Temp. After Forging (°C)	Lower Die Temp. Before Forging (°C)	Upper Die Temp. Before Forging (°C)	Lower Die Temp. After Forging (°C)	Upper Die Temp. After Forging (°C)
18	206	210	207	214	200	205	207	200
19	200	198	198	210	199	195	191	198
20	193	200	196	202	184	190	182	265
21	191	195	190	194	180	210	184	219
22	185	190	189	189	172	199	179	187
23	187	185	182	180	168	182	172	167
24	-	-	-	-	-	-	-	-
25	167	165	174	159	-	-	-	-
26	170	148	171	145	150	167	154	189
27	164	139	157	142	-	-	-	-
28	150	136	138	134	-	-	-	-
29	210	227	213	228	-	-	-	-
30	200	225	205	225	-	-	-	-
31	196	220	202	219	-	-	-	-
32	198	212	190	209	-	-	-	-
33	183	205	181	200	-	-	-	-
34	176	190	177	192	-	-	-	-

Table 5.3 Experimental Data of the Dies (cont'd).

	Preform Die				Finish Die			
Sample No	Lower Die Temp. Before Forging (°C)	Upper Die Temp. Before Forging (°C)	Lower Die Temp. After Forging (°C)	Upper Die Temp. After Forging (°C)	Lower Die Temp. Before Forging (°C)	Upper Die Temp. Before Forging (°C)	Lower Die Temp. After Forging (°C)	Upper Die Temp. After Forging (°C)
35	172	187	179	184	-	-	-	-
36	175	176	171	180	-	-	-	-
37	167	178	169	179	205	230	197	263
38	167	175	160	176	190	255	196	258
39	155	170	157	169	190	251	214	246
40	150	162	164	166	205	238	209	240
41	156	160	157	160	196	230	182	270
42	150	155	152	156	176	256	170	232
43	148	151	147	156	160	220	180	200
44	145	157	147	152	168	184	188	212
45	140	148	144	145	166	200	156	207
46	138	140	132	139	150	186	157	214

During the experiments forging loads are recorded using Decade-260 Series load monitor. Technical data of the load monitor is given in Appendix D. The maximum forging loads are presented in Figures 5.4-7 for samples 7, 17, 35 and 46. Sample 7 and 17 are for preform and finish stage for initial billet temperature of 1000 °C, sample 35 and 46 are for preform and finish stage for initial billet temperature of 1150 °C.

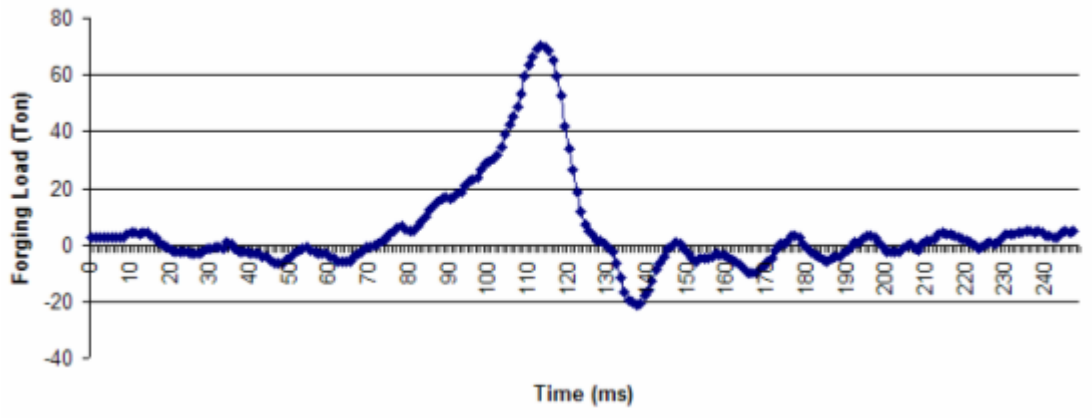

Figure 5.4 The Forging Load for Sample 7.

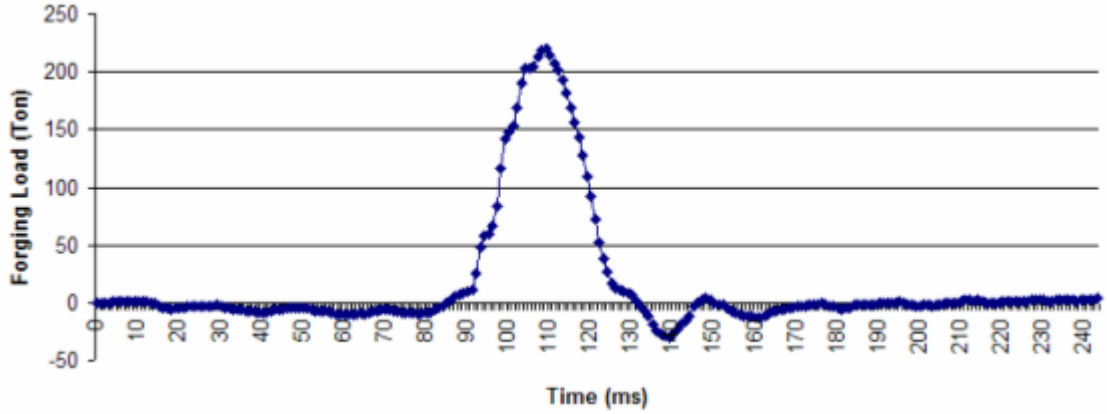

Figure 5.5 The Forging Load for Sample 17.

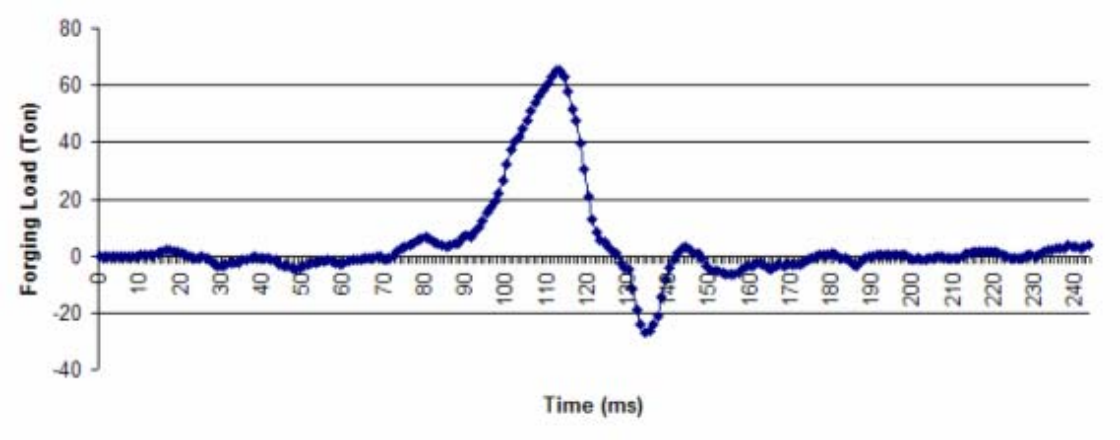

Figure 5.6 The Forging Load for Sample 35.

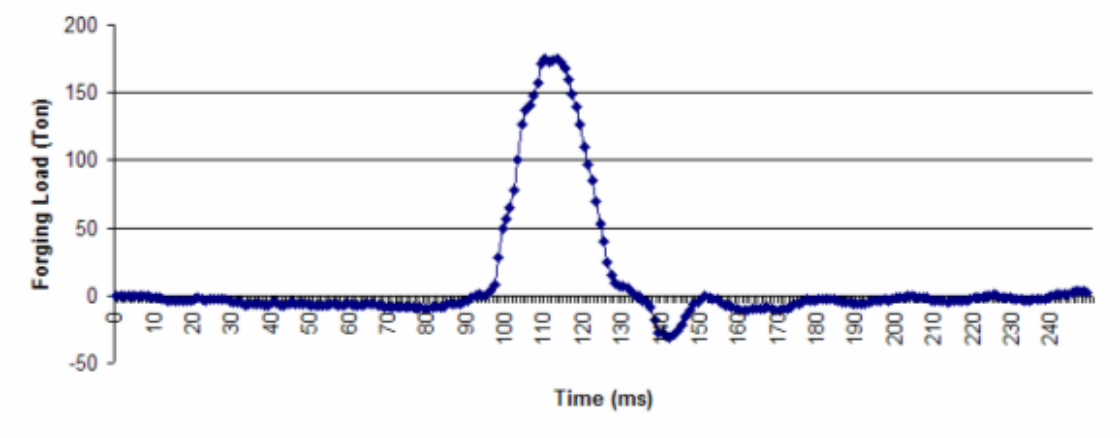

Figure 5.7 The Forging Load for Sample 46.

5.3 Discussion of Experiment Results

From the results of the experiments, it is observed that the temperatures of the billets are between 1180 °C to 1120 °C when the desired temperature is 1150 °C, and 997 °C

to 1068 °C, when the desired temperature is 1000 °C. This is mainly because it is not possible to heat the billets to the exact forging temperature in induction heater. Also while taking measurements the billets are carried between induction heater and pyrometer and cool down below the desired temperatures.

The temperature measurements from dies are between 132 to 265 °C which was defined as 200 °C in the simulations. Since some measurements are recorded in each forging stage the production rate is low and dies are cooled down by convection and radiation during the period. In some parts of experiments dies are reheated to satisfy the specified temperature. Some high temperatures are recorded because of these intermediate heating operations. Also in some measurements, it is observed that temperature of the dies after forging operation is lower than the temperatures before forging. This is possibly due to not taking measurements just after the forging operation. Dies cool down by the time measurements can be taken. Also since the temperature measurements are taken by optical pyrometer, average value of different points is taken as measurement. It is not possible to focus the local peak values as calculated in the simulations.

Visual inspection of the parts shows that there are no forging defects like folds, laps and unfilled regions on the finished parts, which is consistent with the simulation results. Flash formation around the part is reduced considerably compared with the current practice applied in the forging company. There is almost no flash formation in the preform stage and the flash thicknesses on the finished parts are measured to be between 1.99 to 2.11 mm, which was designed to be 2 mm. Some of the forged parts are shown in Figure 5.8.

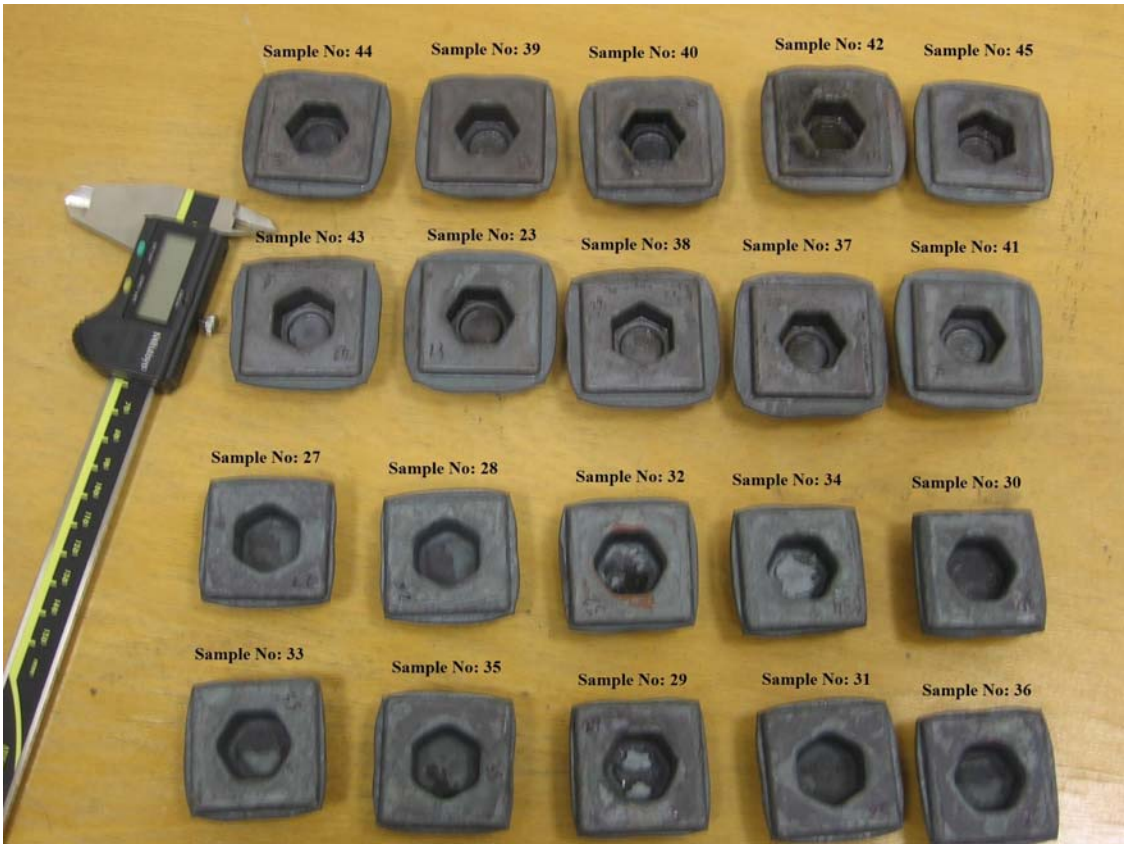

Figure 5.8 Some of the Forged Parts.

The hexagonal cavity dimensions are in the range of 19.02 to 19.07 mm for the finished part, which satisfy the part's dimensional tolerance of ±0.5. The dimensions of width and length of the parts are in the range of 39.98 to 40.10 mm which also satisfies the dimensional tolerance.

Scale layer formation is observed on the parts and mass of the parts after forging operation is reduced approximately 0.5 g.

Maximum forging load of 687 kN for the preform stage and 2150 kN for the finish stage is monitored for initial billet temperature of 1000 °C. 711 kN for the preform

stage and 2355 kN for the finishing stage are obtained from the simulation results for the same initial billet temperature. For initial billet temperature of 1150 °C, punch loads of 636 kN for the preform stage and 1717 kN for the finish stage are measured in the experiments. Maximum forging loads obtained for the same billet temperature are 610 kN for the preform stage and 1344 kN for the finish stage from the computer simulations. From comparison of the results, it is observed that the experimental results are in good agreement with the numerical results.

CHAPTER 6

CONCLUSIONS AND FURTHER RECOMMENDATIONS

6.1 General Conclusions

The conclusions can be summarized as follows:

1. Detailed analysis of the forging process for a particular industrial part and the related dies has been performed using elastic-plastic finite element method.

    - In the finite element simulations, it is observed that the maximum equivalent stress values on the dies increase as the initial billet temperature is reduced. These maximum equivalent stress values occur at the similar locations for all the simulations.
    - The peak temperatures on the dies are observed at the locations which are in contact with the workpiece for the longest duration. Similarly, the locations where the maximum temperatures occur on the dies do not change for all the simulations.

2. Computer simulations have been done for the process design proposed by a previous study [13] by using Deform 3D. Results obtained by Deform 3D have been compared to the results of MSC Superform of the previous study.

- It is observed that the stress, strain and temperature distributions are in good agreement with each other in elastic deformation range for both workpiece and dies. Also temperature distributions on the dies obtained by both codes are in good agreement.
- In the simulations, plastic deformation was observed on the finish dies by both codes for the billet temperature of 950 °C and below. However, plastic strain is observed for the billet temperature of 1000 °C on the lower finish die and for the billet temperature of 850 °C on the preform dies by Deform 3D whereas MSC Superform showed no plastic deformation for both temperatures. Also it is observed that the maximum effective stress values are relatively higher for the simulations in Deform 3D.

3. Effects of preform die geometry and reduced billet material on the die stresses and the forging load are investigated using finite element method.

    - The simulation results of proposed billet shape showed that maximum equivalent stress, forging load and plastic strain on the dies are reduced. No plastic deformation is observed on preform dies for the billet temperatures of 1150 °C, 1000 °C, 950 °C, 900 °C and 850 °C.
    - The simulations suggest that; plastic deformation occurs on the lower finish die for initial billet temperature of 1000 °C and below, although die stresses can be decreased by changing the preform die geometry.

4. The experimental study has been conducted for the proposed billet geometry at billet temperatures of 1150 °C and 1000 °C.

- It is observed that flash formation on the finished part obtained by the proposed forging process sequence is reduced considerably compared to the current forging practice. Scrap material is reduced by 12.1 %.
- It is observed that there is almost no flash formation in the preform stage.
- It is observed that finite element simulation results and the experiment results are in good agreement for the proposed geometry.
- Experimental results showed that the product obtained by the proposed forging process satisfies the dimensional tolerances required.

6.2 Recommendations for Future Studies

The followings may be suggested as future works of this particular study;

- Tool life and wear analyses can be made for the dies.
- Near-net shape forging of the particular part can be studied.
- More than one performing stage can be designed in the process sequence to avoid plastic deformation for billet temperature of 1000 °C and below.

REFERENCES

1. Semiatin, S.M., "Forming and Forging Volume 14-9th Edition Metals Handbook", ASM International, 1988, pp. 10-58.

2. Tuncer, M.N., "Precision Forging Hollow Parts", Ph d. Thesis, University of Birmingham, 1985.

3. Wikipedia [On-Line], Available at, http://en.wikipedia.org/wiki/Forging, last accessed; February 2009.

4. Boyer, H., "Metals Handbook – Forging and Casting", 8th Edition, ASM handbook committee, 1971.

5. Forging Industry Association, [On-Line], Available at, http://www.forging.org/facts/wwhy6.htm, last accessed; February 2009.

6. Kobayashi, S., Altan, T., "Metal Forming and Finite Element Method", Oxford University Press, 1989.

7. Vazquez, V., Altan, T., "Die Design for Flashless Forging of Complex Parts", Vol. 98, Journal of Materials Processing Technology, 2000, pp. 81-89.

8. Kalpakjian, S., "Manufacturing Processes for Engineering Materials", 3rd Edition, Addison Wesley Longman Inc., California, 1997.

9. Sabroff, A.M., Boulger, F.W., Henning, H.J., “Forging Materials and Practices”, Reinhold Book Corporation, Ohio, 1986.

10. Sheridan, S.A., Unterweiser, P.M., “Forging Design Handbook”, American Society for Metals , 1972.

11. Vural, O., Özdöngül, N., Sertkaya, S., Alanyalı, E., “Dövme hataları kataloğu”, Ford Otosan, 2004.

12. Dieter, G., Kuhn, H., Semiatin, S.L., “Handbook of Workability and Process Design”, ASM International, 2003.

13. Saraç, S., “Design and Thermo-mechanical Analysis of Warm Forging Process and Dies”, M. Sc. Thesis, Middle East Technical University, Ankara, 2007.

14. Aktakka, G., “Analysis of Warm Forging Process”, Middle East Technical University, Ankara, 2006.

15. Civelekoğlu, B., “Analysis of Forging For Three Different Alloy Steels”, Middle East Technical University, Ankara, 2003.

16. Mehta, B.V., Al-Zkeri, I., Gunasekera, J.S., “Evaluation of MSC SuperForge for 3D simulation of streamlined and shear extrusion dies”, Ohio University, USA, 2000.

17. Abachi, S., “Wear Analysis of Hot Forging Dies”, M. Sc. Thesis, Middle East Technical University, Ankara, 2004.

18. Öztürk, H., “Analysis and Design of Aluminum Forging Process”, Middle East Technical University, Ankara, 2005.

19. Kim, D.H., Kim, B.M., Kang, C.G., “Die Life Estimation of Hot Forging for Surface Treatment and Lubricants”, Vol. 5, No. 4, International Journal of Precision Engineering and Manufacturing, 2004, pp. 5-13.

20. Iwama, T., Morimoto, Y., “Die Life and Lubrication in Warm Forging”, Vol. 71, Journal of Materials Processing Technology, 1997, pp. 43-48.

21. Fai, K.T., Chow, C.L., Chui, L.T., “Prediction of a Billet Shape for Axisymmetric Warm Forging Using Variational Analysis”, Vols 274-276, Key Engineering Materials, 2004, pp. 733-738.

22. Aksan Steel Forging Company.

23. WAFAM-The Warm Forging Practical Handbook.

24. Hirschvogel, M., Dommelen, H.V., “Some Applications of Cold and Warm Forging”, Vol. 35, Journal of Materials Processing Technology, 1992, pp. 343-356.

25. Altan, T., “Metal Forming Handbook”, Springer-Verlag Berlin Heidelberg, 1998.

26. Remppis, M., “Warm Forging Technology – Basics and Applications”, Metallurgia, 1997.

27. Schmoekel, D., Sheljaskow, S., Speck, F.D., “Situation der Werkzeugwerkstoffe fur die Halbwarmumformung in Deutschland”, Universitat Stuttgart, 1994.

28. Semiatin, S.M., “Metals Handbook Vol. 10: Failure Analysis and Prevention”, American Society for Metals, 1986, pp. 500-503.

29. Hutchinson, D.W., “The Function and Proper Selection of Forging Lubricants”, Acheson Colloids Company, 1984.

30. Deform 3D Users Manual, Scientific Forming Technologies Corporation, 2008.

31. Bathe, K.J., “Finite Element Procedures in Engineering”, Prentice-Hall Inc., 1982.

32. Pro/Engineer Wildfire III User Guide, PTC, Release 2006.

33. MSC Superforge User Manual, The MacNeal-Schwendler Corporation,2003.

34. ANSYS Icem Cfd Documentation for Release 11.0, ANSYS Inc., 2007.

35. MatWeb, Material Property Data, [On-Line], Available at, http://asia.matweb.com/search/SpecificMaterial.asp?bassnum=MS0001, last accessed; February 2009.

36. MatWeb, Material Property Data, [On-Line], Available at, http://www.matweb.com/search/datasheettext.aspx?matguid=4ad9842a94674606a42e22985585d9e1, last accessed: February 2009.

37. Kutlu, A.E., “Analysis and Design of Preforms for Non-Axisymmetric Press”, M. Sc. Thesis, Middle East Technical University, Ankara, 2001.

38. ASSAB KORKMAZ, [On-Line], Available at, http://www.assabkorkmaz.com/sicak.html, last access: January 2009.

APPENDIX A

TECHNICAL DRAWING OF THE PART

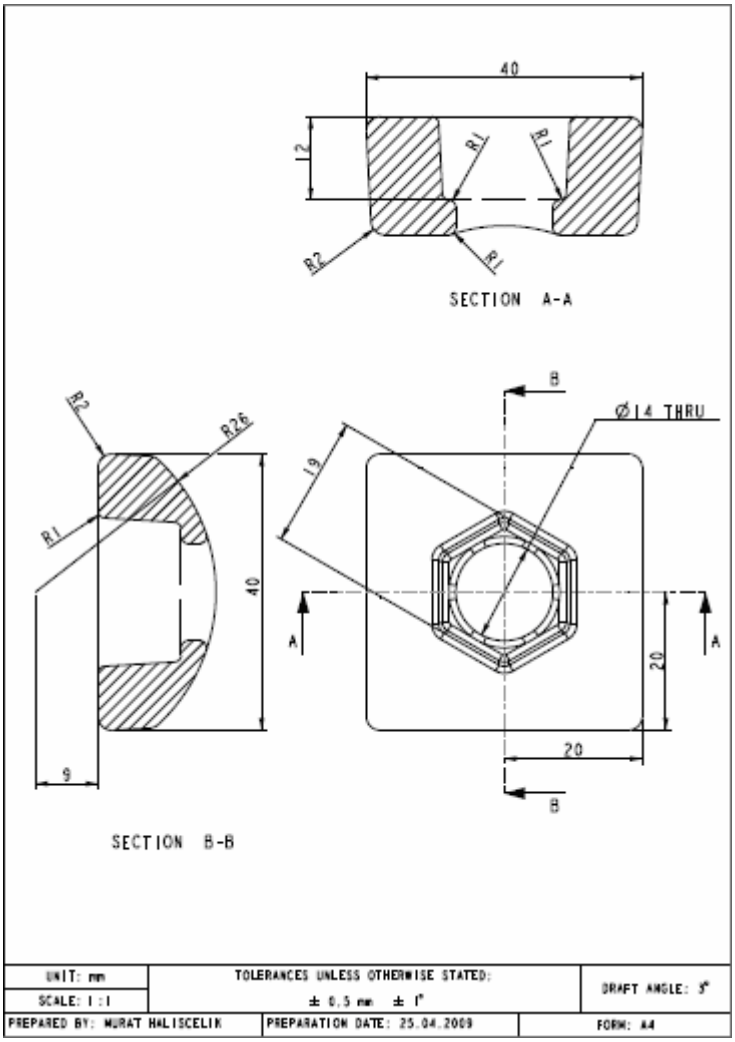

Figure A. 1 Technical Drawing of the Part.

APPENDIX B

TECHNICAL DRAWING OF THE DIES

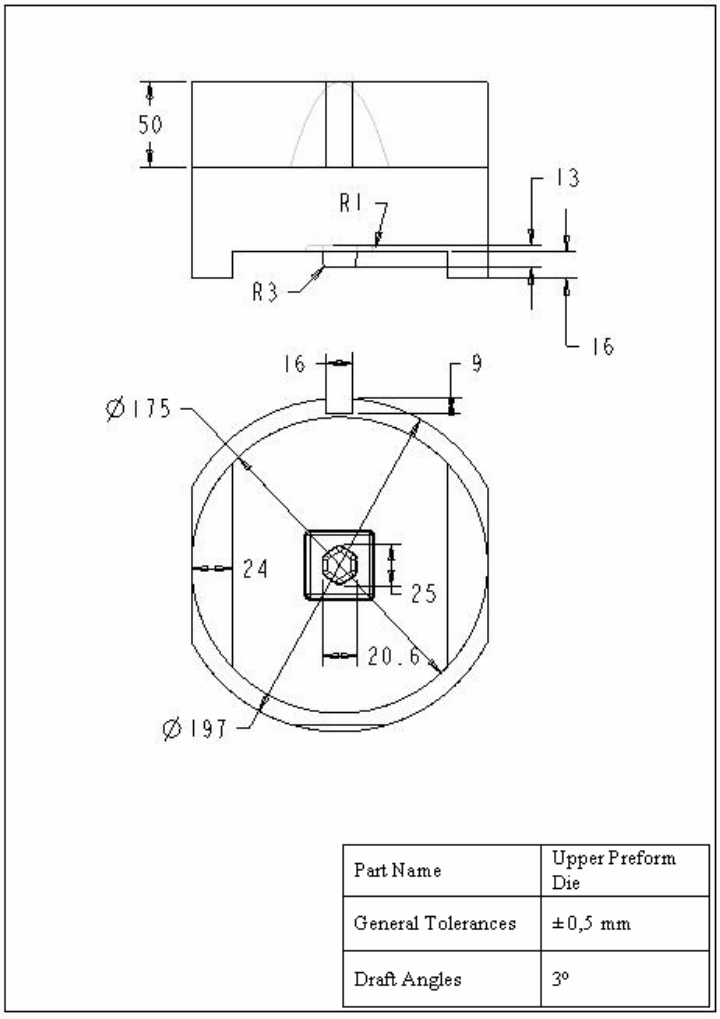

Figure B. 2 Technical Drawing of the Upper Preform Die [13].

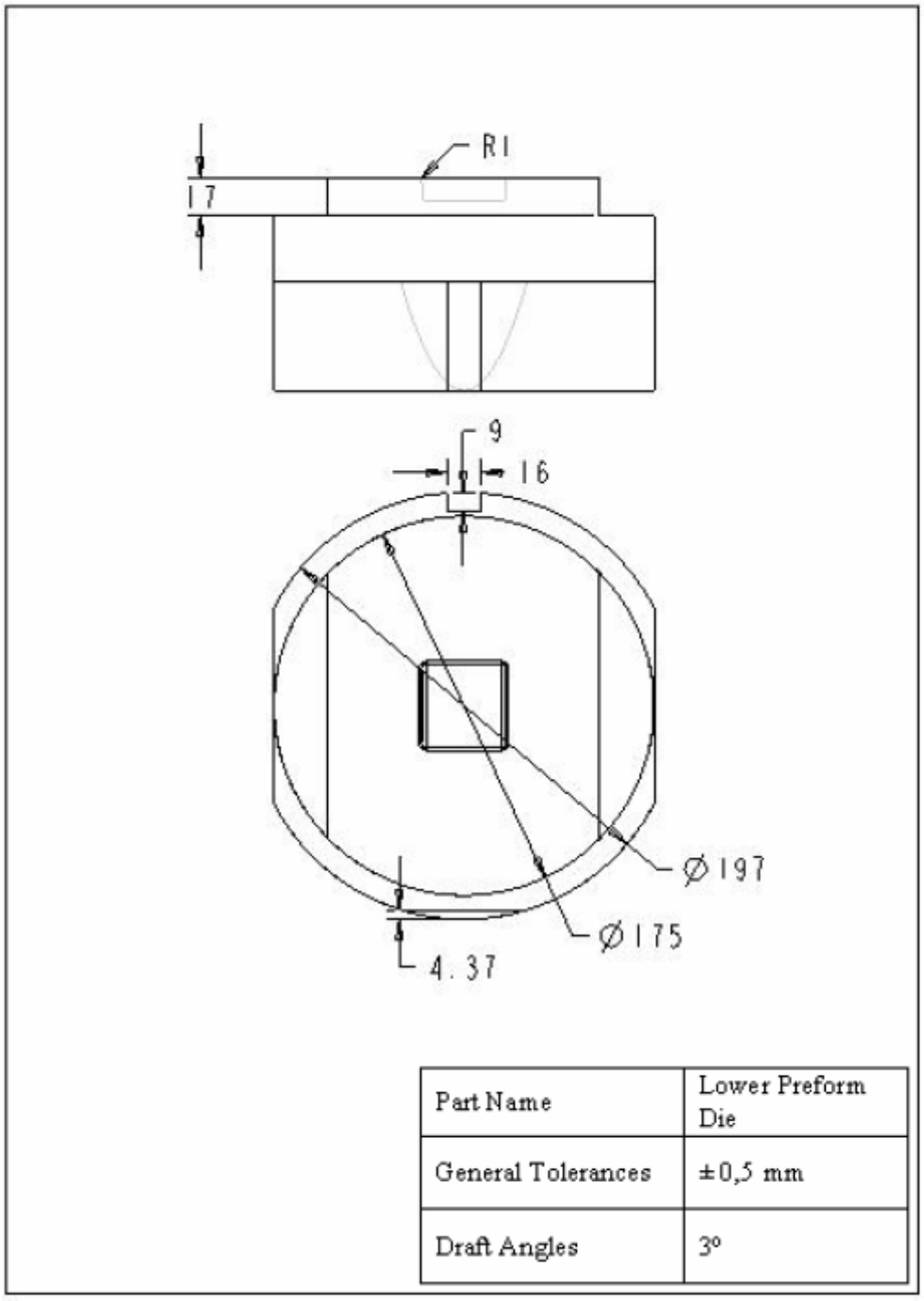

Part Name	Lower Preform Die
General Tolerances	±0,5 mm
Draft Angles	3º

Figure B. 2 Technical Drawing of the Lower Preform Die [13].

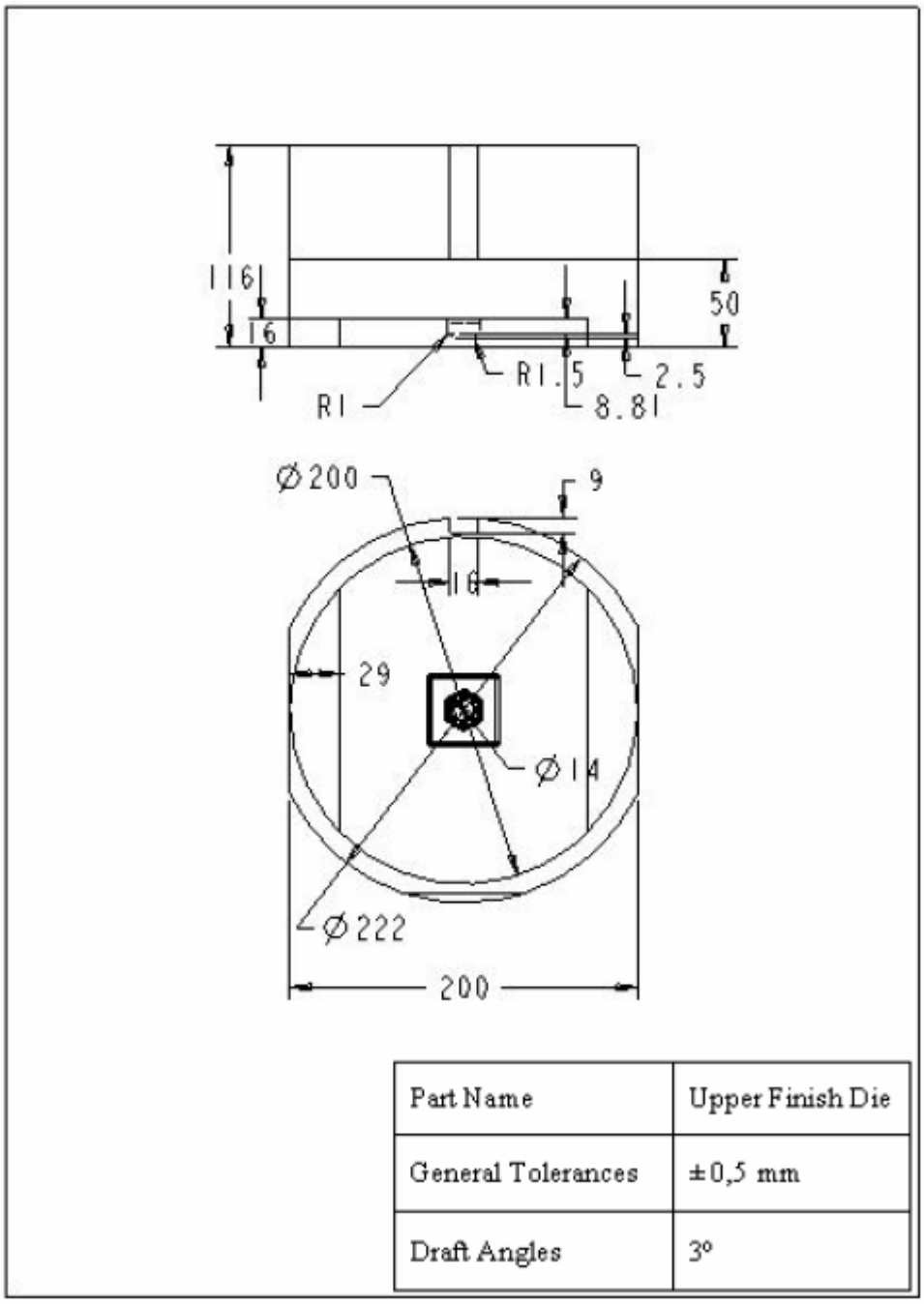

Figure B. 3 Technical Drawing of the Upper Finish Die [13].

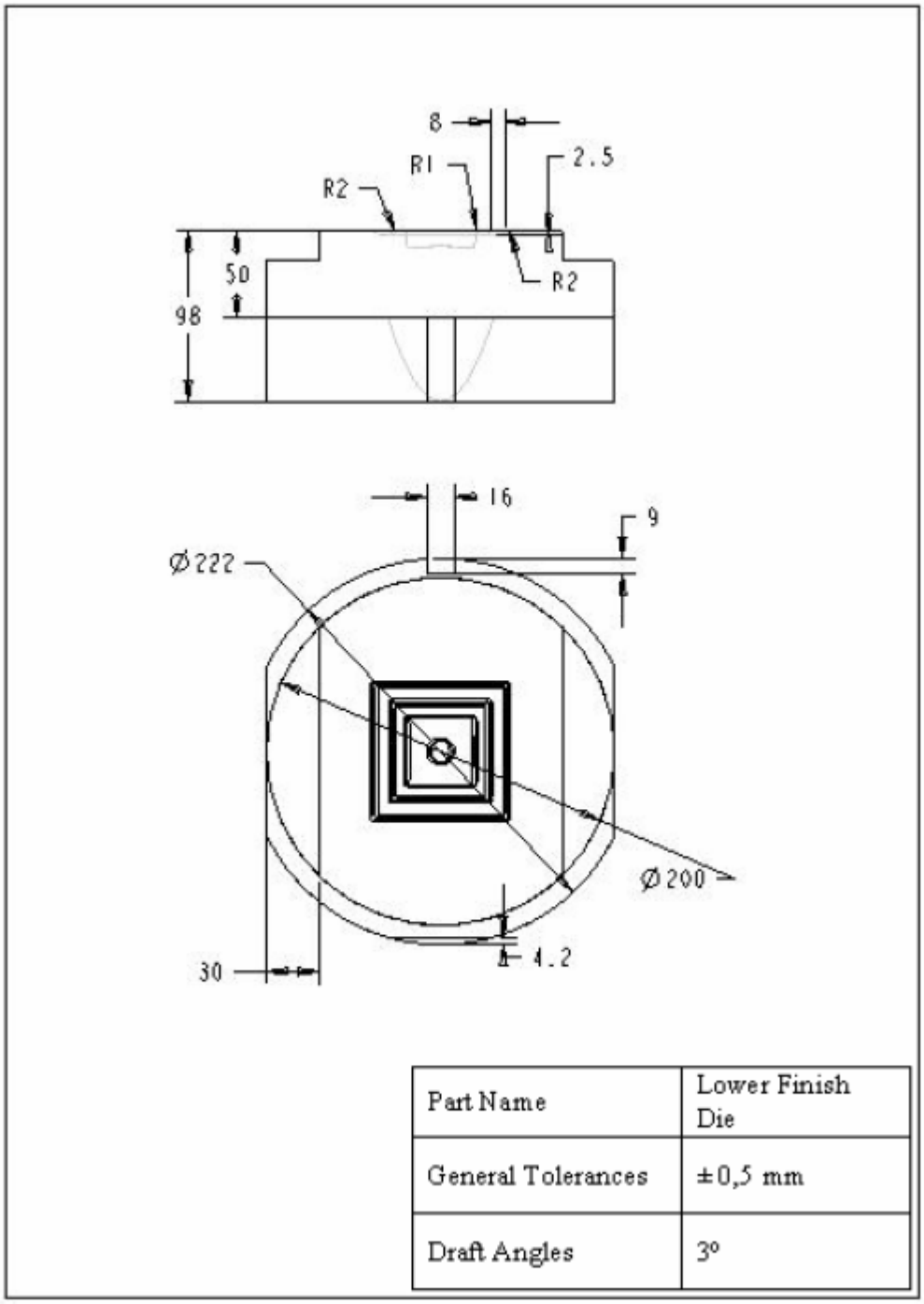

Part Name	Lower Finish Die
General Tolerances	±0,5 mm
Draft Angles	3°

Figure B. 4 Technical Drawing of the Lower Finish Die [13].

APPENDIX C

TECHNICAL DATA OF 1000 TON SMERAL MECHANICAL PRESS

Nominal Forming Force	: 10 MN
Ram Stroke	: 220 mm
Shut Height	: 620 mm
Ram Resetting	: 10 mm
Rod Length	: 750 mm
Crank Radius	: 110 mm
Number of Strokes at Continuous Run	: 100 min^{-1}
Press Height	: 4840 mm
Press Height above Floor	: 4600 mm
Press Width	: 2540 mm
Press Depth	: 3240 mm
Press Weight	: 48000 kg
Die Holder Weight	: 3000 kg
Main Motor Input	: 55 kW
Max. Stroke of the Upper Ejector (without die holder)	: 40mm
Max. Stroke of the Lower Ejector (without die holder)	: 50 mm
Max. Stroke of the Upper Ejector (due to the die holder)	: 20 mm
Max. Stroke of the Lower Ejector (due to the die holder)	: 20 mm
Max. Force of the Upper Ejector	: 60 kN
Max. Force of the Lower Ejector	: 150 kN

APPENDIX D

DECADE 260 LOAD MONITOR SPECIFICATIONS

The Decade 260 Series is a measurement and control system designed to measure and control assembly and test applications. The purpose of the system is to measure force, pressure, torque and position whilst the machine is assembling or testing a component, and from the measured data determine either a pass of failure from the criteria set.

- Provide a PASS of FAIL decision from the measured process data.
- Provide a measure of force/ pressure/ torque and position during the process.
- Provide a database of tools recalled manually or automatically with unique settings.
- Display real-time and history logged information about the process.
- Display third-party machine and process information in the form of programmable messages.
- Large 10.4” TFT colour touch screen for clear display of process data and an intuitive interface.
- Configurable I/O channels, and easy wiring to controlling PLC.